

This dissertation has been 65-11,690
microfilmed exactly as received

COALSON, Jacqueline Jones, 1938-
ELECTRON MICROSCOPICAL AND HISTOCHEMI-
CAL STUDIES ON THE ALVEOLAR-CAPILLARY
MEMBRANE IN ACQUIRED AND CONGENITAL
HEART DISEASE.

The University of Oklahoma, Ph.D., 1965
Health Sciences, pathology

University Microfilms, Inc., Ann Arbor, Michigan

THE UNIVERSITY OF OKLAHOMA
GRADUATE COLLEGE

ELECTRON MICROSCOPICAL AND HISTOCHEMICAL STUDIES
ON THE ALVEOLAR-CAPILLARY MEMBRANE IN ACQUIRED
AND CONGENITAL HEART DISEASE

A DISSERTATION
SUBMITTED TO THE GRADUATE FACULTY
in partial fulfillment of the requirements for the
degree of
DOCTOR OF PHILOSOPHY

BY
JACQUELINE JONES COALSON

Oklahoma City, -Oklahoma

1965

ELECTRON MICROSCOPICAL AND HISTOCHEMICAL STUDIES
ON THE ALVEOLAR-CAPILLARY MEMBRANE IN ACQUIRED
AND CONGENITAL HEART DISEASE

APPROVED BY

William C. Ferguson
John F. Kelly
James H. ...

DISSERTATION COMMITTEE

ACKNOWLEDGMENT

I would like to express my sincere thanks and appreciation to Dr. William E. Jacques whose active interest and support has been inestimable during the course of this study.

Appreciation is also expressed to Drs. Walter Joel, Jeanne Green, and John F. Lhotka for their interest and guidance in all phases of my graduate program. I am especially grateful to Dr. Lhotka for his suggestions, materials, and criticisms in the histochemical aspects of this study.

I am also grateful to Dr. Gilbert Campbell for providing the lung biopsy specimens.

My sincere thanks to Juanetta Anderson and Gerry Stevens for their assistance, materials, and laboratory facilities.

TABLE OF CONTENTS

Chapter	Page
I. INTRODUCTION.....	1
II. MATERIALS AND METHODS.....	4
III. OBSERVATIONS.....	26
IV. DISCUSSION.....	48
V. SUMMARY.....	63
BIBLIOGRAPHY.....	65
APPENDICES.....	74
Appendix A.....	75
Appendix B.....	80

ELECTRON MICROSCOPICAL AND HISTOCHEMICAL STUDIES
ON THE ALVEOLAR-CAPILLARY MEMBRANE IN ACQUIRED
AND CONGENITAL HEART DISEASE

CHAPTER I

INTRODUCTION

After two hundred years of inconclusive findings at the light microscopic level, it has been established by electron microscopic techniques, that the lung does have a continuous alveolar lining epithelium (Low and Daniels, 1952; Low, 1953, 1953a, 1954, 1961; Itagi, 1955; Karrer, 1956, 1956a, 1956b, 1958, 1960; van Breeman and Neustein, 1956; de Groodt, Laguesse, and Sebruyens, 1958; Baker, 1959; Schulz, 1959, 1962; Watson and Valentine, 1959; Kisch, 1960, 1960a; Policard, Collet, and Martin, 1961; Divertie and Brown, 1964; Nagaishi, Okada, Ishiko, and Daido, 1964; van Breeman, 1965).

The septal wall or the alveolar-capillary membrane has been a subject of much disagreement as to the number and exact nature and composition of the layers which constitute the wall. The data that have been accumulated tend to be confusing due in great part to misused terminology and interpretation of tissue components. The interpreta-

tion given by Low (1961) has been substantiated by most workers and it has proved to be the most meaningful in this study.

It was suggested in 1936, by Parker and Weiss that many of the functional observations and clinical findings in mitral stenosis could be correlated with morphological findings on gross and light microscopic material. Indeed, Bucci and Cook (1961) demonstrated a decreased diffusing capacity of the pulmonary membrane in twenty four patients with increased pulmonary blood flow and suggested that an alteration of the volume/surface area ratio and/or increased thickness of the pulmonary capillary membrane might explain the mild increase in the membrane/intracapillary resistance ratio of change observed in the patients. At the electron microscope level, Schulz (1956) described changes in endothelial cells accompanied by thickening of the basement membrane and perivascular components in a case of mitral stenosis. These results were substantiated by Meessen (1956).

The present study was undertaken to obtain data on the morphological changes observed in the alveolar-capillary membrane in patients with functional evidence of acquired and congenital heart disease, particularly those associated with pulmonary hypertension. Histochemical data were obtained in order to try to correlate ultrastructural findings with histochemical changes, if any. It should be emphasized that the lung has been largely neglected in histochemical studies, therefore, a comprehensive battery of histochemical reactions

has been incorporated in this study. However, only the results which contributed substantially to the ultrastructural findings are included in the observations.

CHAPTER II

MATERIALS AND METHODS

In the ensuing study, twelve lung biopsies were obtained from University Hospital clinical patients at thoracotomy; one specimen was obtained at autopsy.

It is essential that short case histories be included presenting the clinical and surgical procedures employed in obtaining a diagnosis for these thirteen patients.

Case I

This thirty-nine month old white male was without symptoms until the age of nine months. At this time, he developed an upper respiratory infection and was found to have a heart murmur. This child exhibited a cyanosis which was increased by exertion or crying. The patient also tired easily and had shortness of breath.

Physical examination revealed a slightly cyanotic individual with signs of early clubbing. Chest examination showed a bulging precordium especially on the left. There was no palpable thrill in the precordium. There was a high pitched, jet-like ejection murmur of grade IV/VI which radiated to the axilla and clavicle and which was heard

best at the left sternal border in the second intercostal space.

The electrocardiograms suggested right atrial and right ventricular hypertrophy.

Cardiac catheterization data indicated a right to left shunt but the site of the shunt was not known. The pressure tracings suggested that it was not at the ventricular level. Angiocardiograms indicated an interatrial septal defect with pulmonary stenosis. A post-stenotic dilatation of the pulmonary artery was noted.

Surgery revealed pulmonary valvular stenosis and infundibular stenosis just below the valve ring. After resection of the infundibular muscle and pulmonary commissurotomy the post-operative course has been excellent.

Case II

This ten year old Indian female was admitted to University Hospital for cardiac evaluation. A heart murmur was first noted at six weeks of age, but she was generally asymptomatic apart from moderate dyspnea and easy fatigability until the last few years during which her symptoms have become progressively worse.

Pertinent physical findings revealed decreased breath sounds over the right posterior and lateral areas just below the scapula. A diffuse point of maximal intensity was heard in the third and fifth intercostal spaces, approximately one centimeter from the left sternal border and extending to the anterior axillary line. A grade III/VI, harsh

systolic murmur, crescendo type and radiating to the left shoulder was noted in the third intercostal space. A grade IV/VI systolic murmur which did not radiate was heard at the apex and fourth intercostal space one to two centimeters from the left sternal border. The second pulmonic, with a split second sound, was greater than the second aortic sound.

Cardiac catheterization was performed and the child was diagnosed as having a left superior vena cava, a ventricular septal defect and pulmonary hypertension. Electrocardiograms revealed a right bundle branch block and right ventricular hypertrophy.

A banding of the pulmonary artery was accomplished at thoracotomy at which time a lung biopsy was obtained.

Case III

This thirty-six year old white male had previously been diagnosed as having rheumatic heart disease at the age of fourteen with subsequent development of mitral stenosis and mitral insufficiency. He was first admitted to University Hospital fifteen years ago with complaints of dyspnea on exertion of many years duration. At that time a closed finger-fracture of the mitral valve was accomplished at thoracotomy. He did well until fourteen years later at which time he noted fatigue and occasional episodes of dyspnea. Subsequently he developed pedal edema, orthopnea, and hemoptysis.

The physical findings showed a few fine basilar rales in the posterior chest. The point of maximal intensity was at the left mid-clavicular line with a prominent left ventricular heave. There was atrial fibrillation on palpation. A grade III/VI systolic murmur and a diastolic murmur were audible at the left sternal border. The second pulmonic sound was accentuated.

A cardiac catheterization was performed during the last admission at which time a diagnosis of mitral stenosis with pulmonary hypertension was made.

A lung biopsy was obtained during surgery. The patient did not respond well post-operatively and died on the fifteenth post-operative day. The findings at autopsy were consistent with the clinical diagnosis.

Case IV

This nineteen month old white female had been found to have congenital heart disease at birth. Upon her first hospital admission, she was diagnosed as having right upper pneumonia, bilateral otitis media, and patent ductus arteriosus with pulmonary hypertension. Seven months later she was admitted for a division and ligation of the patent ductus arteriosus.

Her physical findings showed a labored respiratory rate of 150 and she was in moderate respiratory distress. There were decreased breath sounds on the left side of the chest and rales were heard through-

out the lung fields. The point of maximal intensity was heard at the sixth intercostal space at the midclavicular line. There was a grade II/IV systolic murmur over the precordium throughout the cycle.

X-rays showed cardiomegaly with right ventricular predominance and increased pulmonary vascularity.

Electrocardiograms revealed an incomplete right bundle branch block and right ventricular hypertrophy.

Cardiac catheterization data were consistent with a large left to right shunt.

In spite of successful duct ligation at thoracotomy, pressure readings indicated that the pulmonary hypertension persisted. Post-operatively, the patient developed tachycardia. The second pulmonic sound remained greatly increased and there was a long systolic murmur of grade III/IV intensity with a questionable diastolic murmur at the apex. The precordium was quite active.

Five months later the patient developed bilateral bronchopneumonia which did not respond well to treatment and expired two months later.

At autopsy the following observations were made: (1) atresia of the left common pulmonary vein, (2) small interventricular defect, (3) hypertrophy of the right atrium and right ventricle, (4) enlargement of the pulmonary artery, (5) small patent ductus arteriosus, ligated and divided.

Case V

This patient was a fourteen year old white male with a history of congenital heart disease. A murmur was heard at six months of age but the family refused treatment until the age of fourteen. At the time of admission the patient was dyspneic and intolerant of exercise. Cyanosis was not present.

Pertinent physical findings revealed palpable peripheral pulses with a slow upstroke, a plateau, and a slow fall. Reclining blood pressure, measured by auscultation in the upper extremity, was 90/60. Precordial activity was increased with a strong apical thrust. A definite systolic thrill was felt over the base, along the left sternal border, suprasternal notch and over the carotid artery. A harsh ejection-type systolic murmur of grade III/IV was heard over the entire chest radiating well into the great vessels of the neck. There was paradoxical splitting of the second basal sound.

Electrocardiograms were indicative of left ventricular hypertrophy with some degree of heart strain.

X-rays were suggestive of a definite left ventricular contour and possible post-stenotic dilatation of the aorta.

Cardiac catheterization was performed and the patient was diagnosed as having severe aortic stenosis with mild pulmonary hypertension.

At thoracotomy, a subaortic stenosis of the heavy membranous type was found just below the aortic cusps. The stenotic defect was corrected and the post-operative course has been satisfactory.

Case VI

This fifty-three year old white male with a long history of rheumatic involvement had his first attack of acute rheumatic fever at the age of four. He was without symptoms until fourteen years ago when he suffered a left hemiplegia followed by an almost complete return of function. Seven years ago, a finger-fracture mitral valvulotomy was performed after the patient had developed a marked decrease in exercise tolerance, in addition to an oppressive retrosternal chest pain during times of stress.

Pertinent physical findings revealed a blood pressure of 120/60 with an irregular pulse rate of 60. Percussion indicated enlargement of the heart to the left and right. The point of maximal intensity appeared in the left fifth intercostal space beyond the midclavicular line. The first mitral and second pulmonic sounds were accentuated. In addition to a well localized apical diastolic rumble of grade II/VI, an apical systolic murmur of grade II/VI was present which radiated to the left axilla.

An electrocardiogram showed the following: (1) atrial fibrillation, (2) occasional ventricular extrasystole, (3) left ventricular hypertrophy, (4) primary T-wave changes.

Cardiac catheterization data and left ventricular angiocardiography were compatible with a diagnosis of marked mitral stenosis and minimal mitral insufficiency of rheumatic origin. Anatomically the patient had left atrial and right ventricular hypertrophy; physiologically the patient exhibited atrial fibrillation and congestive heart failure.

The mitral stenosis was corrected surgically and the post-operative course has been satisfactory.

Case VII

Two months prior to hospital admission, this fifty-four year old white male was diagnosed as suffering from congestive heart failure of insidious onset. At this time, he was found to have atrial fibrillation and was started on digitalis.

Physical examination on this admission showed a blood pressure of 142/60 with an irregular pulse rate of 48. A well localized grade II/IV diastolic murmur was heard only in the left decubitus position. A grade II/IV systolic murmur was heard at the apex; an opening sound was heard but the second pulmonic sound was not remarkable.

Electrocardiograms were suggestive of left ventricular hypertrophy.

Cardiac catheterization data revealed an elevated pulmonary wedge pressure indicating mitral insufficiency and stenosis. Pressure

data from the right heart was consistent with a mild pulmonary hypertension. Mitral stenosis was the predominant lesion with moderate mitral and aortic insufficiencies.

Surgical procedure revealed a moderately to markedly stenotic mitral valve. The stenosis was of a fibrous type. There was no gross evidence of either mitral or aortic insufficiency.

After commissurotomy, the post-operative course has been satisfactory.

Case VIII

The patient was an eleven year old white female who had a diagnosis of patent ductus arteriosus with a reversal of flow and pulmonary hypertension. This diagnosis was confirmed by cardiac catheterization and angiocardiography.

Pertinent physical findings revealed a blood pressure of 130/84 with a regular pulse of 84. The chest was clear to auscultation and percussion. The heart rhythm was regular; the point of maximal intensity was three centimeters lateral to the midclavicular line. A grade II/VI diastolic murmur was heard maximally at the left sternal border in the second intercostal space. The pulmonary second sound was greatly accentuated. The other physical findings and laboratory data were within normal ranges.

A bilateral pulmonary artery banding was accomplished and a lung biopsy was obtained during the surgery. The patient responded

well post-operatively and is being followed in the out-patient and cardiology clinics.

Case IX

This eleven year old white female was admitted to the hospital for evaluation of a heart murmur. A year earlier, the patient began having episodes of dizziness and fatigue and had noted a gradual development of shortness of breath. Two months prior to admission the patient complained of chest pain and a smothering sensation during rest and exercise. Since that time, the patient has had fever once or twice weekly. Six weeks prior to admission the patient's left knee became swollen and warm but these signs disappeared spontaneously two days later.

At the time of admission, a physical examination showed a blood pressure of 118/78 and was unremarkable except for a grade IV/VI middle to late diastolic crescendo murmur heard at the apex which radiated throughout the left hemithorax. A grade I/VI systolic murmur was heard at the apex with a systolic opening snap. The physical diagnosis was indicative of mitral stenosis with a question as to whether this was of rheumatic or of congenital origin.

Cardiac catheterization data indicated pulmonary arterial hypertension but a shunt was not demonstrated.

Commissurotomy was performed and the post-operative course has been satisfactory.

Case X

This sixty-four year old white male with a chief complaint of slight dyspnea on exertion was admitted to University Hospital for cardiac catheterization and cardiac evaluation. Fifteen years earlier the patient had received I¹³¹ treatment for Grave's disease. Thirteen years after this the patient began receiving dessicated thyroid for hypothyroidism. One year prior to this admission the patient suffered an acute myocardial infarction, became hypotensive and developed congestive heart failure. Digitalis treatment was begun and the patient developed a loud systolic murmur which was thought to be caused by papillary muscle rupture.

The physical examination at this admission revealed a blood pressure of 130/90 with a regular pulse of 80. The patient exhibited marked exophthalmus and was unable to move the left eye upward and laterally. The jugular vein was large and pulsatile. Decreased breath sounds and dullness were noted at the right lung base. The heart was slightly enlarged to the left with a prominent epigastric impulse. A loud harsh pansystolic murmur with a thrill was heard maximally at the apex. A grade IV second sound was widely split. Pedal pulses were palpable and questionable clubbing was noted.

X-ray examination revealed cardiomegaly, a prominent right ventricle and increased pulmonary vasculature.

The electrocardiogram showed an old anteroseptal and anterolateral myocardial infarction with complete right bundle branch block.

Cardiac catheterization data revealed a small left to right shunt which suggested a ruptured interventricular septum secondary to the myocardial infarction. Cineangiocardiograms demonstrated mild to moderate left to right shunt in the lower interventricular septal region. Because of the left to right shunt the pulmonary wedge pressure was at the upper limits of normal or slightly elevated. There was no mitral regurgitation.

The septal defect was repaired with Teflon felt during surgery and the post-operative condition has been good.

Case XI

This sixty-nine year old diabetic white female was referred to University Hospital for evaluation of a solitary mass in the upper lobe of the right lung which was discovered during hospitalization for congestive heart failure. Two years prior to this admission a mass, diagnosed as undifferentiated spindle cell sarcoma (probably liposarcoma or rhabdomyosarcoma) was removed from the distal part of the left thigh. Two months later a recurrent mass was excised from the scar. Seven months later a high amputation was performed for a second tumor recurrence. There was no history of hemoptysis or chest pain and the patient was without signs or symptoms until a year and a half later when the lung mass was discovered. A metastatic survey was negative and

planigrams revealed only the solitary pulmonary lesion.

The admitting diagnosis was as follows: (1) metastatic sarcoma in the right lung, (2) well compensated atherosclerotic heart disease with congestive heart failure, (3) senile diabetes mellitus.

Physical diagnosis revealed a blood pressure of 160/70 with a regular pulse of 84. The lungs were clear to auscultation and percussion. The heart showed a grade III/VI systolic murmur radiating to the neck which was heard best at the left sternal border in the seventh intercostal space.

Electrocardiographic findings indicated left ventricular hypertrophy with primary T-wave changes.

No cardiac catheterization data were obtained from this patient.

A right upper lobectomy was performed. At surgery neither pleural or gross nodal involvement was noted. There was no evidence of mediastinal extension. The biopsy was obtained at a site free from tumor involvement.

The surgical pathology report diagnosed the tumor mass as a metastatic malignant spindle and giant cell tumor consistent with rhabdomyosarcoma of the right upper lobe. The resected margin was free of tumor.

The patient was discharged fifteen days post-operatively.

Case XII

This eleven year old white female has had numerous hospital admissions for chronic lung disease, pneumonia, and other congenital anomalies. In addition to the above disorders the patient had an admitting diagnosis of congenital spherocytosis, right hemiparesis due to cerebro-vascular accident, mild mental retardation, blindness in the left eye due to vitreous hemorrhage, pulmonary fibrosis of unknown etiology, and coarctation of the aorta.

Family history revealed that one sibling had chronic lung problems, that another died at fifteen months of age from pulmonary fibrosis (*pneumocystis carinii*), and that the mother was known to have spherocytosis.

Physical examination revealed a blood pressure of 135/90 in the right arm and 120/65 in the left arm. The pressure in both legs was 90/60. The chest showed some increase in anterior-posterior diameter. There were no rales but occasional coarse rhonchi were heard in the posterior lung fields. The point of maximal intensity was in the midclavicular line of the fifth intercostal space with some apical thrust. A thrill was not present. A systolic murmur was heard at the base which radiated into the neck; it was also well heard over the back. A grade I/II systolic murmur was heard over the pulmonary valve area.

X-ray revealed generalized pulmonary fibrosis and emphysema.

Because of the prominent pulmonary involvement, lung biopsies were obtained for histopathologic and electron microscopic evaluation at this time. The surgical pathology findings indicated a minor degree of interstitial fibrosis with slight pleural thickening.

At a later time, cardiac catheterization data were obtained for evaluation of the aortic coarctation. The cardiac catheterization data indicated no intracardiac communication. Pressures in the right heart were essentially in the normal range. Systolic pressures in the left ventricle, ascending aorta, and left brachial artery were elevated. Pressure recordings across the area of coarctation revealed a gradient of 50-60 mm. of mercury. These data were consistent with the admitting diagnosis of coarctation of the aorta.

Case XIII

This one year old white female was admitted with a clinical diagnosis of congenital mitral stenosis. Since the age of three months, the patient had exhibited cyanotic episodes lasting up to five minutes and associated with breath holding. Respiratory distress was not apparent during these periods. A heart murmur was found three weeks prior to admission.

Physical examination revealed an asymmetrical thorax with prominence of precordium and left chest anteriorly. The lungs were clear. A grade III/IV systolic murmur was heard over the fourth to fifth intercostal space at the left sternal border and also over the pre-

cordium to the axillary line and upward along the left sternal border. Pulses were equal. The liver was palpable four fingerbreadths below the right costal margin.

Chest x-ray with barium swallow showed moderate cardiomegaly with a very large left atrium and hypertrophy of the right ventricle.

The electrocardiogram showed right axis deviation.

Cardiac catheterization data revealed increased pressure in the pulmonary vein, right ventricle, and pulmonary artery.

At surgery, an enlarged left atrium and right ventricle with a very small mitral valve was found. There was questionably some sclerotic changes in the pulmonary artery.

Post-operative condition was poor and after being taken off the pump, the heart rate slowed and effective systemic pressures could not be maintained. The patient was put on a bypass pump and drugs were given. Despite these measures, the patient took a progressive downhill course and expired.

The lung specimen was taken thirty to forty-five minutes after death.

The cardiac catheterization data can be found on pages twenty, twenty-one, and twenty-two.

TABLE I
CARDIAC CATHETERIZATION DATA

	CASE I	CASE II	CASE III	CASE IV	CASE V	CASE VI	CASE VII
SVC	-	-	m 12	-	-	-	-
RA	- m 5	2 m 2	13 m 10	- m 4	-	- m 6	- m 8
RV	114/10/0	110/0/10	98/0/13	75/0	-	36/6	43/0/7
RPA	- -	120/57 m 85	- -	- -	22/9 m 16	- -	- -
LPA	12/4 m 8	- -	100/40 m 65	- -	- -	- -	- -
MPA	12/4 m 8	105/45 m 70	93/45 m 65	80/48 m 60	- -	44/7 m 26	42/18 m 30
WEDGE	- -	- m 5	- m 30	- -	14/5 m 9	27 -	- m 18
BA	98/55 m 73	102/65 -	140/80 m 100	- -	90/50 m 70	- -	- -

SVC - superior vena cava; RA - right atrium; RV - right ventricle; RPA - right pulmonary artery; LPA - left pulmonary artery; MPA - mean pulmonary artery; WEDGE - wedge pressure; BA - brachial artery; m - mean. All readings are in millimeters of mercury.

TABLE I

Continued

	CASE VIII	CASE IX	CASE X	CASE XI	CASE XII	CASE XIII
SVC	-	-	m 4	-	-	-
RA	5 m 3	-	- m 4	-	- m 2	-
RV	140/0/10	53/0/3	49/2/4	-	-	-
RPA	140/80 m 100	47/28 m 37	-	-	20/8 m 14	-
LPA	130/75 m 100	-	-	-	-	-
MPA	-	48/22 m 35	42/22 m 30	-	24/8 m 14	-
WEDGE	- m 4	31/16 m 24	- m 13	-	-	-
BA	130/75 m 100	-	132/85 m 105	-	170/60 m 90	-

SVC - superior vena cava; RA - right atrium; RV - right ventricle; RPA - right pulmonary artery; LPA - left pulmonary artery; MPA - mean pulmonary artery; WEDGE - wedge pressure; BA - brachial artery; m - mean. All readings are in millimeters of mercury.

TABLE I

Continued

PERCENT OXYGEN SATURATION

CASE NUMBER	I	II	III	IV	V	VI	VII	VIII	IX	X	XI	XII
SVC	58	72	65	53	77	-	-	-	65	56	-	-
RA	59	78	43	49	75	-	-	83	66	53	-	-
RV	-	83	62	63	-	-	-	76	66	68	-	-
RPA	-	83	-	-	75	-	-	77	66	-	-	-
LPA	60	-	62	-	-	-	-	-	-	-	-	-
MPA	60	83	64	70	-	-	-	75	63	70	-	-
WEDGE	-	-	-	-	93	-	91	-	100	-	-	-
BA	81	97	97	-	99	-	-	99	-	-	-	-

SVC - superior vena cava; RA - right atrium; RV - right ventricle; RPA - right pulmonary artery; LPA - left pulmonary artery; MPA - mean pulmonary artery; WEDGE - wedge pressure; BA - brachial artery.

At the time of thoracotomy, the lung biopsy was obtained which was immediately fixed in the following manner. For electron microscopic study, a piece of the tissue was cut into small pieces and fixed in Zetterqvist's fixative (Pease, 1964) for a period of forty five minutes to one hour. The procedure used for Maraglas embedding was the one developed by Freeman (1963). The Epon embedding procedure of Luft (1961) was utilized with the following modification: seven parts of the Epon mixture "A" plus three parts of mixture "B" was used as the final embedding resin to produce a somewhat softer block. This embedding mixture had been found previously in this laboratory to enhance thin sectioning of lung material.

The specimens for electron microscopic observations were sectioned with the Porter-Blum ultramicrotome fitted with a Du Pont diamond knife or with glass knives.

After procuring thin sections on formvar coated grids, they were stained using various electron staining procedures: Watson's lead hydroxide stain (1958), Watson's saturated uranyl acetate stain (1958a), Millonig's lead tartrate stain (1961), Reynold's lead citrate stain (1963), Callahon and Horner's vanadatomolybdate stain (1964), Pease's five per cent uranyl acetate stain (1964). The stain employed has been designated in the plate descriptions.

The ultrathin sections were examined with an RCA EMU-3F electron microscope.

When desired fields were viewed in the electron microscope, photographic plates were exposed to the electron beam to secure electron micrographic data.

In the histochemical and cytological study, seven different fixatives were employed for each biopsy. These were: ten per cent neutral-buffered formalin, Bouin's solution, Carnoy I solution, calcium acetate-formalin, alcohol-neutral formalin, calcium-formol, and cetyl pyridinium-formalin (Pearse, 1960; Barka and Anderson, 1963). For some of the enzyme and lipid studies, it was mandatory to use frozen sections, and the specimens were immediately frozen on dry ice and stored in the deep freeze at -30° C. until appropriate sections were cut on the International Harris Cryostat, Model CT. Optimal times for fixation were used for all of these fixatives. Due to the small size of the lung biopsy, in some cases, it was necessary to omit several of the fixatives.

With the exceptions of the calcium-formol fixed specimens and the fresh frozen blocks, all of the tissues were embedded in Paraplast. Seventy five to one hundred slides were prepared from every fixative from every biopsy procured. Paraplast embedded tissues for empirical cytological staining and for some histochemical procedures were sectioned at four to ten micra on a Minot rotary microtome. The calcium-formol and fresh frozen sections were cut at six to twelve micra on the cryostat.

The histochemical study was initially undertaken to obtain a comprehensive battery of reactions on lung. The histochemical methods and modifications and the empirical cytological methods, which were used routinely to augment and clarify some of the histochemical data, have been listed in Appendix A.

Photomicrographic data were obtained from selected histochemical and cytological procedures which could be correlated with ultrastructural findings.

The light microscopic apparatus consisted of the Zeiss photomicroscope which was suited for microscopy and photomicrography with trans- and epi- illumination as well as for work with polarized light. This photomicroscope was particularly valuable in that the operator could take a series of properly exposed photographs in rapid succession of labile histochemical reactions. The following accessories were utilized in taking color photomicrographs: (1) a blue filter, (2) a neutral density filter, when desired. A red-green filter was utilized in photographing specimens for black and white exposures.

CHAPTER III

OBSERVATIONS

Case I

This patient had pulmonary stenosis with no pulmonary hypertension and served as a functional control in this study. The figures for all the cases were included in Appendix B.

The lumina of the capillaries were continuously lined by endothelial cells. The cytoplasmic extensions were normally quite thin in this case. The endothelial lining was not widened although in comparison with the alveolar epithelial lining, it did appear more prominent (Figures 1 and 2). Vesicles and ribosomes were dispersed throughout the cytoplasm, but large pinocytotic vesicles were not evident.

Both the capillary endothelial and the pulmonary epithelial cells rested on distinct basement membranes. These membranes had two components, an inner lamina densa, which faced the perivascular space, and a translucent lamina lucida, which rested upon the plasma membranes of the endothelial and epithelial cells. The capillary basement membrane was slightly thicker than that of the atten-

uated alveolar basement membrane (Figure 1 and 2). In some instances, both basement membranes merged into the perivascular fiber components (Figures 1 and 3).

The perivascular space included the area which was situated between the two basement membranes. Collagen, reticular fibers, and mesenchymal cell derivatives were observed in the perivascular space (Figure 2). However, there were no large increments of these three components in this functional control. There may have been some edema present in Figure 2, but the wall was still not thickened appreciably.

It has been suggested that the pulmonary surface lining consists of two cell types, the alveolar type I cell and the alveolar type II cell. The alveolar type I cell forms the attenuated flattened epithelial layer. Cellular organelles and nuclei are infrequent, but when present the cytoplasm becomes increased in width. The alveolar type II cell does not have long cytoplasmic extensions, but contains inclusion bodies and microvilli. There are none demonstrated in the electron micrographs for this case. The pulmonary epithelium was conspicuously attenuated in this case (Figures 1, 2, and 3). Occasional vesicles and infrequent cellular organelles were noted in the epithelial cytoplasm.

In a thick area of the septal wall, a mast cell with its characteristic inclusions was noted (Figure 3). Astrablau and toluidine

blue histochemical preparations showed an appreciable number of mast cells with very intensely stained granules.

The cytological and histochemical tests for collagen, elastic and nucleic acids (for cellular definition) were all unremarkable in that no increased amounts of the various components were demonstrated. The reticular fibers appeared to be within normal range in the Gomori preparations, consequently the capillaries were not well-defined.

Case II

The diagnosis of this patient was determined as left superior vena cava, ventricular septal defect, and pulmonary hypertension.

The endothelial lining appeared to be slightly increased in width and contained vesicles of varying sizes (Figures 4, 5, 6, and 7). Several large pinocytotic vesicles were well seen in Figures 4 and 5. An interdigitation of the endothelium and the capillary basement membrane was seen in Figure 6. This was a normal configuration in which endothelial cells overlaid each other with an intervening portion of the capillary basement membrane found between the two cell borders.

The capillary basement membrane was slightly thickened in some areas (Figures 4, 5, and 6). The alveolar basement membrane showed a slight size increase in this case (Figure 4). Mesenchymal cell derivatives within the septal wall appeared closely adherent to

the alveolar basement membrane (Figures 4, 5, and 6).

In Figures 4, 5, and 6, the perivascular space showed widening due to increased collagen and reticular fiber deposition. Many cytoplasmic elements of mesenchymal cells containing small dense ribosomal particles were seen in the perivascular space (Figure 4).

Alveolar type I cell cytoplasmic extensions, forming a continuous lining, rested upon the alveolar basement membrane. Some large pinocytotic vesicles were evident in the epithelial investments (Figures 5, 6, and 7). Dense ribosomal particles within the epithelium were observed in Figures 4 and 7. An alveolar type II cell, resting directly upon the underlying basement membrane with no intervening cell layer interposed, was seen in Figure 6.

The pulmonary macrophage contained many inclusion bodies of varying shapes and densities in addition to other normal cellular organelles (Figure 7). The ribonucleoprotein particles were quite abundant in this particular macrophage. Although the macrophage appeared to form part of the epithelial lining, it was separated from the underlying basement membrane by the attenuated alveolar type I cytoplasmic border.

The histochemical and cytological studies augmented the ultrastructural findings in this case. The Gomori and periodic acid-Foot techniques for reticulum definitely showed an increase in the reticular fiber content. The elastic tissue, visualized by the orcein method, did not show any appreciable increase. The collagen fibers appeared

slightly increased in the Masson-type trichrome preparations. The gallocyenin-chrome alum, the Feulgen, and the methyl green-pyronin methods indicated that there was an appreciable increase of mesenchymal cells within the septal walls.

Case III

Acquired mitral stenosis with pulmonary hypertension was diagnostically determined in this patient.

The endothelial cytoplasmic lining did appear to show an increase in thickness (Figures 8, 10, and 11). Ribosomes and numerous small vesicles were observed in the investing cytoplasm in all instances (Figures 8, 9, 10, and 11). Interdigitations that formed an open channel between the capillary lumen and the capillary basement membrane were observed between contiguous cell boundaries (Figure 11).

Both basement membranes were extensively thickened in this case of acquired mitral stenosis (Figures 8, 9, 10, and 11). The demarcation between the lamina densa and the lamina lucida of the basement membranes was lacking in most areas (Figures 8, 9, and 11). Although the basement membrane appeared very homogeneous, collagen, elastic and reticular fibers were observed which augmented the prominent thickening of the septal wall (Figures 8, 9, and 10). Mesenchymal cell components were closely adherent to the alveolar basement membranes in Figures 8 and 9. Ribosomal particles were

again discerned in these cellular portions (Figures 8, 9, and 10).

Vesiculation and vacuolization of the alveolar type I cell were observed (Figures 8, 9, 10, and 11). However, the epithelial investment was not increased in width.

Histochemical and cytological studies were not obtained in this case due to the small size of the lung biopsy procured.

Case IV

This patient was clinically diagnosed as having patent ductus arteriosus with pulmonary hypertension. The final pathologic diagnosis was atresia of a left common pulmonary vein, a small interventricular septal defect, enlargement of the pulmonary artery, and hypertrophy of the right atrium and the right ventricle.

The lumen of the blood vessel in Figure 13 depicted two endothelial cells. This was suggestive of a marked endothelial proliferation since normally only occasional nuclei were seen. This interpretation was fortified by light microscopic studies of cytological material. The endothelial cytoplasm contained abundant ribosomal particles and many vacuoles.

The capillary basement membrane showed minimal thickening, whereas the alveolar basement membrane appeared essentially normal (Figure 13). In Figure 12, a nucleated mesenchymal cell was seen in close proximity to the alveolar basement membrane.

The perivascular space was markedly dilated in this case. Edematous conditions had separated the densely packed collagenous and elastic elements which were definitely increased in amount (Figures 12 and 13). The mesenchymal cell contained numerous ribosomes and a well-defined Golgi zone (Figure 12).

The alveolar type I cell contained numerous vacuoles and vesicles, some of which were closely adherent to the alveolar basement membrane (Figure 13). Ribosomes and mitochondria were infrequently seen in the epithelial cytoplasm (Figures 12 and 13). Other than the sites of vacuolization, the continuous epithelial lining did not appear to be increased in width.

The ultrastructural observations were augmented and clarified by histochemical and cytological studies. The vessels showed marked intimal proliferation and an extremely large amount of reticular fibers were observed investing the capillaries. Both the orcein and aldehyde-fuchsin methods for elastic tissue depicted a substantial increase in elastic tissue within the septal walls. The connective tissue stains, Masson-type and Koneff, showed an increase in collagen deposition, but a more delicate fibrous element, thought to be reticular fibers, were even more evident. The alkaline fast green method for histones, the Feulgen for deoxyribosenucleic acid, the gallocyanin-chrome alum and the Turchini for nucleic acids indicated a substantial increase of cells within the septal wall. Enzyme

studies, including di- and tri- phosphopyridine nucleotide reductase, esterase, acid and alkaline phosphatases, gave positive results in these cells and were helpful in discerning the increased cellularity in the septal wall. In the preparations stained for tyrosine by the diazocoupling reaction, many granules were observed within the septal cells. A Prussian blue for hemosiderin gave the same staining distribution of the positive granular material.

Case V

This patient had congenital aortic stenosis with mild pulmonary hypertension.

The normally narrow endothelial lining appeared slightly thickened with increased vacuolization and vesiculation (Figures 14, 15, 17, and 18). In these same figures, there were large, irregular spaces near the capillary basement membrane which appeared to contain a fibrillar or reticular substance (Figures 14, 15, 17, and 18). Reference was particularly called to Figure 18 in which an apparent change was noted within the endothelial cytoplasm. Finger-like cytoplasmic extensions and a fiber bundle resembling collagen were both seen in the clear area near the capillary basement membrane.

In this case, the capillary basement membrane was somewhat thickened. In Figures 15 and 17, it looked attenuated at one point but this could have been an artifact. The alveolar basement membrane was within normal limits, and in many instances had a mesenchymal

cell portion closely apposed (Figures 15, 16, 17, and 18).

The perivascular space of the alveolar septal wall was widened with increased amounts of collagen (Figure 18) and elastic fibers (Figure 14) and swelling probably due to edema (Figures 14, 15, 16, 17, and 18). In the alveolar septa of Figure 15, two fibroblastic type cells were observed from which thin cytoplasmic processes extended into the surrounding perivascular spaces. In Figures 17 and 18, leucocytes were seen within the septal wall. Light microscopic observations substantiated the findings of abundant cells in the perivascular space.

The alveolar type I cells were not increased in width, but there were a few pinocytotic vesicles (Figures 15 and 17) and innumerable smaller vesicles present (Figures 14, 15, 16, 17, and 18). The alveolar type II cell (Figure 16) contained numerous osmiophilic inclusions of varying configurations and rested directly upon the alveolar basement membrane.

In the cytological and histochemical preparations, the reticulum appeared to be increased in amount and the capillaries were particularly well-invested with fine reticular fibers. The elastic stains: orcein, aldehyde-fuchsin, and Verhoeff hematoxylin, did not show any demonstrable increase in the elastic fiber content except in occasional thickened septal walls. In these thickened areas, the elastic stains did show an amorphous type of deposition. In the Goldner and Masson preparations, the collagen appeared to be palely stained and was slightly in-

creased in amount. In these areas, the edematous transudate appeared fuchsinophilic and masked the collagen staining. Collagen appeared to be more abundant and was well stained even in the edematous areas in the Van Giesen preparations. The Turchini, gallocyanin-chrome alum, alkaline fast green, and Feulgen methods did demonstrate minimal cellular increase in the wall, but the thickness of the septal wall was not always associated with this increased cellularity. The thickening of the septal wall appeared to be more dependent on the edematous swelling present. A typical layering effect was noted in the gallocyanin-chrome alum preparations. The septal cells appeared pushed to the epithelial borders with a hollow edematous area occupying the center of the wall.

Case VI

This case was a patient with acquired mitral stenosis and minimal mitral insufficiency.

The lumen of the capillary was lined by endothelium which was quite granular and vesiculated. A slight increase in width was discerned (Figures 19, 20, and 21).

The basement membranes of the capillaries were thickened considerably (Figures 19, 20, and 21). The alveolar basement membrane, when separate, was also thickened in width. In Figures 19 and 21, continuous canals interdigitated between the endothelial cells allowing contact between the capillary basement membrane and the capillary lumen.

The perivascular space was markedly widened in Figures 19 and 21. Increased deposition of both collagen and elastic fibers were involved in this thickening. In Figure 19, the amorphous material, which was interpreted as altered elastic fiber tissue, was very smudgy with no clear delineation of borders. Mesenchymal cells were observed in apposition with the alveolar basement membrane (Figure 21). The cell in Figure 19 had unusual inclusion bodies. In cross section they appeared as cylinders of symmetrical size and in longitudinal section they appeared as short rods with two outer osmiophilic borders and an inner osmiophobic center. These inclusions resembled those seen in the mast cell in Figure 3.

Ribosomal particles and vesicles were observed in the alveolar type I cell. There was no increased vacuolization or prominent thickening of this layer.

The Gomori and periodic acid-Foot techniques showed a minimal reticular fiber increase at the light microscopic level. Elastic tissue preparations did indicate increased amounts of elastic deposition. The connective tissue stains exhibited minimal increased accumulation of collagen. Mildly increased cellularity within the septal walls were demonstrated by the Turchini, alkaline fast green, and methyl green-pyronin tests.

Case VII

The diagnosis of the patient was acquired mitral stenosis, moderate mitral insufficiency and moderate aortic insufficiency.

The endothelial cell layer was markedly widened with increased vesiculation and vacuolization, which may have been due in part to the gross pulmonary edema present (Figures 22, 23, and 24).

Both the capillary and alveolar basement membranes were intact even though the alveolar spaces contained red blood cells and copious transudate. The capillary basement membrane was markedly thickened (Figures 22, 23, and 24). In Figure 22, a portion of mesenchymal cell cytoplasm was seen embedded in the homogeneous matrix of the capillary basement membrane. The alveolar basement membrane was attenuated in some instances (Figure 22) due to the edema present. It was again noted that the alveolar basement membranes were closely apposed to mesenchymal cells (Figures 22, 23, and 24).

A preponderance of collagenous elements, which greatly thickened the air-blood barrier, filled the perivascular space (Figures 22, 23, and 24). In the mesenchymal cells, large pinocytotic vacuoles showed a demonstrable increment (Figure 23).

In one instance, the epithelial cell lining was not evident (Figures 22 and 23). This was probably a deleterious result of the transudative fluid pressure in the alveoli. Otherwise, pinocytotic vacuolization was

was the only remarkable finding in the alveolar type I cell lining (Figure 22). In Figure 24, attention was called to a fat embolus which could have been responsible for the edematous condition in this tissue.

The Gomori reticulum stain demonstrated a tremendous increase of reticular fibers in the alveolar walls. A concomitant increase in elastic and collagen fibers were likewise seen in the orcein, aldehyde-fuchsin, Koneff, Goldner, and Van Giesen preparations. The cellularity was not markedly enhanced within the septal wall. However, in the gallocyanin-chrome alum and Turchini sections, a layer of cuboidal epithelial cells was seen lining the alveoli.

Case VIII

This patient had a diagnosis of patent ductus arteriosus with reversal of flow and pulmonary hypertension.

The lumen of the capillary was continuously lined by endothelial cells. The cytoplasm appeared slightly thickened and several large pinocytotic vacuoles and numerous vesicles were observed (Figures 25 and 27). Occasionally a mitochondrion was seen in cytoplasmic extensions of the endothelial cell (Figure 25). There was no formed endoplasmic reticulum; only ribosomal particles were evident.

Both the capillary endothelial and the pulmonary epithelial cells rested on distinct basement membranes (Figures 25, 26, 27, and 28). The capillary and alveolar basement membranes were approximated

and coalesced in Figure 25. There was no appreciable size increase in the basement membranes in this case (Figures 25, 26, 27, and 28).

The perivascular space contained an increased amount of reticular fibers and collagen with its characteristic periodicity. This was more prominently pronounced in Figure 28, which was a longitudinal section of an alveolar capillary wall. Occasional cellular components were noted in the perivascular space (Figures 25, 26, and 28). In one instance, the perivascular space was seen to be lined by a cell resembling the endothelial cell which lined the capillary (Figure 27). There was also a free cell, probably a macrophage with an ingested red blood cell, in the space. The perivascular space was noted to contain densely packed collagen and elastic fibers. It has been suggested that the perivascular space may function as a lymphatic channel at this level of the respiratory tissue. The only vesicles noted in this area were found in the cytoplasmic extensions of the mesenchymal cells.

Numerous vesicles were seen in the epithelial layer some of which appeared to abut on the alveolar basement membrane (Figure 25). The alveolar type II cell was seen in Figure 26. It was characterized by dense laminated structures, the inclusion bodies, and microvilli. Its cytoplasm did not form tenuous cytoplasmic extensions as compared to the alveolar type I cell. It rested upon the alveolar basement membrane. This cell, like that of the alveolar type I cell, did not have a formed endoplasmic reticulum, but many ribosomes were evident.

The free alveolar cell had an abundant cytoplasm which contained numerous ribosomes, inclusion bodies, mitochondria, and microvilli (Figure 28). It was noted that some of the inclusion bodies were found free in the alveolar space. In this free macrophage, one inclusion body adjacent to the cytoplasmic border, was suggestive of either an extrusive or phagocytic activity of the macrophage.

Histochemical studies were not available for this case, since the biopsy specimen size was only adequate for electron microscopic studies.

Case IX

This patient had mitral stenosis probably of rheumatic origin. Remarkable endothelial swelling was found in Figure 30, concomitant with an increase in small cytoplasmic vesicles which were seen more abundantly at the endothelial plasma membrane. Large pinocytotic vacuoles were also noted. Two darkly staining bodies were observed in the endothelial cytoplasm. One of these bodies was enclosed by a double membrane whereas the other appeared to be invested by only a single membrane. The identification and significance of these bodies were undetermined. The endothelial lining in Figure 29 was not remarkably different from those observed in other cases of mitral stenosis.

The basement membranes were fused in Figure 20 and were

markedly thickened. The capillary basement membrane was well-defined and increased in width in Figure 30.

Fine reticular fibers (Figure 29) and elastic fibers (Figure 30) were observed in the perivascular space. However, the overall increase in thickening was attributed to the basement membrane components in this case. The mesenchymal elements in Figure 29 showed vacuolization.

The epithelial components of the pulmonary surface epithelium in this instance were not appreciably widened (Figure 29).

The reticular, collagen, and elastic fibers were increased in amount as demonstrated by the cytological methods. A marked cellularity was observed in the Feulgen, Turchini, and methyl green-pyronin histochemical tests. In the Goldner and Masson stained preparations, intimal proliferation was noted in the small arterioles. In some instances, the lumen was markedly compromised.

Case X

A diagnosis of acquired interventricular septal defect with a mild to moderate left to right shunt was determined in this case.

The capillaries showed very prominent endothelial cell thickening. Innumerable vesicles were noted throughout the cytoplasm (Figures 31, 32, and 33), however, no large pinocytotic vacuoles were evident.

Both the capillary and alveolar basement membranes exhibited

outstanding increases in thickness (Figures 31, 32, and 33). Some dispersed collagenous and reticular elements fused into the basement membrane investments.

Mesenchymal cell derivatives were commonly encountered throughout the perivascular space. A fat inclusion was observed in the mesenchymal element in Figure 33. Collagen and reticular fiber deposition were not markedly pronounced in these figures (Figures 31, 32, and 33).

The alveolar type I cell lining did show some increase in width. Many small vesicles were interspersed throughout the cytoplasm. The alveolar type II cell in Figure 32 was depicted with microvilli but no inclusion bodies were present in the field. Underlying the alveolar type II cell, vacuolization was noted and the alveolar basement membrane was markedly attenuated (Figure 32).

The reticular network showed only a minimal increase and the capillaries were not well-invested with reticulum in the Gomori preparations. Significant findings in the connective tissue studies demonstrated only a slight increase of delicate collagenous fibers but some areas of cuboidal alveolar epithelial cells were observed. The pulmonary veins showed an augmented deposition of smooth muscle fibers in the Goldner preparations. Cellularity within the septal wall was negligible in this case.

Case XI

This patient was a diabetic who presented in congestive heart failure and atherosclerotic heart disease.

The endothelial lining did not show an increment of vesicles or vacuoles in this case, nor was there any widening of the investing layer. There were two fat inclusions observed in the endothelial cytoplasm in Figure 34. Otherwise, the endothelium was unremarkable.

There was no increase in width in either the alveolar or the capillary basement membranes. They both appeared well-delineated.

The most prominent changes were found in the perivascular area. In a cross section of the septal wall in Figure 34, numerous collagen fibers and a large amount of elastic tissue, which was quite homogeneous and osmiophilic, were seen. The longitudinal section of a septal wall (Figure 35) was quite remarkable in that a tremendous increase of closely packed collagen and elastic fibers was observed. The elastic tissue had indistinct borders and appeared amorphous, whereas the collagen was well-demarcated and had its typical periodicity.

The pulmonary surface epithelium was not thickened and did not show any remarkable vesiculation. The ribosomes were clearly demonstrated by their intense staining.

Although the elastic tissue was markedly enhanced at the ultrastructural level, the orcein, aldehyde-fuchsin, and Verhoeff hematoxy-

lin preparations showed only minimal elastic fiber deposition. The collagenous elements were very delicately stained in the Koneff and Masson preparations, and did not appear markedly increased in deposition. No hypercellularity within the septal walls was noted in the Turchini and gallocyanin-chrome alum preparations.

Case XII

This patient was diagnosed as having extensive pulmonary fibrosis of unknown etiology.

The endothelium that lined the lumen of the capillary did not appear to be increased in width (Figures 36 and 37).

It was possible only to depict typical basement membranes in Figure 37. In this figure, the alveolar basement membrane was quite narrow and extremely well-delineated. It did not appear to fuse into the perivascular components. However, the alveolar basement membrane appeared to be discontinuous under the alveolar type II cell in Figure 37. It was further observed that a space resembling vacuolization was again seen (refer to Figure 32) underlying the alveolar type II cell. In other figures of this series, alveolar and capillary basement membranes could not be distinguished clearly. Only an intense fibrosis which involved both basement membranes was seen (Figures 36, 38, and 39).

Figure 36 was a low field magnification which was helpful

in determining the extent of fibrosis. The perivascular areas were labelled due to the extreme difficulty in orientation. Tremendous collagen deposition filled the perivascular spaces and mesenchymal cells were very numerous. Alveolar air spaces appeared narrowed due to the fibrosis of the surrounding structures. In Figures 38 and 39, cell types encountered in the fibrotic spaces were depicted. In Figure 38, careful attention was called to the light appearing areas in the upper and lower portions of the plate. This material was collagen with its characteristic periodicity, but it appeared very pale in comparison with the surrounding structures. The cell was probably a monocyte with a well-defined Golgi zone, mitochondria, and ribosomes. The other cellular elements in the figure were mesenchymal in origin, such as those observed in the perivascular spaces in other cases. Figure 39 depicted two other cells seen in the fibrotic areas. The cell on the right had the characteristics of a plasma cell with numerous mitochondria, a closely layered rough endoplasmic reticulum and secretion products. The cell on the left, likewise had mitochondria and a rough endoplasmic reticulum but the "layering effect" and the secretion products were lacking. The nucleus contained a very large nucleolus. The material lying between the endoplasmic reticulum borders was noted to be slightly dense and stippled in appearance. This cell type could not be definitely identified.

The pulmonary alveolar type I lining was within normal limits

in Figures 36 and 37. Scanty vesiculation was noted (Figure 37).

Tissue for histochemical and cytological studies was not available for examination in this case.

Case XIII

This child had congenital mitral stenosis with pulmonary hypertension.

The endothelial lining of the capillary lumen appeared slightly widened. There was prominent vesiculation in the cytoplasm (Figures 40, 41, and 43).

The capillary basement membrane was markedly increased in width (Figures 40, 41, and 43). The alveolar basement membranes were likewise involved (Figures 41 and 43). In Figure 42, both basement membranes were observed to merge into "pockets" of the perivascular space. In this particular figure, no gross enlargement of the basement membranes was noted.

Mesenchymal cell elements with prominent vacuolization (Figures 40 and 42), collagen and reticular fibers (Figures 41, 42, and 43) were observed in increased amounts in the perivascular space. These tissue components plus the widened basement membranes resulted in a demonstrably increased air-blood barrier.

The alveolar type I cytoplasmic extensions were increased in width and contained numerous vesicles and vacuoles (Figures 41, 42,

and 43). An alveolar type II cell with characteristic inclusion bodies had many large vacuoles throughout the cytoplasm (Figures 42 and 43). The alveolar basement membrane was extremely attenuated in this area, but no large intervening vacuolization or widening was noted between the pulmonary alveolar type II cell and the underlying perivascular space.

Significant increases of intraseptal mesenchymal cells and reticular fibers were found at the light microscopic level. The mesenchymal cell nuclei were characterized by finely stippled chromatin and two or three large nucleoli. The orcein preparations showed a normal amount of elastic tissue. Collagen fibers were minimally increased in the Koneff and Goldner preparations.

In summary, it may be said that congenital and acquired mitral stenosis and the acquired interventricular septal defect showed the most prominent basement membrane changes with or without an accompanying increase of collagen, elastic, and reticular fiber deposition. The other cases with increased pulmonary hypertension showed primary increased collagen, elastic and reticular fiber changes with no substantial increase in the basement membrane width. A functionally normal case was presented, as was a case with extensive fibrosis for a comparative study of the ultrastructural changes observed in the lung.

CHAPTER IV

DISCUSSION

The causes of pulmonary hypertension in this study can be grouped into two broad classes: 1.) mitral stenosis and left-sided heart failure of any cause leading to pulmonary congestion which results in an increased vascular resistance distal to the capillaries and 2.) congenital cardiac lesions in which there occurs an increased pulmonary blood flow or perfusate such as ventricular septal defect, in which the pulmonary circulation is exposed to left-sided pressures with small vessel disease; atrial septal defect, in which the vascular bed is exposed to high flow with resultant pulmonary arteriolar disease; and patent ductus arteriosus with vascular disease of the lung resulting from high flow and/or high pressure.

As demonstrated in this study of the ultrastructural changes in the air-blood barrier in pulmonary hypertension, the cases examined fall into two categories. That is, 1.) those cases in which the basement membranes were the primary tissue components altered with or without increased fibrous deposition, and 2.) those cases in which the alteration was due to an increased deposition of connective tissue com-

ponents, with no significant changes in the basement membranes. The first category included the cases of acquired mitral stenosis, congenital mitral stenosis, and acquired interventricular septal defect. The cases that comprised the second category were the patent ductus arteriosus, the patent ductus arteriosus with atresia of a common pulmonary vein and congenital interventricular septal defect, congenital interventricular septal defect with a left superior vena cava, aortic stenosis and congestive heart failure.

Structural changes in the pulmonary parenchyma in mitral stenosis have been described by various investigators at the light microscopic level (Parker and Weiss, 1936; Bell, 1943; Larrabee, Parker, and Edwards, 1949; Moschowitz, 1949; Meessen, 1956). Although there were various interpretations as to the tissue component within the septal wall showing the significant changes, these workers were in complete agreement on the increased width of the air-blood barrier seen in mitral stenosis. Meessen (1956), Hatt and Rouiller (1958), Schulz (1959), and Asano, (1964), in ultrastructural studies, observed increased fibrous tissue in the septal wall in patients with mitral stenosis.

In this study, the cases of mitral stenosis were primarily characterized by alveolar and capillary basement membrane thickening; this consistent change in the basement membranes being augment-

ed in most of the cases by increased collagen, reticular, and elastic fiber deposition.

With respect to the capillary basement membrane, there is almost uniform agreement by workers at the light or electron microscopic level in regard to its increased thickness in mitral stenosis (Larrabee, Parker, and Edwards, 1949; Moschcowitz, 1949; Meessen, 1956; Hatt and Rouiller, 1958; Schulz, 1959). The only exception is Asano (1964) who reported that one case out of his series did not show any thickening of the capillary basement membrane at the ultrastructural level. Larrabee, Parker, and Edwards (1949) were the only investigators to report an increased thickening of the alveolar basement membrane such as that observed in this study, but their observations were done at the light microscopic level.

These changes in the air-blood barrier lend credence to the findings of pulmonary function tests performed on patients with mitral stenosis (Palmer, Gee, Mills, and Bates, 1963). This investigatory group observed that the diffusing capacity of the pulmonary membranes was reduced in some cases of mitral stenosis. They suggest that this decreased diffusion capacity paralleled the pulmonary vascular congestion and pulmonary fibrosis seen pathologically.

It has been stated, that at birth, the elastic fibers are confined to the edges of the alveolar entrance and do not appear in the inter-alveolar septa until the age of five years or more and that elastic

fibers do not become noticeable in the walls of the alveolar portions of the lungs until the age of eighteen or more years (Loosli and Potter, 1959). In this study, eight of the thirteen patients were under eighteen years of age, and three of these eight cases were under five years of age. The functional normal control for this study was thirty nine months old and light microscopic studies indicated that elastic tissue was present but not increased. In the orcein, aldehyde-fuchsin, and Verhoeff hematoxylin slide preparations, elastic tissue was demonstrated in all the cases in which tissue for cytological work was available. At the ultrastructural level, many workers have demonstrated elastic tissue to be normally present in mammalian lung (Low, 1953, 1953a, 1954, 1961; Giesecking, 1956; Giese and Giesecking, 1957; Chase, 1959; Schulz, 1959; Takahashi, Kawano, Ota, and Otsuka, 1961; Diver-tie and Brown, 1964). Giese and Giesecking (1957) conjectured that the elementary fibrils of the reticular tissue participated in the formation of the elastic fibers since they observed a tuft-like splitting of fibrils at the borders of the elastic tissue. This fibrillary synthesis of elastic fibers could not be substantiated in this study.

It has been reported that the elastic tissue content of the lung increases with age (Briscoe and Loring, 1958; Pierce, Hocott, and Ebert, 1959, 1961; Wright, Kleinerman and Zorn, 1960). In Wright, Kleinerman, and Zorn's study (1960), they observed that although the elastic content of lung increased with age, the hexosamine content of the elastic

fraction decreased with advanced age. In Case XI, a sixty nine year old female, there was an obvious increase of elastic tissue in the septal wall at the electron microscopic level. However, the light microscopic studies for elastin were not indicative of a pronounced elastic tissue. This lack of correlation could possibly be explained by a decreased staining propensity of the elastic fibers since the elastic tissue appeared smudgy in many areas of the electron microscopical and cytological preparations. It was however, noteworthy that the elastic tissue "stained" quite intensely at the ultrastructural level. The intensity of "staining" of elastic tissue seen in electron micrographs of Case VI was not noted in any of the other cases stained with lead citrate and uranyl acetate, and this finding is suggestive of an altered state of the elastic tissue in this particular case of congestive heart failure. The finding of increased elastic tissue in this patient with chronic passive congestion is in agreement with Giesecking (1960) who studied the ultrastructural changes in lungs in chronic passive congestion and observed increased elastic and reticular tissue, as well as, increased mesenchymal cells within the perivascular space.

In Case IV, patent ductus arteriosus, atresia of a left common pulmonary vein and interventricular septal defect, a definite increase of elastic fibers was observed at the light and electron microscopic levels. The other cases involving congenital heart defects did not show the marked elastic fiber increase that was evident in Case IV.

This difference between these cases could be explained by two physiological mechanisms. The patent ductus arteriosus lesion, in which there is a communication between the high resistance greater circulation and the low resistance pulmonary system, would produce an increased pulmonary blood flow or perfusate ultimately resulting in pulmonary hypertension. Secondly, the atretic pulmonary vein, by causing passive congestion in the lungs, would enhance the already severe condition caused by the patent ductus arteriosus. These two factors are felt to explain the tremendous fibro-cellular changes in the septal wall causing a severe embarrassment of oxygen diffusion in Case IV.

The increased fibro-cellular deposition seen in the congenital cardiac lesions (excluding Cases I, V, and XII) would substantiate the pulmonary function findings on patients with increased pulmonary blood flow (Bucci and Cook, 1961). They demonstrated a decreased diffusing capacity of the pulmonary membrane in twenty four patients and suggested that the changes observed indicated an alteration of the volume surface area ratio and/or an increased thickness of the pulmonary capillary membrane.

Collagen fibers were considered to be scarce (Miller, 1923; Policard, 1942) in the normal alveolar wall. Some investigators (Müller, 1929; Mollendorff, 1942; Policard, 1949) quoted by Bertalanffy (1964), have stated that collagenous fibers do not occur at all in the alveolar walls. Hesse and Loosli (1949), and Loosli, Adams, and

Thornton (1949), in light microscopic studies, observed that collagen fibers did constitute a normal component in the septal wall. This has been verified by numerous electron microscopic investigations (Low, 1953, 1953a, 1953b, 1954, 1961; Karrer, 1956; van Breemen and Neustein, 1956; Baker, 1959; Takahashi, Kawano, Ota, and Otsuka, 1961; Divertie and Brown, 1964; Nagaishi, Okada, Ishito, and Daido, 1964; van Breemen, 1965). At the ultrastructural level, Schulz (1959) referred to the fibrous element present in normal and pathological lung as reticular fibers even though in many of his plates, the characteristic appearance of collagen can be determined. He further agreed with Giese and Giesecking (1957) that the reticular fibers of the pulmonary stroma were not pre-collagen, since no maturation to collagen fibers were observed in the septa.

It has been widely agreed that reticular fibers constitute the main fibrous component of the septal wall (Miller, 1923; Josselyn, 1935; Policard, 1942, 1949; Leblond and Bertalanffy, 1951; Bertalanffy, Glegg, and Eidinger, 1954; Low, 1954; Giese and Giesecking, 1957; Schulz, 1959; Gross, 1961). However, most investigators have found the reticular fibers to be generally associated with collagen fibers, differing morphologically primarily by their smaller diameter and their greater tendency to form a network (Copenhaver, 1964).

In this study, the functional control of pulmonary stenosis was the only case which did not show a marked increase in collagen

and/or reticular fibers. Prominent collagen deposition was seen in Cases IV, VII, and XI. Case VII was a lesion of acquired mitral stenosis of long duration which had resulted in congestive heart failure. Physiologically, this patient would have had increased vascular resistance in the pulmonary circuit and chronic passive congestion of the lungs. Case XI was also in congestive heart failure which likewise had resulted in chronic passive congestion of the lung. Collagen fibers (Case VII), and collagen and elastic fibers (Case XI) were responsible for the increased air-blood barrier. These findings are supported by those of Gieseck (1960), who observed a four to ten-fold increase in width was attributed to an increase in reticular and elastic fibers and mesenchymal cells within the perivascular space.

Increased vascular resistance, resulting from the atresia of a left common pulmonary vein, plus an increased pulmonary artery flow from a patent ductus arteriosus, were physiologically present in Case IV. Both of these hemodynamic alterations would have been conducive to the remarkable increase of fibrous deposition observed in the air-blood barrier.

Unlike elastic tissue, collagen has been reported not to increase with age (Pierce, Hocott, and Ebert, 1959, 1961; Wright, Kleinerman, and Zorn, 1960). However, other investigators, using colorimetric determinations, have reported that hydroxyproline, thus the collagen content of the lung, increased with age (Briscoe and Loring,

1959; Briscoe, Loring, and McClement, 1959).

It has been reported and verified in this study that the alveolar lining of the lung consists of two types of cells (Karrer, 1956a, 1960; Kisch, 1957, 1960a; Policard, Collet, and Martin, 1961; Campiche, Gautier, Hernandez, and Reymond, 1963; Balis and Conen, 1964; Nagai-shi, Okada, Ishiko, and Daido, 1964). The majority of ultrastructural investigators have indicated that the alveolar epithelium is of endodermal origin (Low and Sampaio, 1957; Campiche, Gautier, Hernandez, and Reymond, 1963; Balis and Conen, 1964) in contrast to Policard, Collet, and Pregermain (1957), who believe both cell types are of mesenchymal origin and to Marinozzi (1960), who claims that only the alveolar type II cell is mesenchymal in origin. Further controversy has been particularly directed to the function of the alveolar type II cell. There is evidence that the characteristic inclusion bodies (also referred to as "typical" inclusion bodies (Karrer, 1956a); osmiophilic bodies (Policard, Collet, and Pregermain, 1957); "characteristic" inclusion bodies (Woodside and Dalton, 1958); lamellar transformed mitochondria (Schulz, 1959); lamellar inclusions (Campiche, Gautier, Hernandez, and Reymond, 1963) of the alveolar type II cell are the source of the surface tension reducing substance or surfactant (Macklin, 1954; Pattle, 1955, 1963; Clements, 1957, 1962; Klaus, Reiss, Tooley, Piel and Clements, 1962). This surfactant is probably a lipoprotein that contains a phospholipid, palmityl lecithin (Klaus, Clements, and Havel, 1961; Pattle and Thomas,

1961; Bolande, 1964) and is thought to be an important stabilizing factor in pulmonary mechanics (Pattle, 1955; Clements, 1957; Clements, Brown, and Johnson, 1958). Chase (1959) using special techniques, has demonstrated a surface lining layer at the electron microscopic level.

In this study, osmiophilic inclusion bodies and microvilli are associated with both the alveolar type II cell and the free alveolar macrophage. Because of this marked morphological similarity, it is tempting to suggest that the free alveolar macrophage is derived from the alveolar type II cell. The alveolar type II cells were also often noted to have vacuolization which separated the cell from the underlying connective tissue elements. The alveolar basement membrane appeared quite attenuated in these areas, but a definite rupture was never observed. This observation is in disagreement with Marinozzi's (1960) observations in which he claimed the supporting basement membrane to be discontinuous under the alveolar type II cell.

In the lungs of newborn infants, Balis and Conen (1964) described a similar vacuolization in their ultrastructural observations and referred to it as separations by rows of vesicles or cisternae which they believed were indicative of degenerative type II cells. They concluded that the inclusion bodies within the alveolar type II cells were lysosomal structures which were active in the transformation of the fetal cuboidal alveolar epithelium into the attenuated (alveolar type

I) form. Their embryological conclusions can not be evaluated in this morphologic study.

Palade (1956) and Moore and Ruska (1957) reported numerous small vesicles in contact with the endothelial cell membrane in the blood capillaries of normal rat myocardium. Palade (1956) suggested that the vesicles either developed by a pinocytotic mechanism or that they arose within the endothelial cytoplasm and then attached to the cell membrane. It has been suggested by Bennett (1956) that this vesiculation process enables ions and larger particles to pass through the cells without actual disruption of the cell membrane. This process of invagination and pinching off of the plasma membrane to form small vesicles which move across the cytoplasm has been termed cytopempsis (Moore and Ruska, 1957). Moreover, these investigators suggested that the cytopemptic process constituted a means of active and selective transmission of substances within the capillary walls.

The vesiculation of the epithelial and endothelial cells has been observed in mammalian lung by Schulz (1959). He stated that the vesicles were of importance in cell metabolism. De Groodt, Lagasse, and Sebruyens (1958), studying the normal septal wall in various mammals, reported membrane infolding and vesicle formation and noted that some of the vesicles were in contact with the alveolar basement membrane. Leeson and Leeson (1964) suggested that the micropinocytotic vesicles in epithelial and endothelial cytoplasm of fetal rat lung indicated absorp-

tion of amniotic fluid from the alveolar space. They wondered if the number of micropinocytotic vesicles would be increased in pathological conditions where fluid was present in excess in air passages, e. g., pulmonary hypertension and inflammation.

In this study, vesiculation was noted in both the capillary endothelium and the alveolar epithelium in all cases, however, the vesicles appeared to be more abundant in the endothelial lining than in that of the epithelial lining. Although vesiculation in Case I, the functional control, appeared decreased, it was felt that this was due to the decrease in the width of the air-blood barrier and not to an actual decrease in the number of vesicles. It would appear that the smaller vesicles are found in both normal and pathologic lung. Schulz (1959) has suggested that the criterion of a pathological change is the size of the vesicle. The larger vacuoles seen in both the endothelium and epithelium of Cases II, IV, V, and VIII, would be indicative of a pathological state. The vacuolization in Case VII was obviously due to the fat embolism. The patient with congenital mitral stenosis showed the large vacuolar changes only in the mesenchymal derivatives and the alveolar epithelial lining. In Case IX, the vacuoles were noted only in the endothelial lining investment. If it is assumed that the pinocytotic vacuoles are for resorptive and transportive processes (Schulz, 1959), then the above cases would have exhibited conditions in which these two processes were increased. It is interesting to note that the most extensive changes were seen in

cases of congenital heart lesions. At the ultrastructural level, it is possible to separate the pinocytotic vacuoles from the smaller vesicles which are described under "cytopempsis". It should be indicated that further investigations would be necessary to elucidate the different functions, if any, between the two processes.

In regard to the lymphatics of the pulmonary tissue, it has been classically thought that they did not extend below the respiratory bronchioles. Yet, physiologists recognized that particulate matter in the peripheral alveoli somehow was delivered back to the hilar nodes more rapidly than could be explained by simple phagocytosis and amoeboid transport of the matter toward the lymphatic vessels (Drinker, 1954; Krahl, 1964).

Only a few investigators have demonstrated lymphatics at the level of the alveoli (Rouviere, 1938; Tobin, 1954, 1959; Parfenova, 1960; Engel, 1962). Engel (1962) reported that he saw lymphatic vessels within the septal wall, but his low magnification pictures were not convincing. Parfenova (1960), using injection methods, also claimed that she observed lymphatic capillaries in the alveolar wall. She felt that the lymphatic capillaries participated with the pulmonary blood capillaries in the exchange of gas. Tobin (1954), using India ink and latex injection methods, plastic injected corrosion and air-dried specimens, and pathological and histological specimens, demonstrated lymphatics accompanying the smaller branches of the pulmonary artery

and the pulmonary veins. These vascular tributaries were closely related to the alveolar wall, so that the distance from an alveolus to a lymphatic vessel would be quite small. Rouviere (1938) also stated that lymphatics rested directly against the alveolar bed and although no lymphatics were seen in the interalveolar partitions, one part of the alveolar wall was immediately adjacent to the lymphatic spaces.

In Figure 27, a cell, markedly resembling the endothelial cell lining the capillary, appears to invest the perivascular space. This might indicate that the perivascular space represents a terminal lymphatic ramification in the alveolar walls. It is conjectured that the presence of collagen and elastic fibers within the perivascular space may be present to maintain the patency of these channels in the presence of increased pressure gradients at the alveolar-capillary level.

Excluding Cases I and X, there was an increased cellular component, referred to as mesenchymal cells, in the perivascular spaces of all other cases. This was observed ultrastructurally and the empirical and histochemical techniques greatly augmented these findings except in Case XI. This increase in mesenchymal cells has also been observed in other pathological pulmonary studies (Hatt and Rouiller, 1958; Giesecking, 1960). It would appear that the cellular increase correlated with the increased amount of collagen and reticular fibers

present within the perivascular space. The study of aortic stenosis was quite remarkable at the electron microscopic level, in that fibroblastic-like cells and leucocytes were very abundant within the septal wall. These findings correlated well with the light microscopic studies done on this tissue. The lack of a really demonstrable increase of cells in Case X is probably due to the short duration of this patient's disability. The lack of increased cellularity in the functional control (Case I) is in agreement with other normal lung studies (Gieseck, 1960; Divertie and Brown, 1964).

This study, utilizing electron microscopical, histochemical, and cytological techniques, definitely indicate that pulmonary hypertension is associated with a thickening of the alveolar-capillary membrane in congenital heart disease, originally associated with increased pulmonary flow, and in acquired heart disease. Those lesions associated with acquired heart disease all exhibited basement membrane changes with varying fibro-cellular manifestations. The majority of congenital heart lesions did not show appreciable basement membrane thickening, but did show markedly increased fibro-cellular changes in the alveolar capillary (septal) wall. It is felt that the morphological changes in the alveolar-capillary wall, which are present in these cases, would provide anatomic evidence of a decreased diffusing capacity manifested functionally by these patients.

CHAPTER V

SUMMARY

Congenital and acquired heart disease with pulmonary hypertension show an increased thickening of the alveolar-capillary wall.

The cases of mitral stenosis (acquired and congenital) exhibit prominent changes in alveolar and capillary basement membranes, with or without increased fibro-cellular deposition. The case of acquired interventricular septal defect (Case X) showed the same morphological changes.

The congenital heart disease cases did not show appreciable thickening of the basement membranes, but were characterized by an increased deposition of collagen and/or reticular fibers, elastic fibers, and mesenchymal cells. Cases XI and XII were both characterized by these same morphological changes.

In this study, there is no apparent correlation between the severity of thickening of the alveolar wall with the duration of symptoms or to the age of the individual.

It is suggested that the perivascular spaces may function as terminal lymphatic spaces in the alveolar walls.

The congenital heart disease cases were characterized by large pinocytotic vacuolization which has been reported to be indicative of pathological changes.

Regarding the concept of cytopempsis, there was no demonstrable increase of small vesicles in these cases with pulmonary hypertension.

It is suggested that the morphological changes seen in the alveolar-capillary membrane would provide anatomic evidence for the decreased functional capacity of patients with pulmonary hypertension.

BIBLIOGRAPHY

- Asano, H. 1964 Pathohistological and electron microscopic studies of the lung in mitral stenosis with special reference to the correlation between morphological changes and cardiopulmonary dynamics. *Jap. Circulation J.* 28: 801-816.
- Baker, R. F. 1959 Morphology of the human alveolar wall. *J. Appl. Physiol.* 30: 2038.
- Barka, T. and Anderson, P. J. 1963 Histochemistry. Theory, Practice and Bibliography, Hoeber Medical Division, Harper and Row Publishers, Inc., New York.
- Bell, E. T. 1943 Hyperplasia of pulmonary alveolar epithelium in disease. *Am. J. Path.* 19: 901-911.
- Bennett, H. 1956 The concepts of membrane flow and membrane vesiculation as mechanisms for active transport and ion pumping. *J. Biophys. Biochem. Cytol.* 2 (supplement): 99-105.
- Bertalanffy, F. D. 1964 Respiratory tissue: Structure, Histophysiology and Cytodynamics. Part I. Review and Basic Cytomorphology. *International Review of Cytology* 16: 233-328.
- Bertalanffy, F. D., Glegg, R. E., and Eiding, D. 1954 Chemical confirmation of the abundance of reticulin in the lung. *Canad. Med. Ass. J.* 70: 196-197.
- Bolande, R. P. 1964 The morphologic demonstration of an alveolar lining layer and its relationship to pulmonary surfactant. *Am. J. Path.* 45: 449-463.
- Balis, J. U. and Conen, P. E. 1964 The role of alveolar inclusion bodies in developing lung. *Lab. Invest.* 13: 1215-1229.
- Briscoe, A. M. and Loring, W. E. 1958 Elastin content of the human lung. *Proc. Soc. Exp. Biol. Med.* 99: 162-164.

- Briscoe, A. M. and Loring, W. E. 1959 Hydroxyproline content of human lung and of lung collagen. *Fed. Proc.* 18: 470.
- Briscoe, A. M., Loring, W. E., and McClement, J. H. 1959 Changes in human lung collagen and lipids with age. *Proc. Soc. Exp. Biol. Med.* 102: 71-74.
- Bucci, G. and Cook, C. D. 1961 Studies of respiratory physiology in children. VI. Lung diffusing capacity, diffusing capacity of the pulmonary membrane and pulmonary capillary blood volume in congenital heart disease. *J. Clin. Invest.* 40: 1431.
- Burstone, M. S. 1962 Enzyme Histochemistry and Its Application in the Study of Neoplasms. Academic Press, New York.
- Callahan, W. P. and Horner, J. A. 1964 The use of vanadium as a stain for electron microscopy. *J. Cell Biol.* 20: 350.
- Campiche, M. A., Gautier, A., Hernandez, E. I., and Reymond, A. 1963 An electron microscopic study of the fetal development of human lung. *Pediatrics* 32: 976-994.
- Chase, W. H. 1959 Distribution and fine structure of elastic fibers in mouse lung. *Exp. Cell Research* 17: 121-130.
- Chase, W. H. 1959a The surface membrane of pulmonary alveolar walls. *Exp. Cell Research* 18: 15-28.
- Clements, J. A. 1957 Surface tension of lung extracts. *Proc. Soc. Exp. Biol. Med.* 95: 170-172.
- Clements, J. A. 1962 Surface tension in the lungs. *Sci. Amer.* 207: 120-130.
- Clements, J. A., Brown, E. S., and Johnson, R. P. 1958 Pulmonary surface tension and the mucus lining of the lungs: Some theoretical considerations. *J. Appl. Physiol.* 12: 262-268.
- Copenhaver, W. M. 1964 Bailey's Textbook of Histology. Fifteenth edition, Williams and Wilkins Co., Baltimore.
- Dahlqvist, A. and Brun, A. 1962 A method for the histochemical demonstration of disaccharidase activities. Application to invertase and trehalase in some animal tissues. *Jour. Histo. Cyto. Chem.* 10: 294-302.

- de Groot, M., Lagasse, A., and Sebruyns, M. 1958 Fine structure of the alveolar wall of the lung. *Nature (London)* 181: 1066-1067.
- Divertie, M. B. and Brown, A. L. 1964 The fine structure of the normal human alveolocapillary membrane. *J. A. M. A.* 187: 938-941.
- Drinker, C. K. 1954 The Clinical Physiology of the Lungs. Charles Thomas Co., Springfield.
- Engel, S. 1962 Lung Structure. Charles Thomas Co., Springfield.
- Freeman, J. A. 1963 Technical modifications in Maraglas embedding. *J. Cell Biol.* 17: 203-207.
- Giese, W. and Giesecking, R. 1957 Die submikroskopische struktur des fibrillaren Grundgerustes der Alveolarwand. *Beitr. path. Anat.* 117: 17-31.
- Giesecking, R. 1956 Elektronenoptische Beobachtungen im alveolarberisch der Lunge. *Beitr. path. Anat.* 116: 177-199.
- Giesecking, R. 1960 Elektronenoptische Befunde an chronischen Stauungslungen. *Beitr. path. Anat.* 123: 333-382.
- Goldner, J. 1938 A modification of the Masson trichrome technique for routine laboratory purposes. *Am. J. Path.* 14: 237-244.
- Gomori, G. 1937 Silver impregnation of reticulum in paraffin sections. *Am. J. Path.* 13: 993-1001.
- Gomori, G. 1939 Studies on the cells of the pancreatic islets. *Anat. Rec.* 74: 439-460.
- Gomori, G. 1950 Aldehyde-fuchsin: A new stain for elastic tissue. *Am. J. Path.* 20: 665-666.
- Gridley, M. F. 1960 Manual of Histologic and Special Staining Techniques. Second edition, McGraw-Hill Book Co., Inc., New York.
- Gross, P. 1961 Morphology of pulmonary alveolar reticulin tissue. *Arch. Path.* 72: 438-445.

- Hatt, P. Y. and Rouiller, C. 1958 Les ultrastructures pulmonaires et le regime de la petite circulation I. Au cours du retrecissement mitral serre. *Sem. Hop., Path. Biol.* 34: 1371-1397.
- Hesse, F. E. and Loosli, C. G. 1949 The lining of the alveoli in mice, rats, dogs, and frogs following acute pulmonary edema produced by poisoning. *Anat. Rec.* 105: 299-324.
- Itagi, K. 1955 Electron microscopic observation of pulmonary alveolar structures. *Acta tuberc. jap.* 5: 35-52.
- Josselyn, L. E. 1935 The nature of the pulmonary alveolar lining. *Anat. Rec.* 62: 147-171.
- Karrer, H. E. 1956 An electron microscopic study of the fine structure of pulmonary capillaries and alveoli of the mouse. *Bull. Johns Hopk. Hosp.* 98: 65-83.
- Karrer, H. E. 1956a The ultrastructure of mouse lung. General architecture of capillary and alveolar walls. *J. Biophy. Biochem. Cytol.* 2: 241-252.
- Karrer, H. E. 1956b The ultrastructure of mouse lung. Some remarks regarding the fine structure of the alveolar basement membrane. *J. Biophy. Biochem. Cytol.* 2 (supplement): 287-292.
- Karrer, H. E. 1958 The ultrastructure of mouse lung: The alveolar macrophage. *J. Biophy. Biochem. Cytol.* 4: 693-700.
- Karrer, H. E. 1960 Electron microscopic study of the phagocytosis process in lung. *J. Biophy. Biochem. Cytol.* 7: 357-366.
- Kelly, J. W. 1964 Personal communication.
- Kisch, B. 1957 Electron microscopic investigations of lungs. II. Specific cells and other cells with osmiophilic enclosures. *Exp. Med. Surg.* 15: 101-118.
- Kisch, B. 1960 A quantitative method to produce pneumonia for electron microscopic research. *Exptl. Med. Surg.* 18: 243-248.
- Kisch, B. 1960a Electron microscopy of the lungs in acute pneumonia. *Exptl. Med. Surg.* 18: 273-296.

- Klaus, M. H., Clements, J. A., and Havel, R. J. 1961 Composition of surface-active material isolated from beef lung. *Proc. Nat. Acad. Sci.* 47: 1858-1859.
- Klaus, M. H., Reiss, O. K., Tooley, W. H., Piel, C., and Clements, J. A. 1962 Alveolar epithelial cell mitochondria as source of the surface-active lung lining. *Science* 137: 750-751.
- Koneff, A. A. 1936 An iron-hematoxylin-aniline blue staining method for routine use. *Anat. Rec.* 66: 176-177.
- Krahl, V. E. 1964 Anatomy of Mammalian Lung. In Handbook of Physiology, Volume 1, Section 3, Respiration, pp. 213-284.
- Larrabee, W. F., Parker, R. L., and Edwards, J. E. 1949 Pathology of the intrapulmonary arteries and arterioles in mitral stenosis. *Proc. Staff Meet., Mayo Clin.* 24: 316-326.
- Leblond, C. P. and Bertalanffy, F. D. 1951 Reticulin membranes of the framework of the alveolar lung tissue in the albino rat. *J. Canad. Med. Ass.* 65: 263-264.
- Leeson, T. S. and Leeson, C. R. 1964 A light and electron microscope study of developing respiratory tissue in the rat. *J. of Anat.* 98: 183-193.
- Lhotka, J. F. 1952 Histochemical use of lead tetra-acetate I. Cleavage of 1-2 glycols. *Stain Tech.* 27: 213-216.
- Lhotka, J. F. and Myhre, B. A. 1953 Periodic-acid-Foot stain for connective tissue. *Stain Tech.* 28: 129-133.
- Loosli, C. G., Adams, W. E., and Thronton, T. M. 1949 The histology of the dog's lung following experimental collapse. *Anat. Rec.* 105: 697-721.
- Loosli, C. G. and Potter, E. L. 1959 Pre- and postnatal development of the respiratory portion of the human lung with special reference to the elastic fibers. *Am. Rev. Resp. Dis.* 80: 5-23.
- Low, F. N. 1953 The pulmonary epithelium of laboratory mammals. *Anat. Rec.* 115: 343.
- Low, F. N. 1953a The pulmonary alveolar epithelium of laboratory mammals and man. *Anat. Rec.* 117: 241-264.

- Low, F. N. 1954 Ultrastructure of the pulmonary alveolar wall. Anat. Rec. 118: 429-430.
- Low, F. N. 1961 The extracellular portion of the human blood-air barrier and its relation to tissue space. Anat. Rec. 139: 105.
- Low, F. N. and Daniels, C. W. 1952 Electron microscopy of the rat lung. Anat. Rec. 113: 437-449.
- Low, F. N. and Sampaio, M. M. 1957 The pulmonary alveolar epithelium as an entodermal derivative. Anat. Rec. 127: 51-64.
- Luft, J. H. 1961 Improvements in epoxy resin embedding methods. J. Biophys. Biochem. Cytol. 9: 409-414.
- Macklin, C. C. 1954 The pulmonary alveolar mucoid film and the pneumocytes. Lancet 266: 1099.
- Mallory, F. B. 1942 Pathological Technique, W. B. Saunders and Co., Philadelphia.
- Marinozzi, V. 1958 La structure de l'alveole pulmonaire etudiee au moyen de l'impregnation a l'argent. Verh. 4 ten Internat. Kongr. Elektronenmikr., Berlin, Vol. 2, Springer-Verlag, Berlin.
- Masson, P. J. 1929 Some histological methods. Trichrome staining and their preliminary technique. J. Tech. Meth. and Bull. Int. Assn. Med. Mus. 12: 75-90.
- Meessen, H. 1956 Die Lunge bei Mitralstenose. Dtsch. med. Wschr. 81 (Part 2): 1445-1448, 1465-1466.
- Miller, W. S. 1923 A study of the factors underlying the formation of alveolar pores in pneumonia. J. Expt. Med. 38: 707-713.
- Millonig, G. 1961 A modified procedure for lead staining of thin sections. J. Cell Biol. 11: 736-739.
- ¹¹Mollendorff, W. 1942 Z. Anat. Entwicklungsgeschichte. 111: 224-245. quoted by Bertalanffy. (original article not available)

- Moore, D. H. and Ruska, H. J. 1957 The fine structure of capillaries and small arteries. *J. Biophys. Biochem. Cytol.* 3: 457-462.
- Moschcowitz, E. 1949 The association of capillary sclerosis with arteriosclerosis and phlebosclerosis; its pathogenesis and clinical significance. *Ann. Internal Med.* 30: 1156-1179,
- "
Muller, L. 1929 *Beitr. Pathol. Anat. Allgem. Pathol.* 82: 57-91. quoted by Bertalanffy. (original article not available)
- Nagaishi, C., Okada, Y., Ishiko, S., and Daido, S. 1964 Electron microscopic observations of the pulmonary alveoli. *Exp. Med. and Surg.* 22: 81-117.
- Palade, G. E. 1956 The endoplasmic reticulum. *J. Biophys. Biochem. Cytol.* 2 (supplement 4): 85-98.
- Palmer, W. H., Gee, J. B. L., Mills, F. C., and Bates, D. V. 1963 Disturbances of pulmonary function in mitral valve disease. *Canad. Med. Ass. J.* 89: 744-750.
- Parker, F., Jr. and Weiss, S. 1936 The nature and significance of the structural changes in the lungs in mitral stenosis. *Am. J. Path.* 12: 573-598.
- Pattle, R. E. 1955 Properties, function and origin of the alveolar lining layer. *Nature* 175: 1125-1126.
- Pattle, R. E. 1963 The lining layer of the lung alveoli. *Brit. Med. Bull.* 19: 41-44.
- Pattle, R. E. and Thomas, L. C. 1961 Lipoprotein composition of the film lining the lung. *Nature* 189: 844.
- Pearse, A. G. E. 1960 Histochemistry: Theoretical and Applied. Second edition, Little Brown and Co., Boston.
- Pease, D. C. 1964 Histological Techniques for Electron Microscopy. Second edition, Academic Press, New York.
- Pierce, J. A., Hocott, J. B., and Ebert, R. V. 1959 Studies of lung collagen and elastin. *Am. Rev. Resp. Dis.* 80 (supplement): 45-50.

- Pierce, J. A., Hocott, J. B., and Ebert, R. V. 1961 The collagen and elastin content of the lung in emphysema. *Ann. Internal Med.* 55: 210-222.
- Pinkus, H. 1944 Acid orcein Giemsa stain (modification of Unna-Taenzer method). A useful routine stain for dermatologic sections. *Arch. Derm. and Syph.* 49: 355.
- Policard, A. 1942 La couche liquide de recouvrement des alveoles. Considerations histophysiologiques sur quelques mecanismes pulmonaires. *Bull. Histol. Appl. Physiol. Pathol. Tech. Microscop.* 19: 15-26.
- Policard, A. 1949 *J. Franc. Med. Chir. Thorac.* 3: 38-47. quoted by Bertalanffy. (original article not available)
- Policard, A. 1961 Sur l'importance des modifications inframicroscopiques de la paroi alveolaire en pathologic pulmonaire. *Presse Med.* 69: 2589-2592.
- Policard, A., Collet, A., and Pregermain, S. 1957 Structures alveolaires normales du poumon examinees au microscope electronique. *Ann. Rech. Med. Semaine Hop.* 331: 385-398.
- Reynolds, E. S. 1963 The use of lead citrate at high pH as an electron opaque stain in electron microscopy. *J. Cell Biol.* 17: 208-211.
- Rouviere, H. 1938 Anatomy of the Human Lymphatic System. Translated by M. J. Tobias, Edward Brothers, Inc., Ann Arbor.
- Rusnyak, I., Foldi, M., and Szabo, G. 1960 Lymphatics and Lymph Circulation. Physiology and Pathology. First English edition, Pergamon Press, The Macmillian Co., New York.
- Schiebler, T. H. and Schiessler, S. 1959 Über den Nachweis von Insulin mit den Metachromatisch Reagierenden Pseudoisocyanien. *Histochemie* 1: 445-465.
- Schulz, H. 1956 Elektronenoptische untersuchungen der normalen lunge normalen lunge und der lunge bei mitralstenose. *Virchow's Arch. path. anat.* 328: 582-604.
- Schulz, H. 1959 The Submicroscopic Anatomy and Pathology of the Lung. Springer-Verlag, Berlin, pp. 1-199.

- Schulz, H. 1962 Some remarks on the submicroscopic anatomy and pathology of the blood-air pathway in the lung. In: Ciba Foundation Symposium on Pulmonary Structure and Function, Little, Brown and Co., Boston, pp. 205-214.
- Takahashi, K., Kawano, A., Ota, O., and Otsuka, S. 1961 Electron microscopic studies on the lung tissue. *Tokushima J. Exp. Med.* 8: 149-155.
- Tobin, C. E. 1959 Lymphatics of the pulmonary alveoli. *Anat. Rec.* 120: 625-635.
- Tobin, C. E. 1959 Pulmonary lymphatics with reference to emphysema. *Am. Rev. Resp. Dis.* 80: 50-57.
- van Breeman, V. L. 1965 Electron microscopy in clinical medicine. *Norelco Reporter XI*, No. 2, pp. 51-54, 61.
- van Breeman, V. L. and Neustein, H. B. 1956 Electron microscopic studies from guinea pigs and premature infants. *Anat. Rec.* 124: 472-473.
- Verhoeff, F. H. 1908 Some new staining methods of wide applicability; including a rapid differential stain for elastic tissue. *J. A. M. A.* 50: 876-877.
- Watson, J. H. L. and Valentine, V. 1959 Observations on ultra-thin sections of dog lung by methods of electron microscopy. *Henry Ford Hosp. Med. Bull.* 7: 161-173.
- Watson, M. L. 1958 Staining of tissue sections for electron microscopy with heavy metals. II. Applications of solutions containing lead and barium. *J. Biophys. Biochem. Cytol.* 4: 727-731.
- Watson, M. L. 1958a Staining of tissue sections for electron microscopy with heavy metals. *J. Biophys. Biochem. Cytol.* 4: 475-478.
- Woodside, G. L. and Dalton, A. J. 1958 The ultrastructure of lung tissue from newborn and embryo mice. *J. Ultrastr. Res.* 2: 28-54.
- Wright, G. W., Kleinerman, J. K., and Zorn, E. M. 1960 The elastin and collagen content of normal and emphysematous human lungs. *Am. Rev. Resp. Dis.* 81: 938.

APPENDICES

EMPIRICAL METHODS

Cytological Techniques

Hematoxylin and eosin (Mallory, 1942)

Koneff's iron hematoxylin-aniline blue stain (Koneff, 1936)

Collagen Fibers

Goldner's trichrome stain (Goldner, 1938)

Mallory's triple stain for connective tissue (Mallory, 1942)

Mallory-Heidenhain azocarmine method for connective tissue (Gomori, 1939)

Masson's connective tissue stain (Masson, 1929)

Masson's connective tissue stain - AFIP modification (Gridley, 1960)

Van Giesen's connective tissue stain (Mallory, 1942)

Elastic Fibers

Gomori's aldehyde-fuchsin stain for elastic fibers (Gomori, 1950)

Orcein elastic tissue stain (Pinkus, 1944)

Verhoeff's hematoxylin for elastic tissue (Verhoeff, 1908)

Reticular Fibers

Gomori's reticulum stain (Gomori, 1937)

Periodic acid-Foot reticulum stain (Lhotka and Myhre, 1953)

HISTOCHEMICAL METHODS

Proteins

Amino Groups

Chloramine T-Schiff (Chu et al., 1953) (Barka, 1963)

Phenol Groups (Tyrosine)

Diazocoupling reaction (Glenner and Lillie, 1959) (Barka, 1963)

Indole Derivatives (Tryptophan)

Post-coupled p-dimethylaminobenzaldehyde (Glenner and Lillie, 1957)
(Barka, 1963)

Guanidyl Groups (Arginine)

Sakaguchi (Sakaguchi, 1950) (Barka, 1963)

Sulfhydryl and Disulfide Groups

Mercury orange (Bennet and Watts, 1958) (Barka, 1963)

Pseudoisocyanin (Schiebler and Schiessler, 1959)

Histones and Protamines

Alkaline fast green (Alfert and Geschwind, 1953) (Kelly, 1964)

Nucleoproteins

Deoxyribosenucleic Acid

Feulgen (Feulgen and Rossenbeck, 1924) (Barka, 1963)

Ribose and Deoxyribosenucleic Acids

Methyl green-pyronine (Pappenheim, 1899) (Kelly, 1964)

Gallocyanin-chrome alum (Einarson, 1951) (Barka, 1963)

Modified Turchini (Blackler and Alexander, 1952) (Pearse, 1960)

Carbohydrates

Glycogen

Best's carmine (Best, 1906) (Pearse, 1960)

Mucoproteins and Neutral Polysaccharides

Periodic acid-Schiff (McManus, 1948) (Pearse, 1960)

Lead tetra-acetate (Lhotka, 1952)

Acid Polysaccharides

Alcian blue (Wagner and Shapira, 1957) (Barka, 1963)

Astrablau (Kelly, 1964)

Hale's colloidal iron (Hale, 1946) (Barka, 1963)

Toluidine blue (Kelly, 1964)

Lipids

Neutral Fats

Oil red-O (Lillie, 1944) (Pearse, 1960)

Sudan black B (Kelly, 1964)

Phospholipids

Acid hematein method (Baker, 1946) (Barka, 1963)

"
Klüver-Barrera copper phthalocyanine (Klüver and Barrera, 1953)

(Kelly, 1964)

Acetalphosphatides

Plasmal reaction (Hayes, 1949) (Barka, 1963)

Cholesterol

Digitonin reaction (Brunswik, 1922) (Barka, 1963)

Neutral and Acidic Lipids

Nile blue sulfate (Lorrain and Smith, 1908) (Kelly, 1964)

Enzymes

Phosphatases

Alkaline phosphatase (Burstone, 1962)

Acid phosphatase (Burstone, 1962)

Adenosine triphosphatase (Burstone, 1962)

Esterases

Non-specific esterase (Burstone, 1962)

Dehydrogenases

Succinic dehydrogenase (Barka, 1963)

Diaphorases

Diphosphopyridine nucleotide reductase (Burstone, 1962)

Triphosphopyridine nucleotide reductase (Burstone, 1962)

Other Enzymes

Beta-glucuronidase (Burstone, 1962)

Beta-galactosidase (Burstone, 1962)

Carbonic anhydrase (Hausler, 1958) (Pearse, 1960)

Invertase (Dahlqvist and Brun, 1962)

Cations

Dithizone method for zinc (Mager et al., 1953) (Pearse, 1960)

Rubeanic acid method for copper (Okamoto, 1938; Uzman, 1956) (Pearse, 1960)

Pigments

Glenner's method for bilirubin, lipofuscin, and hemosiderin (Glenner, 1957) (Barka, 1962)

Perl's Prussian blue reaction (Perls, 1867) (Barka, 1963)

Figure 1

Case I, pulmonary stenosis. The figure shows the essentially normal air-blood barrier of the functional control. The pulmonary surface lining (al) and alveolar basement membrane (ab) are quite thin. The capillary endothelium (E) and the capillary basement membrane (cb), though not thickened, are thicker than the preceding two alveolar components. The perivascular space (p) is quite narrow and shows a few strands of reticular fibrils (r).

(Reynold's lead citrate and uranyl acetate, 17,200X)



Figure 1

Figure 2

Case I, pulmonary stenosis. This is a section through the septal wall between two capillaries with alveolar spaces (A) on each side. One of the alveolar spaces, which is lined by the thin pulmonary surface lining cells (al), contains a red blood cell. The basement membranes of the capillaries (cb) and alveoli (ab) are not thickened. The perivascular space (p) shows mesenchymal cell remnants (m) and reticular fibers (r). A slight amount of localized edema may be present but even with this, the perivascular space is not markedly widened. Numerous small vesicles are present in the capillary endothelium (E) but no large pinocytotic vacuoles are observed.

(Reynold's lead citrate and uranyl acetate, 13,800X)



Figure 2

Figure 3

Case I, pulmonary stenosis. A section through a thick area of the septal wall showing a well-granulated mast cell (MC) within the perivascular space. The gray fibrillar material above the mast cell is an accumulation of reticular fibers (r) with a few distinct collagen (c) fibrils showing characteristic striations. A mesenchymal cell derivative (m) is seen to be closely apposed to the alveolar basement membrane. The continuous pulmonary surface lining invests the alveolar space (A).

(Reynold's lead citrate and uranyl acetate, 25, 200X)



Figure 3

Figure 4

Case II, left superior vena cava, interventricular defect, and pulmonary hypertension. A comparison of the alveolar basement membrane (ab) and the capillary basement membrane (cb) shows the latter to be slightly increased in thickness. The perivascular space (p) is widened and contains small amounts of collagen and remnants of mesenchymal cells (m). The endothelial cell cytoplasm (E) invests the capillary which contains a coarse precipitate of plasma.

(uranyl acetate, 24,500X)

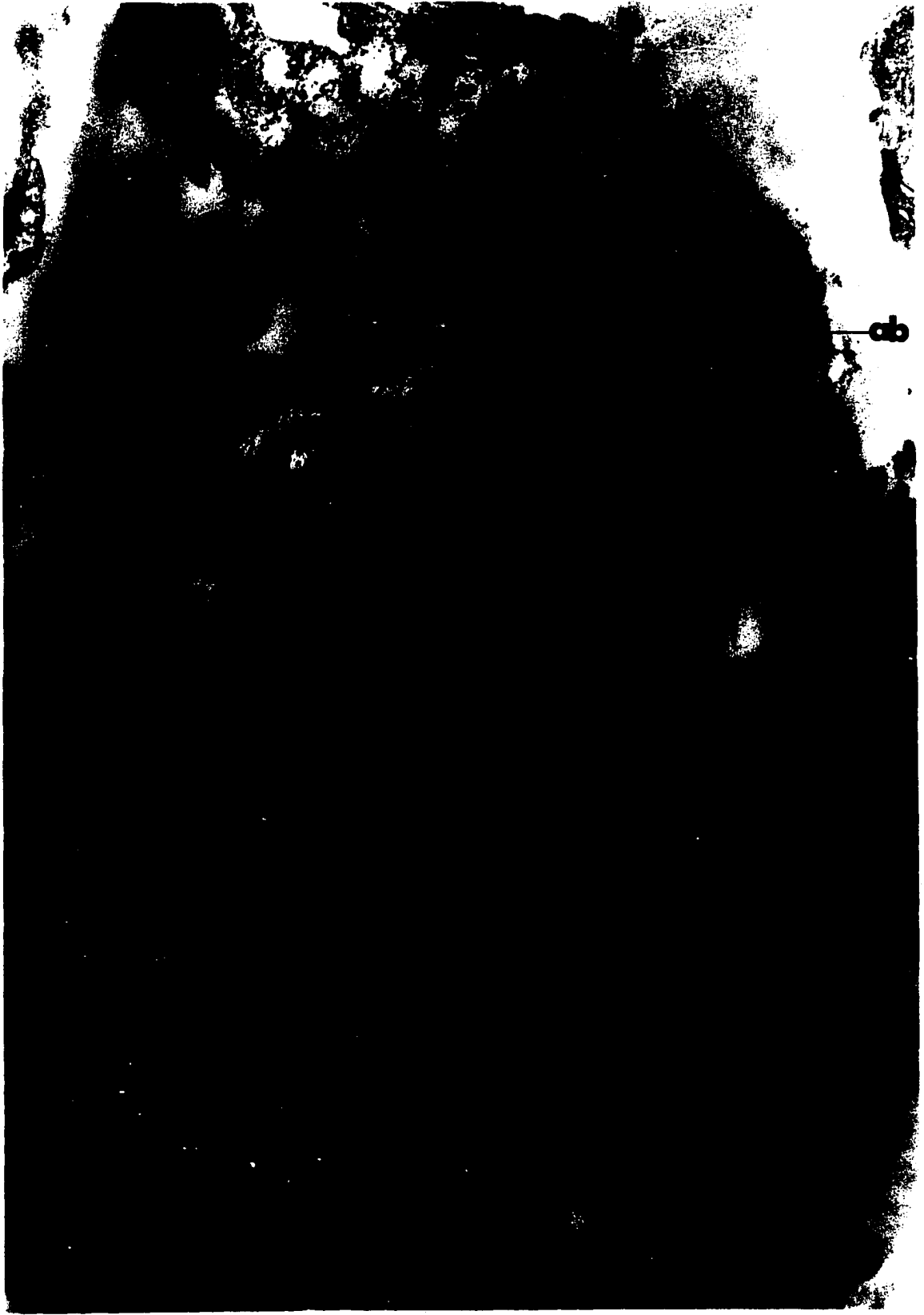


Figure 4

Figure 5

Case II, left superior vena cava, interventricular defect, and pulmonary hypertension. Section through the entire septal wall separating two adjacent alveolar spaces (A). The capillary basement membrane again appears to be slightly thickened when compared to the alveolar basement membrane. The perivascular space (p), as in Figure 4, shows mesenchymal cell remnants and some collagen deposition. Large pinocytotic vacuoles (v) are present in the endothelium, mesenchymal cell derivatives, and the alveolar epithelial lining.

(uranyl acetate, 12,500X)

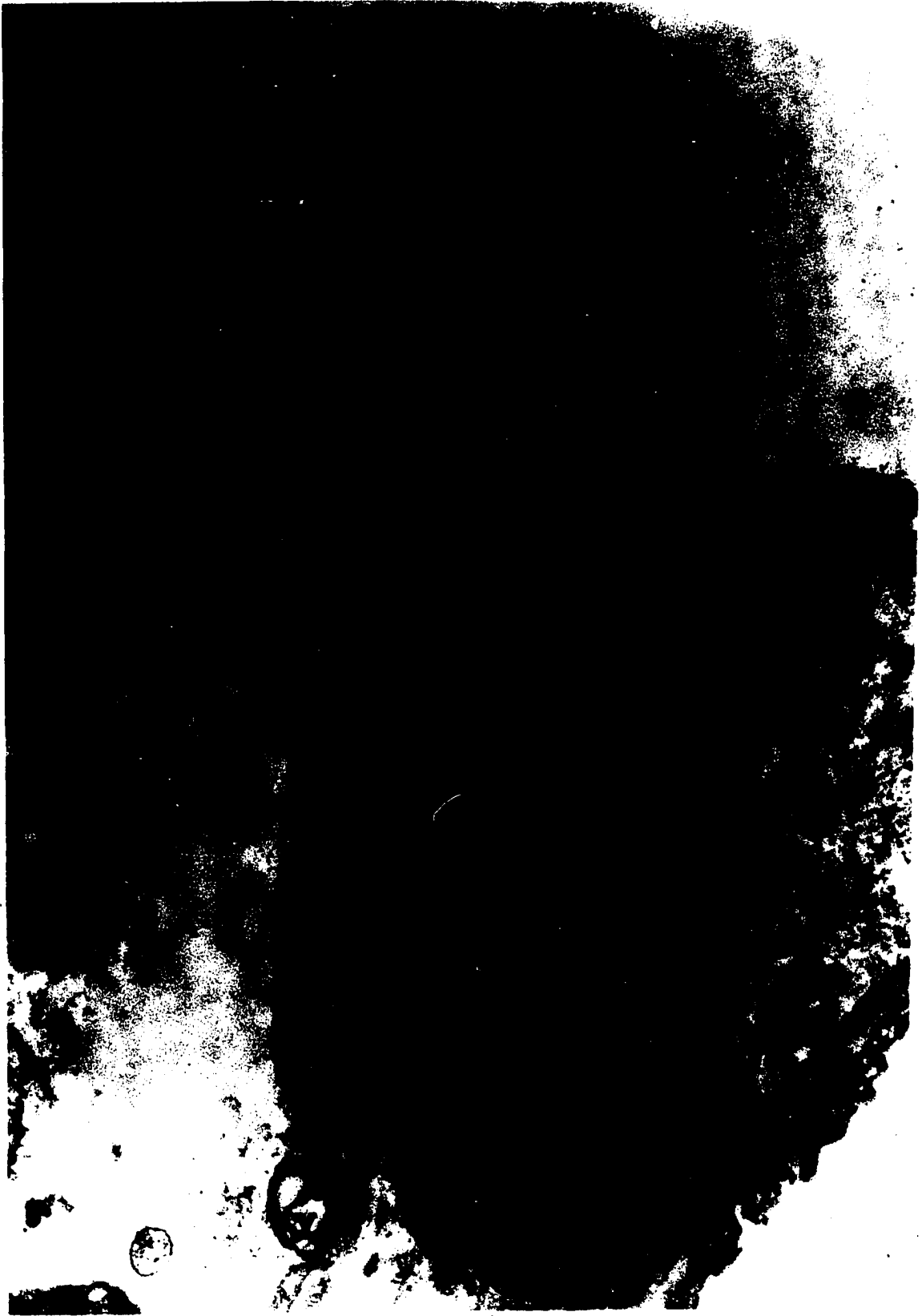


Figure 5

Figure 6

Case II, left superior vena cava, interventricular defect, and pulmonary hypertension. The endothelial cell lining the capillary exhibits some vacuolization (v). Again the capillary basement membrane (cb) appears to be thicker than the alveolar basement membrane (ab). The alveolar type II cell (a2) in this electron micrograph shows only a few microvilli but the characteristic lamellated, osmiophilic inclusion bodies are clearly visible. The surface of the alveolar type II cell projects into the alveolar space (A).

(uranyl acetate, 18,000X)

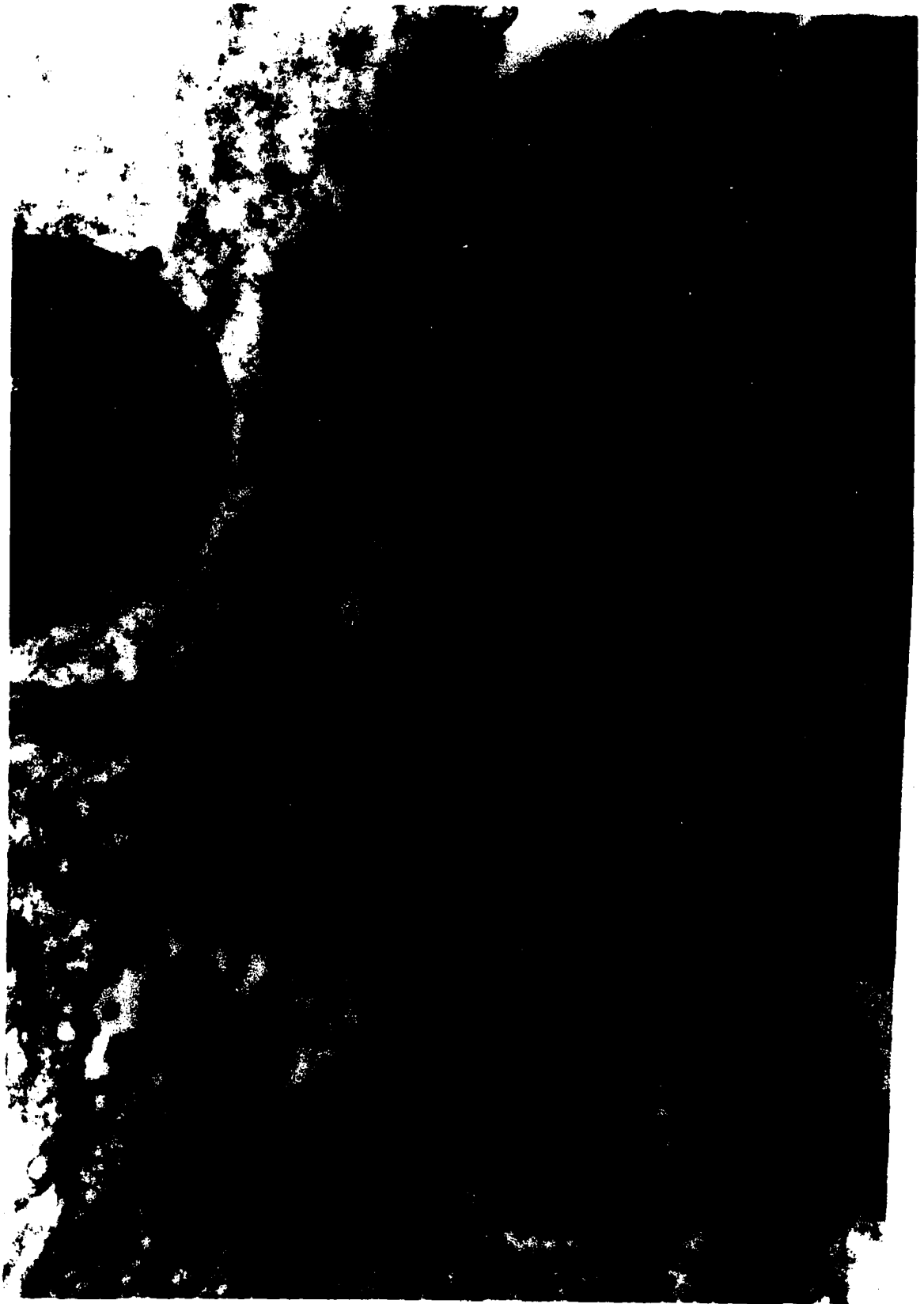


Figure 6

Figure 7

Case II, left superior vena cava, interventricular defect, and pulmonary hypertension. An alveolar macrophage (M) with microvilli and osmiophilic inclusion bodies is free in the alveolar space (A) and occupies most of the center of the field. Attenuated cytoplasmic extensions of the alveolar type I cell (al) can be seen under the alveolar macrophage. In this field, the alveolar and capillary basement membranes have approximated and coalesced. The endothelial lining (E) of the capillary shows numerous small vesicles.

(uranyl acetate, 18,000X)

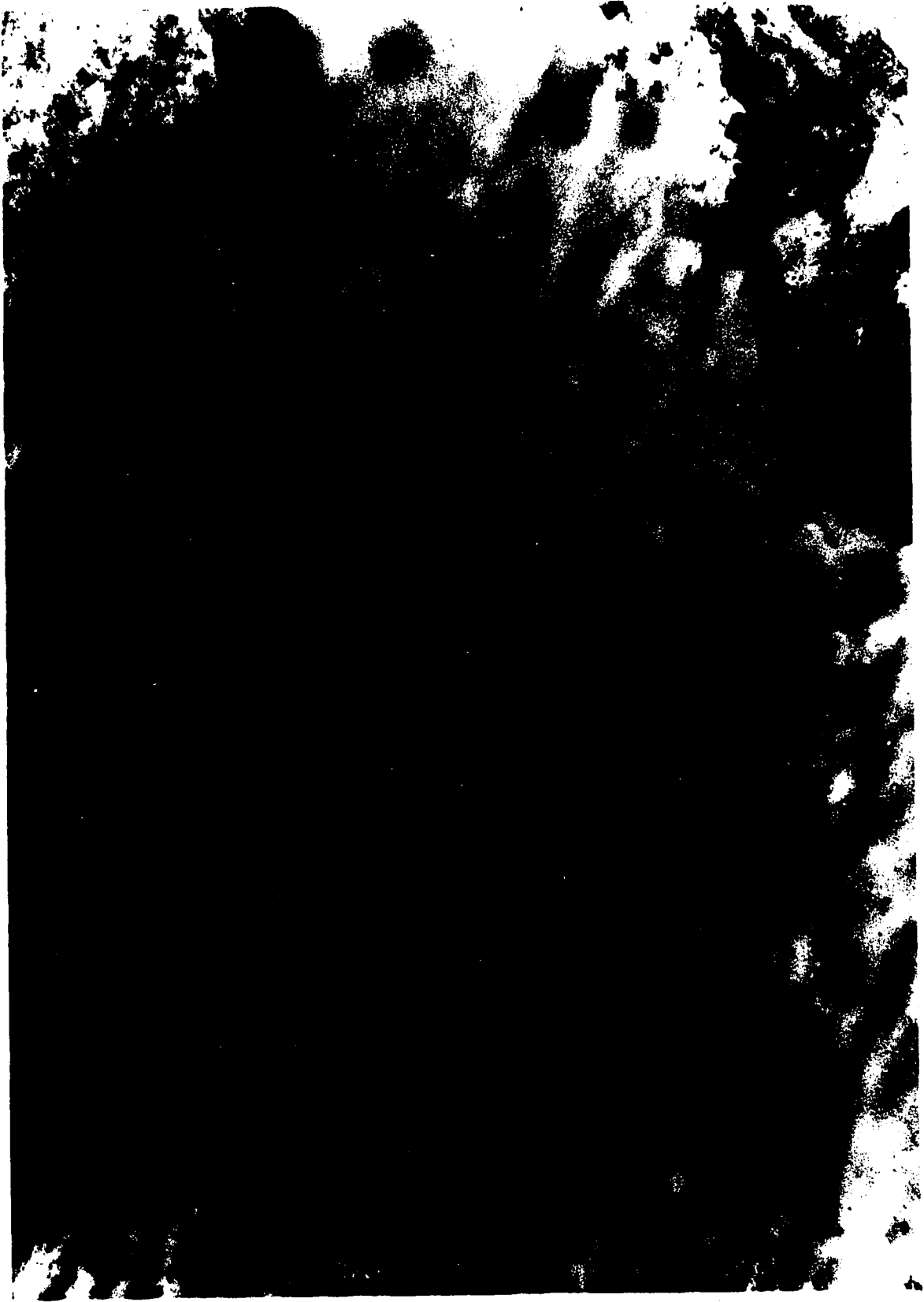


Figure 7

Figure 8

Case III, acquired mitral stenosis with pulmonary hypertension. This is a section through the air-blood barrier which shows marked thickening of both capillary (cb) and alveolar (ab) basement membranes. In many areas, they are indistinguishable as separate structures. The perivascular space (p) shows increased collagen deposition (c) and mesenchymal cell remnants (m). Alveolar spaces (A) are situated in the upper and lower portions of the field.

(uranyl acetate, 20,500X)

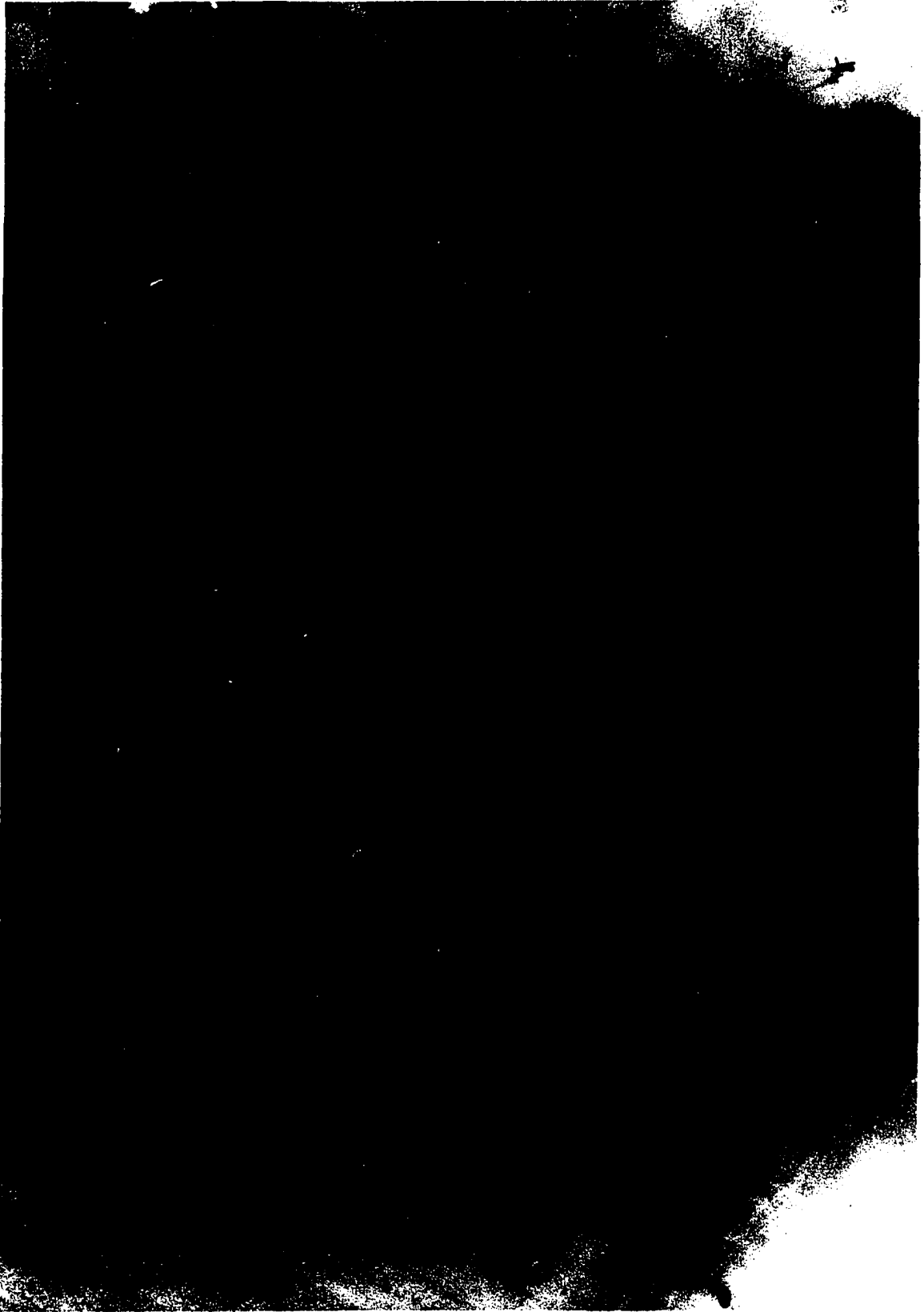


Figure 8

Figure 9

Case III, acquired mitral stenosis with pulmonary hypertension. This figure depicts a region near the nuclear area of an alveolar type I cell (al). The capillary and alveolar basement membranes are markedly thickened and are without distinct limits. Mesenchymal cell remnants (m) near the upper margin of this illustration extend into the basement membrane areas. Increased collagen deposition (c) is seen within the perivascular space.

(uranyl acetate, 27,800X)

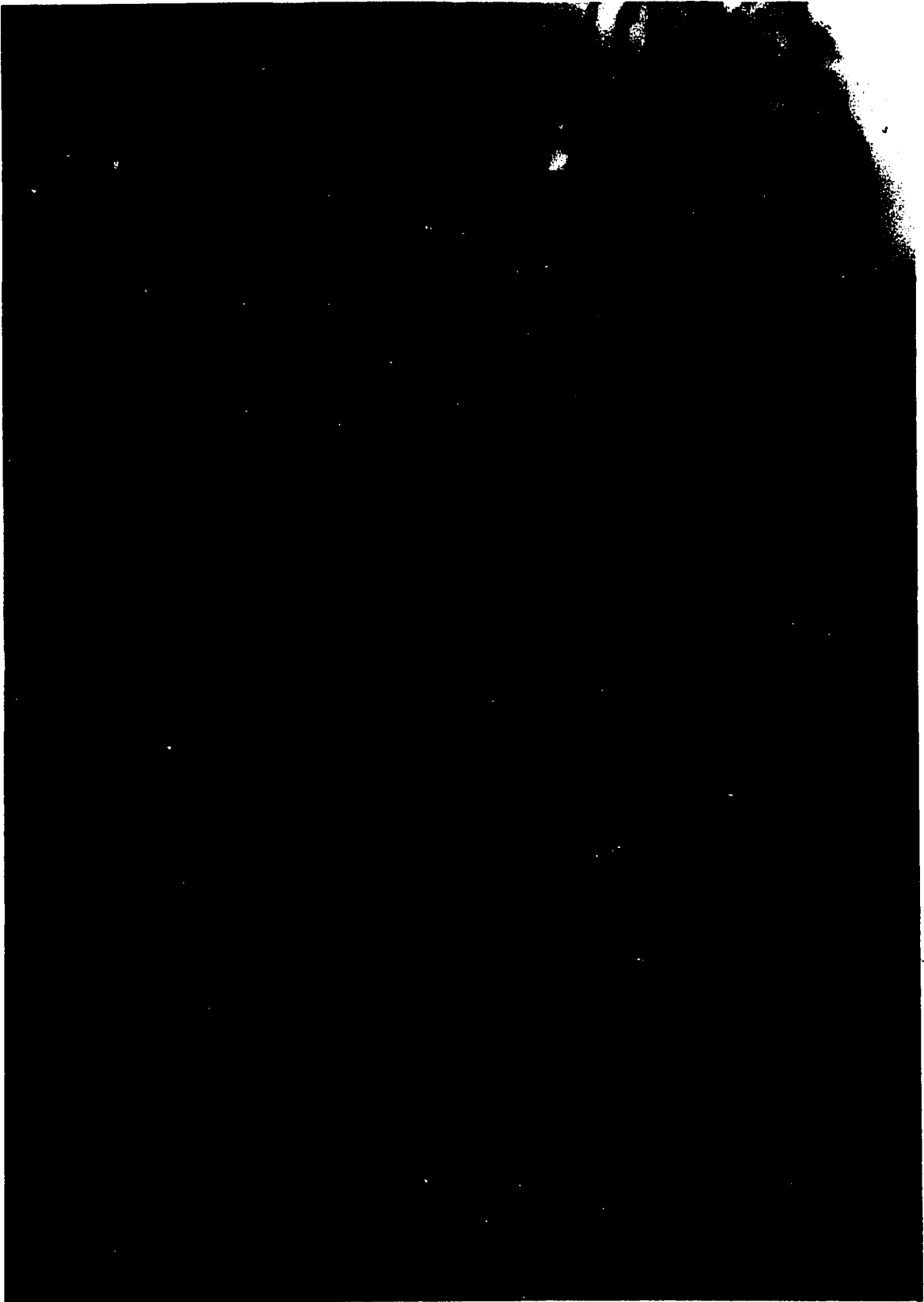


Figure 9

Figure 10

Case III, acquired mitral stenosis with pulmonary hypertension. Two adjacent capillaries (C) are separated from the alveolar space (A) by increased fibro-cellular deposition. Remnants of mesenchymal cells (m) and collagen fibers (c) lie between the thickened alveolar and capillary basement membranes.

(Reynold's lead citrate and uranyl acetate, 23,500X)

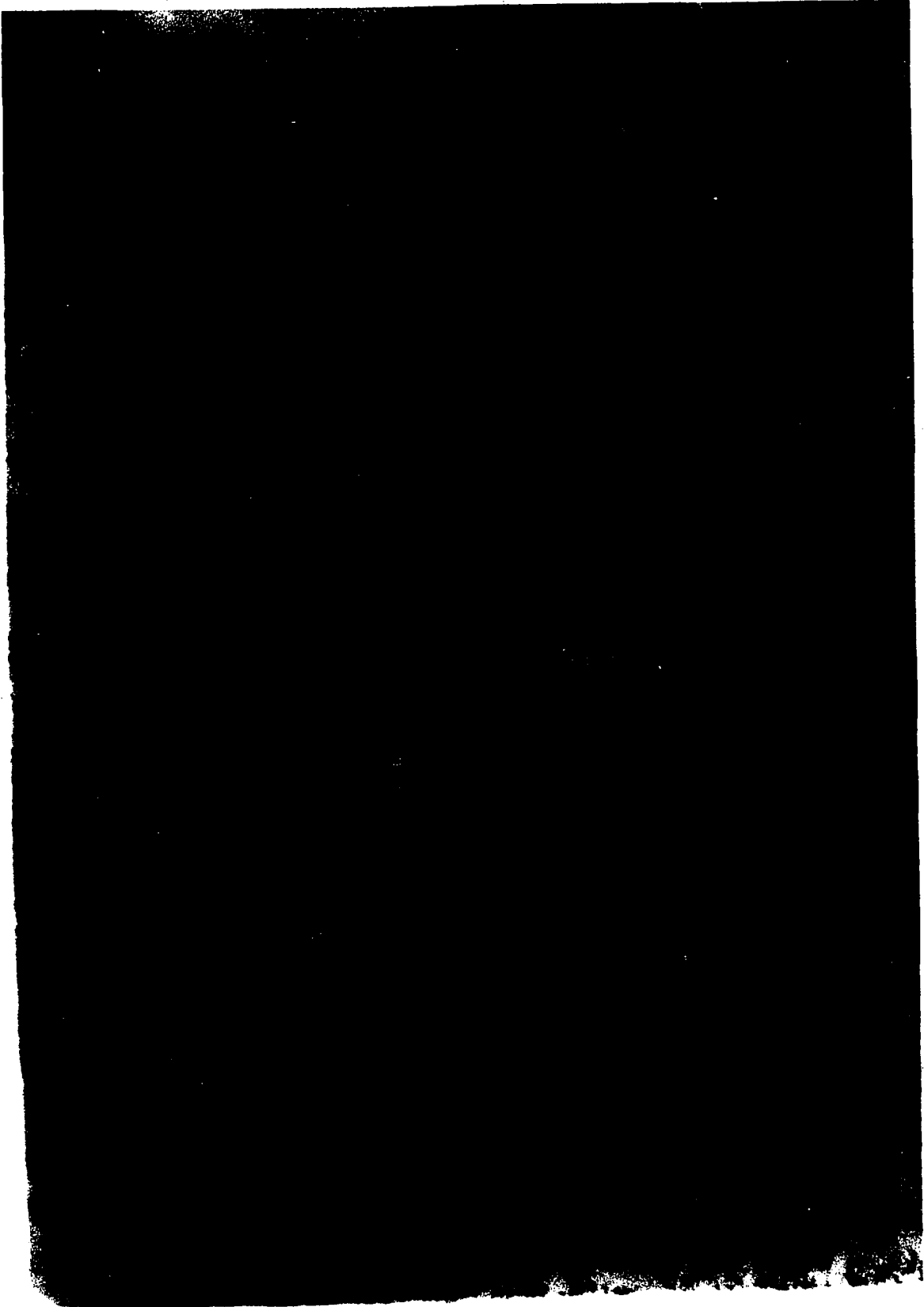


Figure 10

Figure 11

Case III, acquired mitral stenosis with pulmonary hypertension. This figure shows essentially the same changes as the two preceding figures. Note the continuous pulmonary surface lining of the alveolar space (A) which is formed by the attenuated cytoplasmic extensions of the alveolar type I cells. The perivascular space appears to be completely filled with the amorphous basement membrane material. Collagen fibers are not evident. A nucleated mesenchymal type cell (m) is seen within the perivascular space. The capillary lumen (C) is invested by endothelium, and in one area, part of the endothelial cytoplasm appears to fuse with a mesenchymal cell component.

(uranyl acetate, 27,800X)

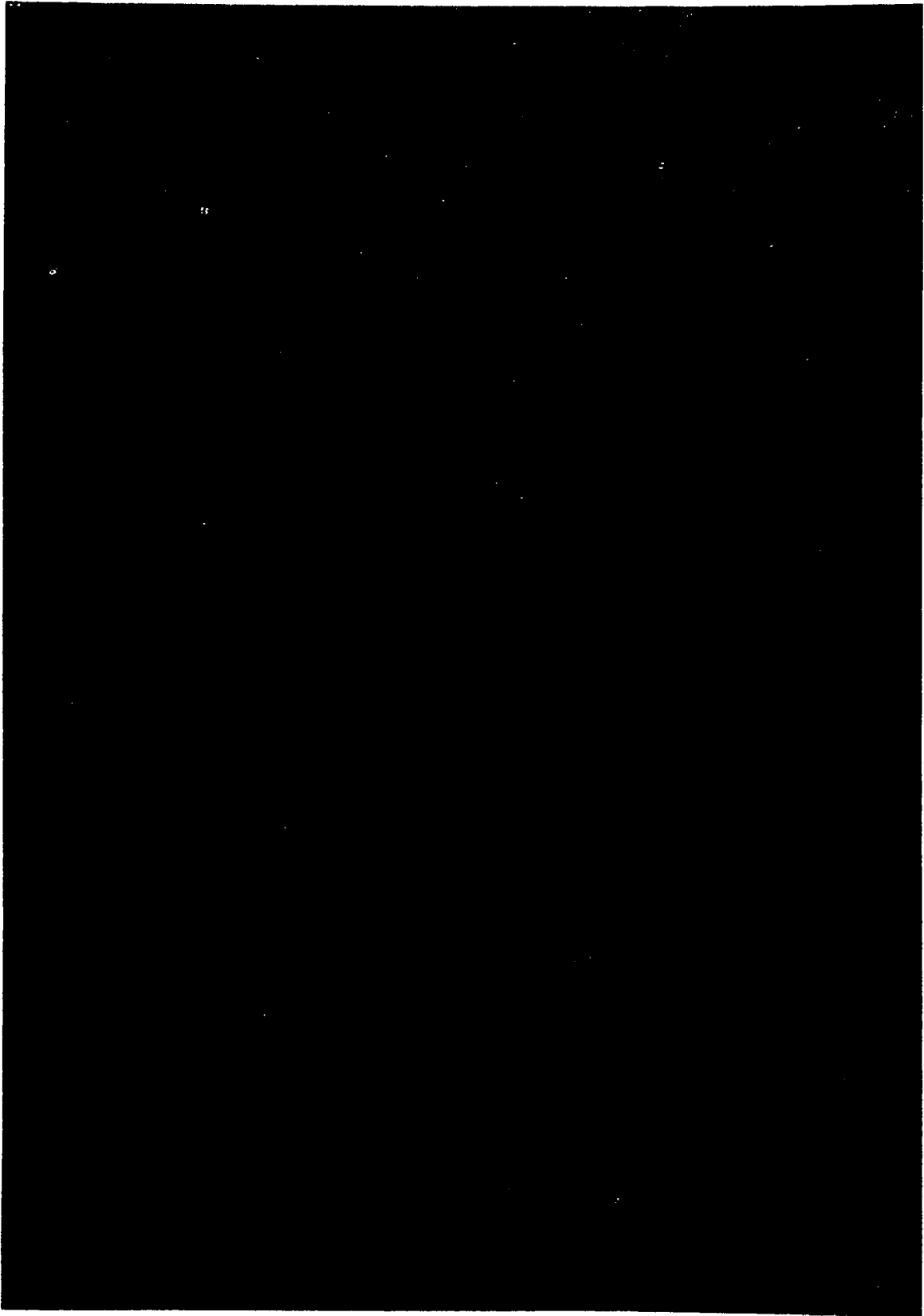


Figure 11

Figure 12

Case IV, patent ductus arteriosus, atresia of a left common pulmonary vein, interventricular septal defect, and pulmonary hypertension. This is a section through only a portion of a septal wall. The alveolar space (A) is indicated for orientation. Note the continuous pulmonary surface lining of attenuated alveolar type I cell cytoplasm. The alveolar basement membrane is distinct and appears essentially normal. A nucleated mesenchymal type cell (m), which shows granulated endoplasmic reticulum, Golgi vesicles (g), and many darkly stained ribosomes, is present in the perivascular space. In addition to the nucleated mesenchymal type cell, the perivascular space shows marked collagen (c) and elastic (e) deposition, gross edema, and remnants of other mesenchymal cells.

(Millonig's lead tartrate and uranyl acetate, 32,500X)

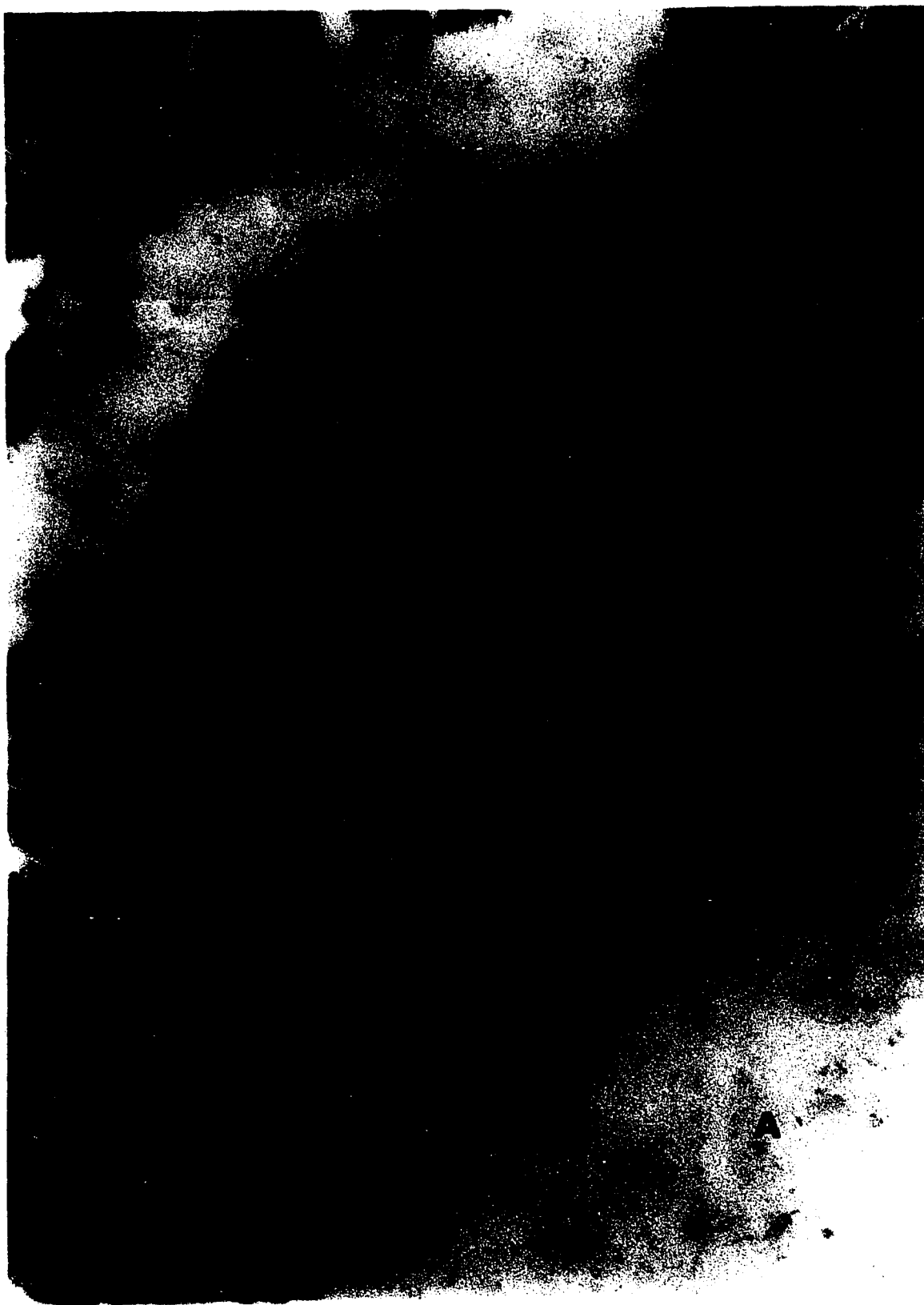


Figure 12

Figure 13

Case IV, patent ductus arteriosus, atresia of a left common pulmonary vein, interventricular septal defect, and pulmonary hypertension. This figure shows a portion of a septal wall, an alveolar space (A) with transudate, and part of a capillary. The capillary endothelium (E) shows vacuolization and prominent ribosomes. At the electron microscopic level, it is very unusual to find two endothelial cell nuclei in the same section of a capillary; two such nuclei in the same area are indicative of endothelial hyperplasia. This was confirmed at the light microscopic level with histochemical and cytological preparations. The capillary and alveolar basement membranes appear to be essentially normal. Deposition of fibrous elements in the perivascular space (p) is not marked in this section but some edema is present. (Millonig's lead tartrate and uranyl acetate, 23,500X)

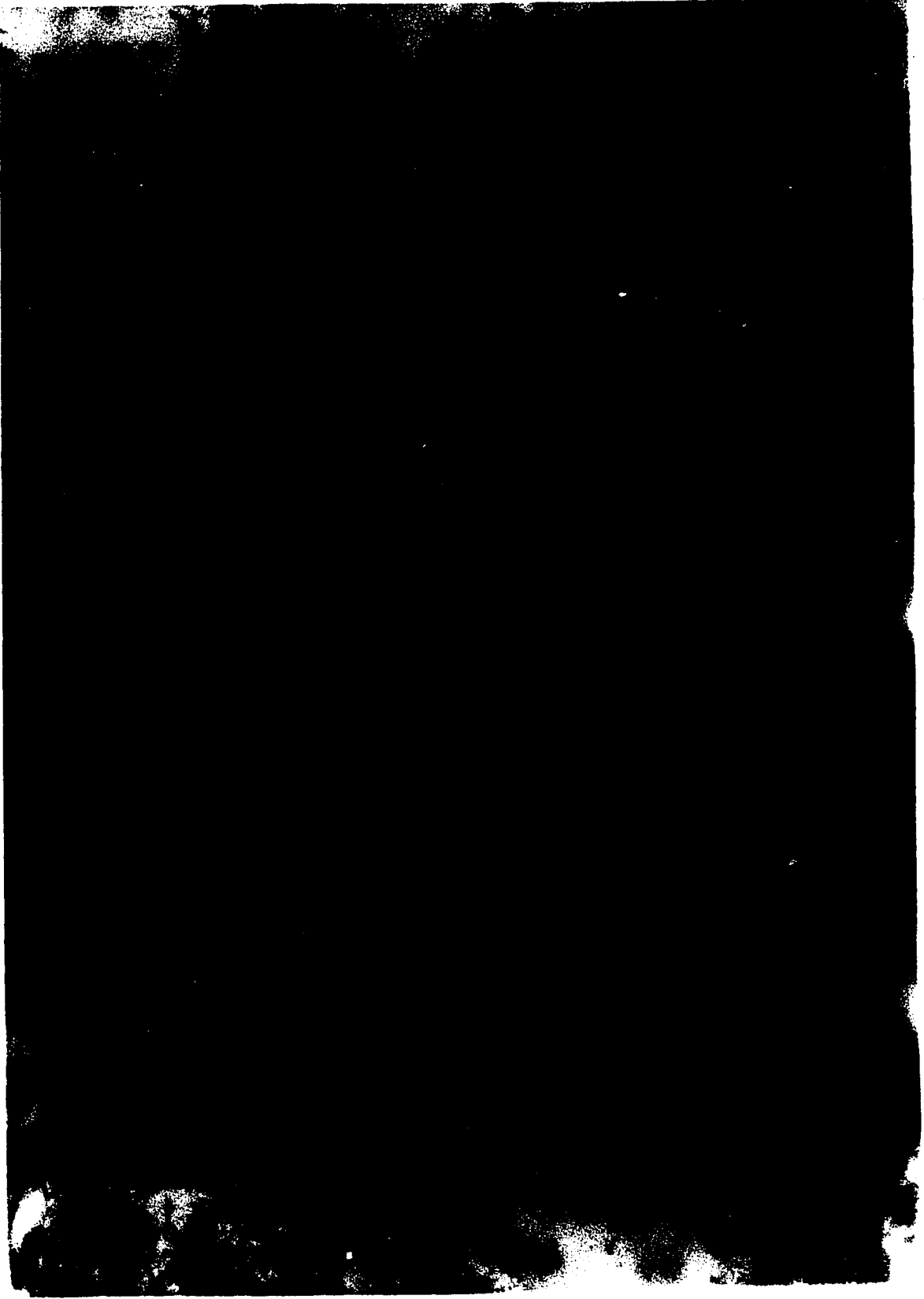


Figure 13

Figure 14

Case V, congenital aortic stenosis. This electron micrograph shows a portion of a septal wall, part of a capillary and the adjacent alveolar space (A). Note the pulmonary surface lining formed by the attenuated cytoplasm of the alveolar type I cells. The capillary endothelium (E) shows vacuolization (v) and vesiculation. The capillary and alveolar basement membranes do not appear thickened but the perivascular space is tremendously increased in width due to increased collagen (c) deposition, mesenchymal cell remnants and reticular fibers. (Reynold's lead citrate and uranyl acetate, 25,200X)



Figure 14

Figure 15

Case V, congenital aortic stenosis. This is a section through an entire septal wall showing portions of two capillaries. The alveolar spaces (A) are indicated for orientation. The capillary basement membrane is thickened but the alveolar basement membrane is still quite thin. Two fibroblast-like cells (m) are seen in the perivascular space (p) between the two capillary walls. Some collagen deposition is seen within the perivascular space, but it is not as pronounced as in Figure 14. Abundant reticular fibers (r) are observed, especially near the cytoplasmic borders of the fibroblast-like cells.

(Reynold's lead citrate and uranyl acetate, 12,900X)

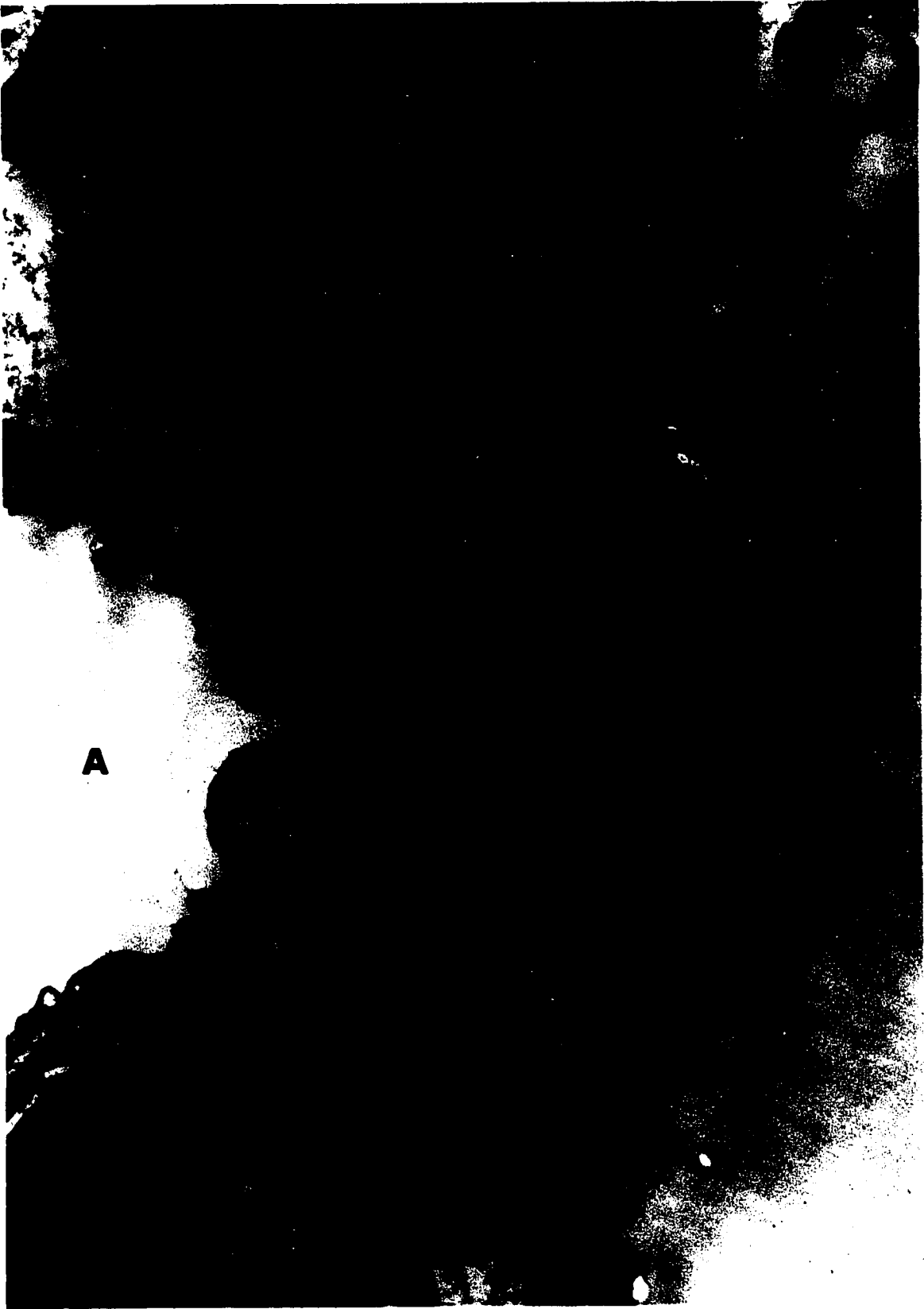


Figure 15

Figure 16

Case V, congenital aortic stenosis. The entire septal wall between the adjacent alveolar spaces (A) is depicted. Mesenchymal cell remnants, increased collagen deposition (c), elastic fibers (e), and edema are seen within the perivascular space. An alveolar type II cell (a2) with microvilli and osmiophilic inclusion bodies is present in the lower left corner of the plate. Note that the attenuated cytoplasmic processes of the alveolar type I cell do not extend under the alveolar type II cell. The alveolar basement membranes appear to be normal but become quite attenuated under the alveolar type II cell.

(Reynold's lead citrate and uranyl acetate, 17,500X)

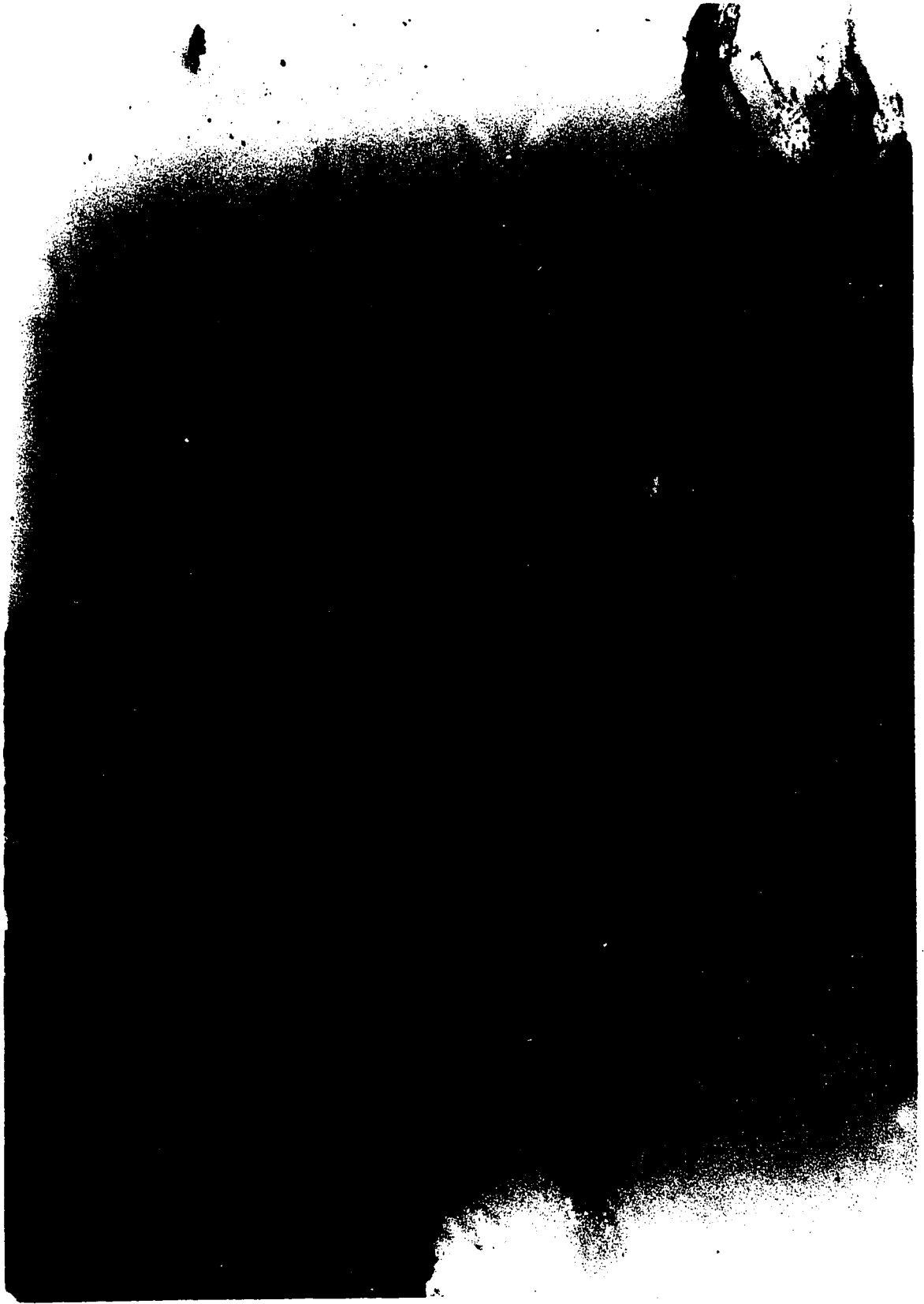


Figure 16

Figure 17

Case V, congenital aortic stenosis. This section shows a markedly widened perivascular space with an enclosed leucocyte (L). The perivascular space (p) also shows edema, mesenchymal cell remnants (m) and patchy collagen deposition. The capillary basement membrane (cb) is slightly thickened. A space (x), extending through the endothelial cells to the capillary basement membrane, can be seen in the lower portion of the field. Attention is called to the vacuolization (v) within the endothelial investment.

(Reynold's lead citrate and uranyl acetate, 12,900X)



Figure 17

Figure 18

Case V, congenital aortic stenosis. The alveolar space (A) is indicated in the lower portion of the micrograph. A leucocyte with a lobulated nucleus is seen within the perivascular space. Collagen (c), reticular fibers, and elastic fibers (e) are prominent in the area surrounding the capillary. The endothelial investment (E) of the capillary is remarkable in that a large area of separation is noted within which some material (x) resembling collagen is seen. The capillary basement membrane is indistinct in an area above this endothelial separation.

(Reynold's lead citrate and uranyl acetate, 12,000X)

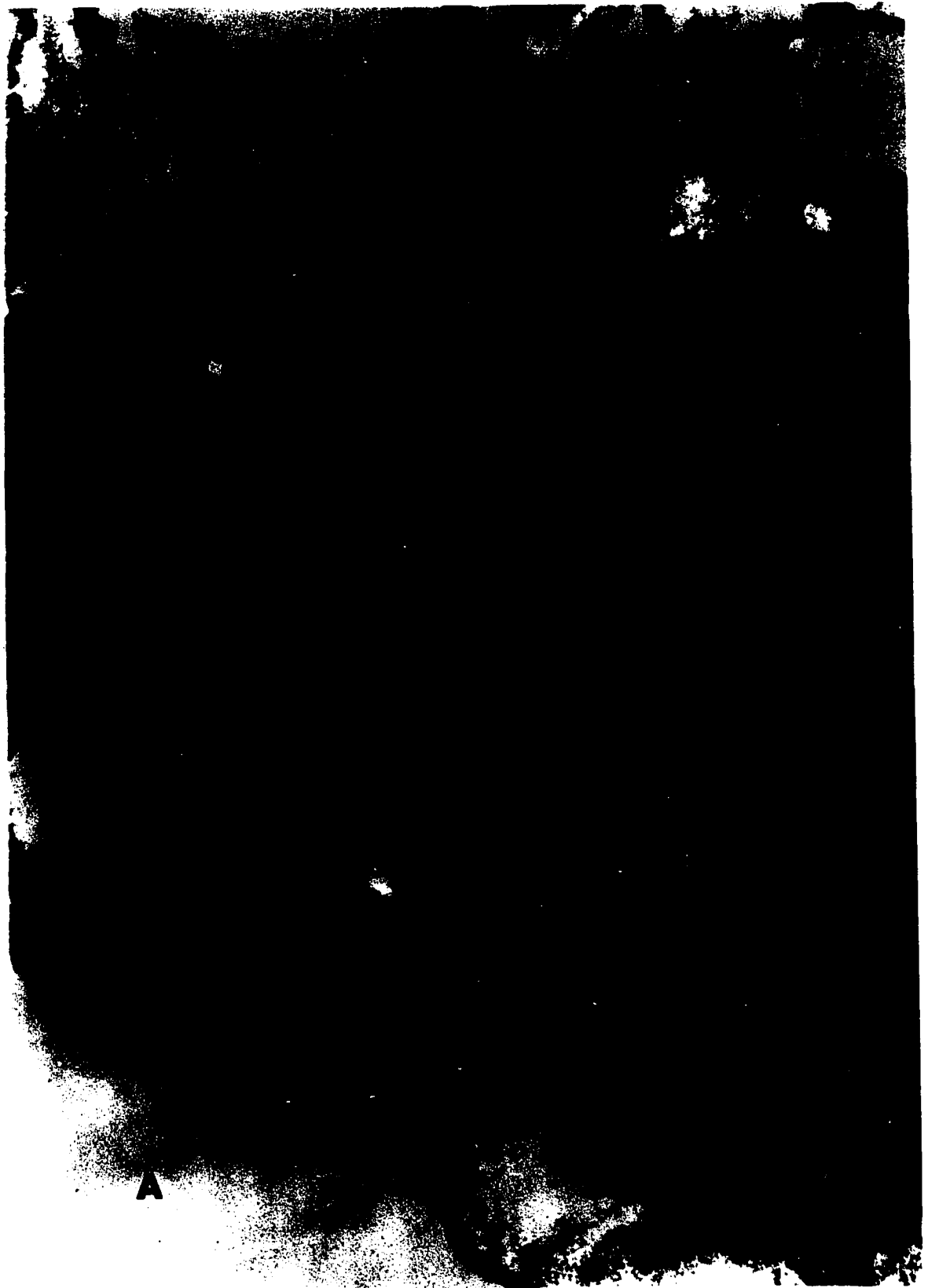


Figure 18

Figure 19

Case VI, acquired mitral stenosis with minimal mitral insufficiency. The central area of this figure is occupied by a capillary lined with endothelium (E). Only small areas of the alveolar spaces are shown at the periphery of the field. The capillary basement membrane is markedly thickened but the segments of alveolar basement membrane visible in this figure appear to be essentially normal. In the lower portion of the figure, the perivascular space contains a cell with long cytoplasmic processes and clusters of osmiophilic inclusions cut in both cross and longitudinal directions. Inclusions near the lower picture margin resemble those filling the cytoplasm of the mast cell in Figure 3. The perivascular space also shows increased collagen (c) deposition and accumulations of amorphous material which is probably elastic tissue (e). The mesenchymal cell (m) above the capillary is probably a pericyte.

(Reynold's lead citrate and uranyl acetate, 17,500X)

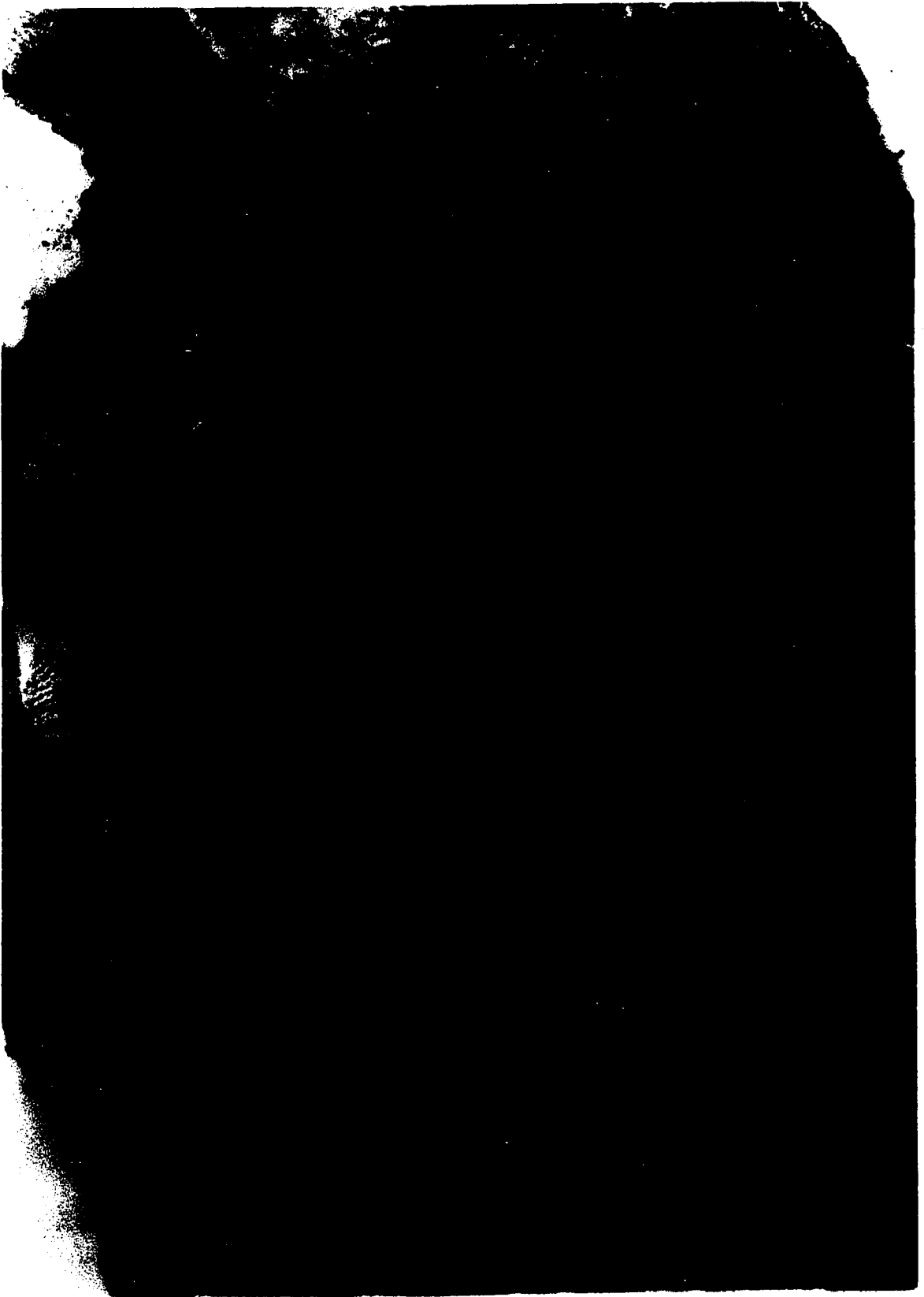


Figure 19

Figure 20

Case VI, acquired mitral stenosis with minimal mitral insufficiency. The alveolar and capillary basement membranes (x) can not be distinguished as separate entities in some areas above the nucleus of the endothelial cell lining the capillary. Toward the bottom of the figure, deposition of delicate reticular fibrils appear to separate the alveolar and capillary basement membranes. In these areas of separation, the alveolar basement membrane appears much thinner than that of the capillary.

(Reynold's lead citrate and uranyl acetate, 20,500X)



Figure 20

Figure 21

Case VI, acquired mitral stenosis with minimal mitral insufficiency. This is a section through a complete septal wall showing the alveolar spaces (A) on both sides. The nucleus of an alveolar type I cell (al) can be seen in the lower right corner of the figure. Note the attenuated cytoplasmic extensions which form the pulmonary surface lining. The capillary basement membrane (cb) and alveolar basement membrane are clearly delineated and slightly thickened. The perivascular space (p) is widened with increased collagen deposition (c), reticular fibers, and mesenchymal cell derivatives.

(Reynold's lead citrate and uranyl acetate, 23,500X)

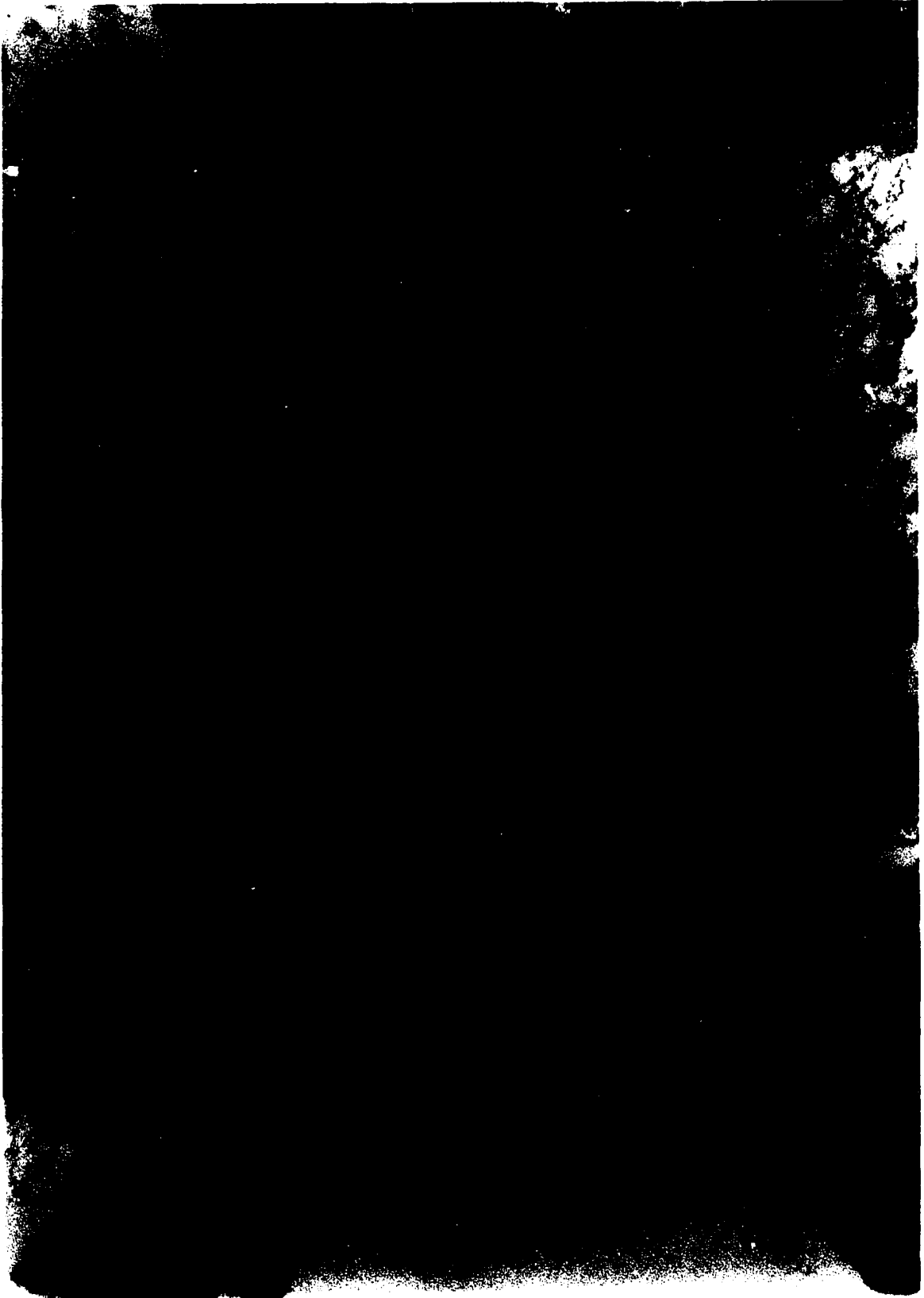


Figure 21

Figure 22

Case VII, acquired mitral stenosis. Two capillaries (C) are seen in the figure with the alveolar space (A) at the right margin. There is copious transudate within the alveolar space. The lumina of the capillaries are lined by an endothelial investment (E) showing an increase in width and prominent vacuolization and vesiculation. The perivascular space contains a tremendous increase of collagen (c) and mesenchymal cell derivatives. The capillary basement membrane (cb) is markedly thickened and in one portion a mesenchymal cell remnant (m) appears to be embedded in the matrix. The alveolar basement membrane shows only slight thickening. The alveolar epithelial layer contains large vacuoles (v) and small vesicles.

(Reynold's lead citrate and uranyl acetate, 18,000X)

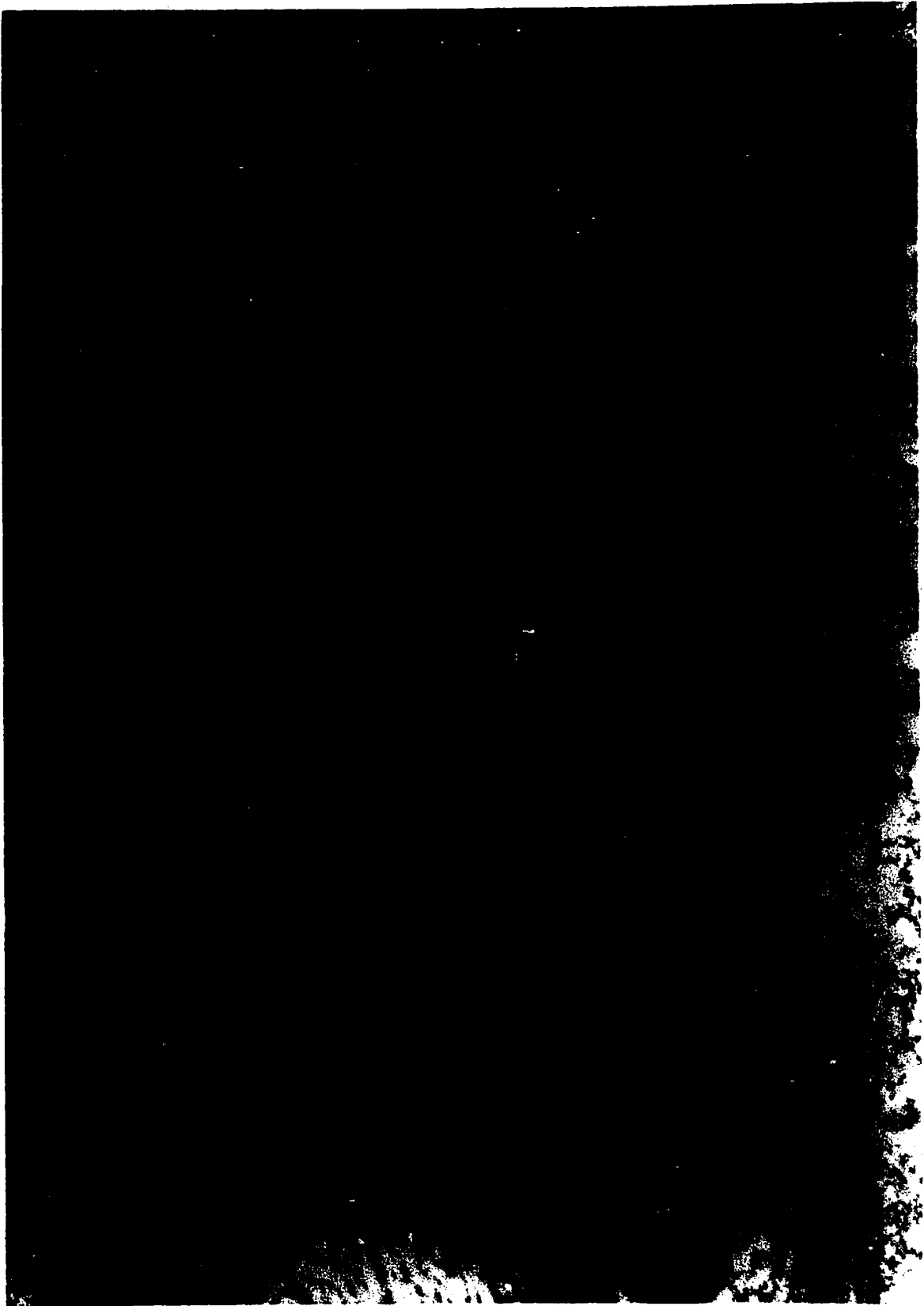


Figure 22

Figure 23

Case VII, acquired mitral stenosis. The alveolar epithelial lining appears to be lost at the right margin of the figure (x). The transudate filled alveolar space (A) superficially resembles a capillary, particularly since it contains a red blood cell, therefore, the capillary (C) has been indicated for proper orientation. The perivascular space is markedly widened with increased collagen deposition (c). There is a mesenchymal cell (m) within the perivascular space which shows prominent vacuolization (v). The capillary basement membrane (cb) is quite thickened whereas the alveolar basement membrane is thin in appearance.

(Reynold's lead citrate and uranyl acetate, 12,500X)

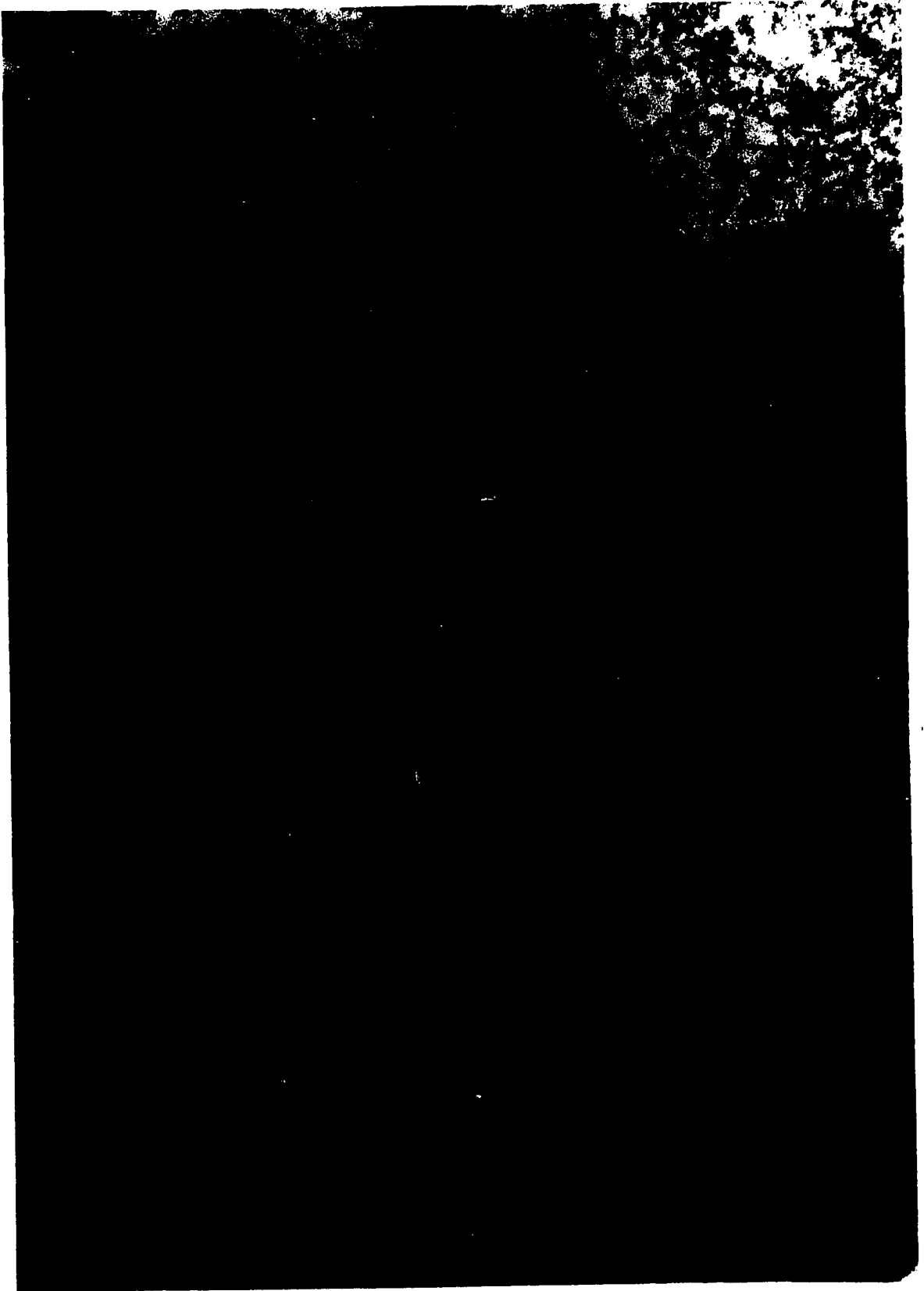


Figure 23

Figure 24

Case VII, acquired mitral stenosis. At the lower right margin, a fat embolism (FE) is depicted in the transudate filled alveolar lumen (A). The capillary and alveolar basement membranes both are increased in width. Increased collagen deposition is noted in the perivascular space (p). The capillary (C) is lined by endothelial cytoplasm which contains numerous vesicles.

(Reynold's lead citrate and uranyl acetate, 18,000X)

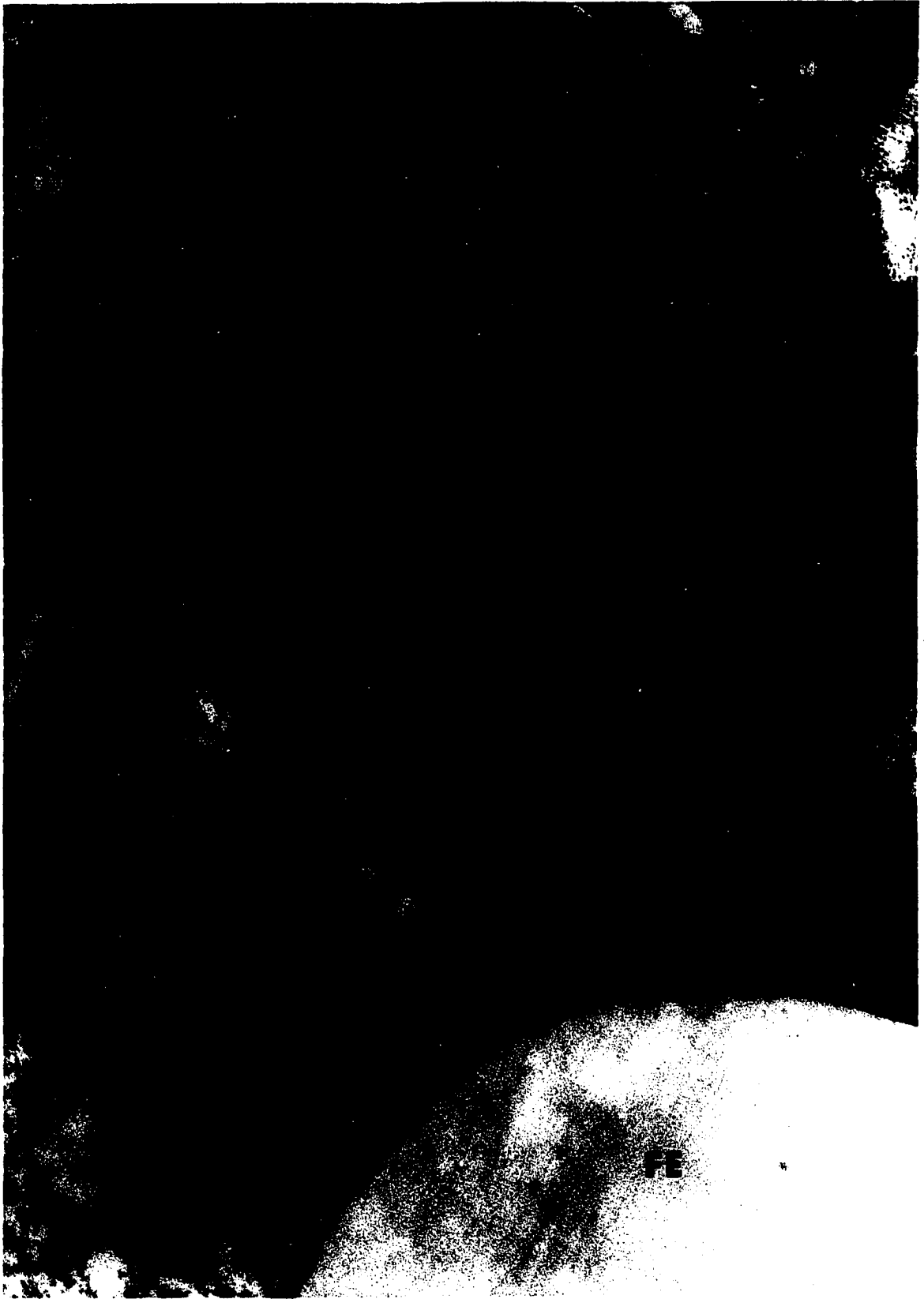


Figure 24

Figure 25

Case VIII, patent ductus arteriosus with reversal of flow, and pulmonary hypertension. The cytoplasm of the pulmonary surface lining contains many small vesicles (x). The alveolar basement membrane appears, in some areas, to fade into the perivascular space (p). However, neither the alveolar basement membrane nor the capillary basement membrane appears to be appreciably thickened. The perivascular space contains portions of mesenchymal cells (m) and shows increased deposition of collagen and reticular fibers (r).
(uranyl acetate, 24,500X)



Figure 25

Figure 26

Case VIII, patent ductus arteriosus with reversal of flow, and pulmonary hypertension. This figure illustrates a typical alveolar type II cell (a2) with its characteristic microvilli and osmiophilic inclusion bodies. Increased deposition of collagen and reticular fibers in the perivascular space (p) is still obvious even at this low power magnification. Mesenchymal cell elements (m) are also seen in the perivascular space. The capillary occupying most of the lower half of the field contains portions of a red blood cell and a lymphocyte.

(uranyl acetate, 12,500X)



Figure 26

Figure 27

Case VIII, patent ductus arteriosus with reversal of flow, and pulmonary hypertension. This figure is a longitudinal section through the alveolar-capillary membrane, oriented so that the capillary lumen (C) and the alveolar space (A) occupy respectively the right and left margins of the page. The alveolar space contains a portion of a free alveolar macrophage which possesses microvilli. Attenuated cytoplasmic extensions of the alveolar type I cells separate the alveolar space from the deeper structures of the septal wall. Portions of two cells are seen in the perivascular space. The upper cell (x) is a macrophage containing an ingested red blood cell. The lower cell (m) resembles very closely the nucleated capillary endothelial cell (E) at the top of the figure. Attenuated cytoplasmic processes of this endothelial-like cell often appear to form a lining for portions of the perivascular space. Increased deposition of collagen and reticular fibers occupies most of the non-cellular regions of the perivascular space (p). The capillary and alveolar basement membranes do not appear to be thickened.

(uranyl acetate, 12,500X)



Figure 27

Figure 28

Case VIII, patent ductus arteriosus with reversal of flow, and pulmonary hypertension. This figure is a longitudinal section through the septal wall which is situated between two adjacent alveolar spaces (A). A portion of an alveolar capillary (C), containing a leucocyte, can be seen in the septal wall. The alveolar and capillary basement membranes do not appear to be thickened, but the perivascular space (p) is widened markedly and shows a definite increase in collagen (c) and elastic (e) fiber deposition. The alveolar space at the bottom of the figure shows a segment of an alveolar macrophage (M) with microvilli and lamellated, osmiophilic inclusion bodies, some of which are free in the alveolar lumen.

(uranyl acetate, 13,300X)



Figure 28

Figure 29

Case IX, acquired mitral stenosis. The lumen of the capillary (C) is invested by anucleated endothelial cell and its cytoplasmic extensions. The capillary (cb) and alveolar basement membranes appear to be fused in some areas and are markedly increased in width. An increased deposition of reticular fibers (r) is observed within the perivascular space. The epithelial lining of the alveolar space (A) does not appear to be increased in width.

(Reynold's lead citrate and uranyl acetate, 19,800X)



Figure 29

Figure 30

Case IX, acquired mitral stenosis. Marked endothelial (E) swelling can be seen in this figure. Large vacuoles and numerous small vesicles are clearly denoted in the endothelial cytoplasm. The darkly staining body (x) is seen to have many small vesicles abutting on its surface. The capillary basement membrane (cb) is quite thick and fine reticular fibers (r) are depicted in the surrounding septal space.

(Reynold's lead citrate and uranyl acetate, 16,300X)

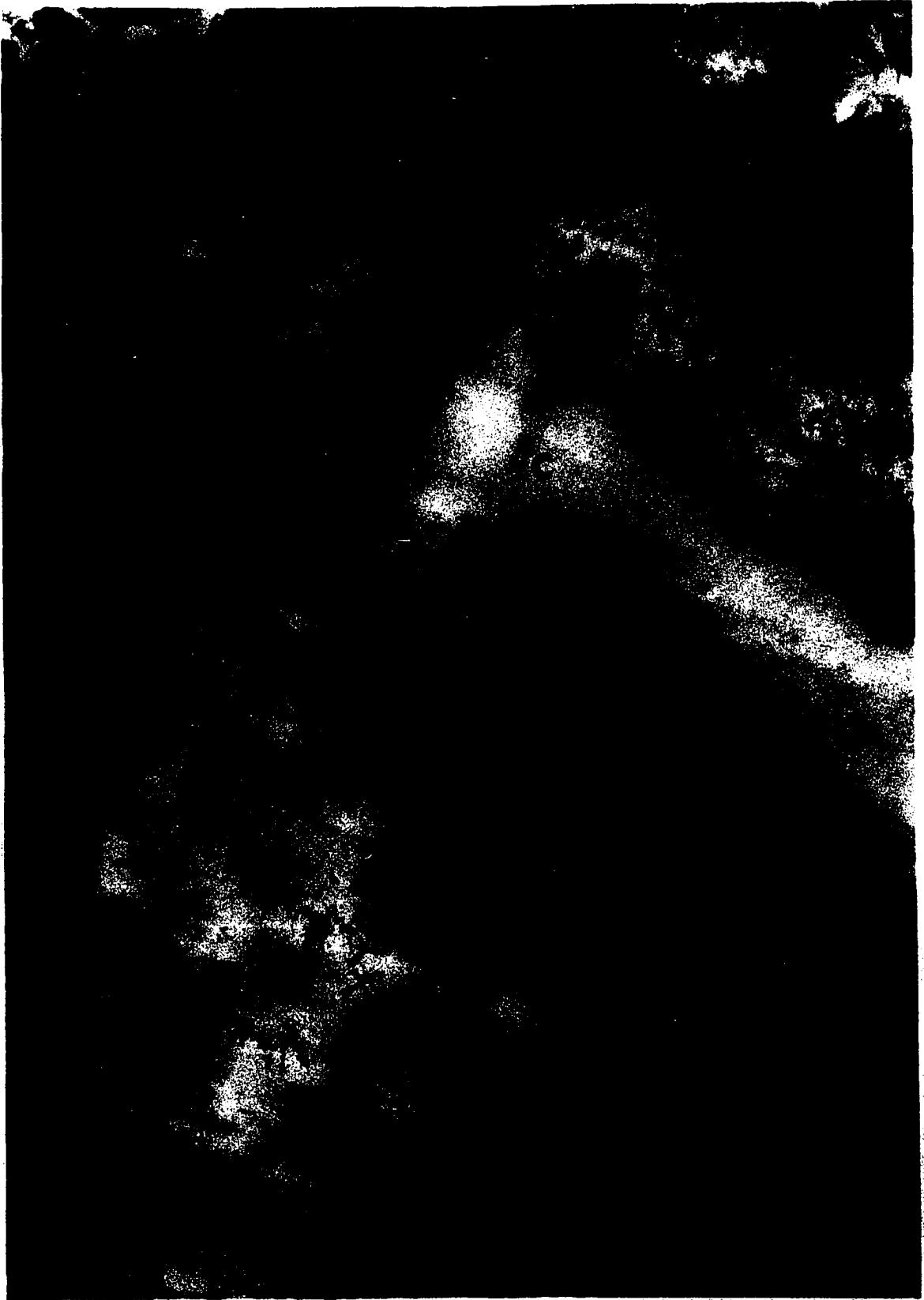


Figure 30

Figure 31

Case X, acquired interventricular septal defect. Portions of two capillaries (C) which appear to project into the alveolar space (A) are demonstrated in this figure. A red blood cell is seen within the alveolus. The capillary basement membrane (cb) is thickened and, in some areas, fuses into the fibrillar material within the perivascular space. The alveolar basement membrane (ab) is also thickened. Fine reticular (r) and collagen fibers are indicated. A few mesenchymal cell derivatives are seen within the perivascular space.

(uranyl acetate, 21,100X)

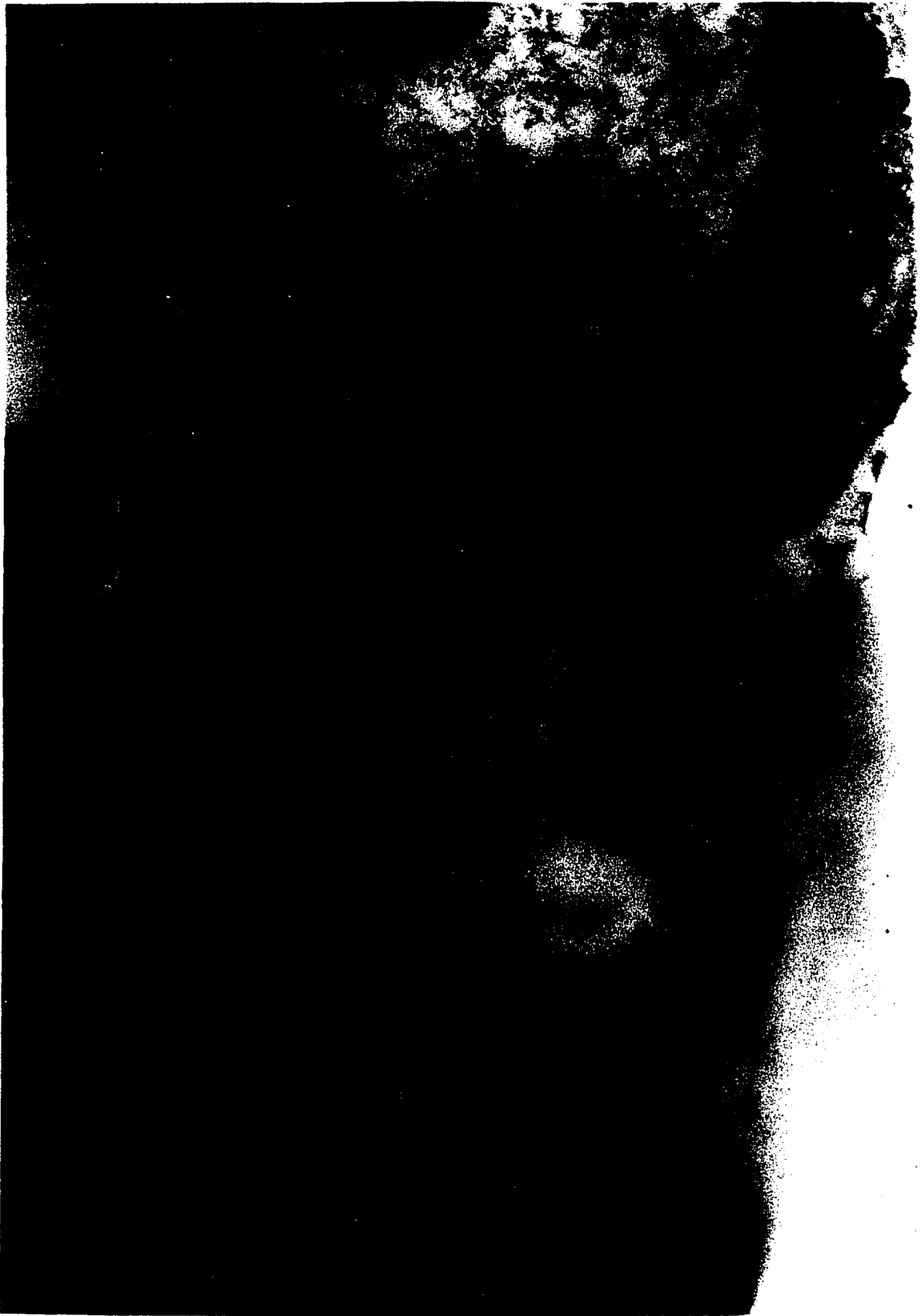


Figure 31

Figure 32

Case X, acquired interventricular septal defect. Underlying the alveolar type II cell (a2) an area of vacuolization (X) is seen. The alveolar basement membrane, although markedly attenuated, is not disrupted in this area. The capillary basement membrane (cb) is increased in width. Fine reticular fibers (r) and a mesenchymal cell component (m) are found in the perivascular space.

(uranyl acetate, 18,000X)

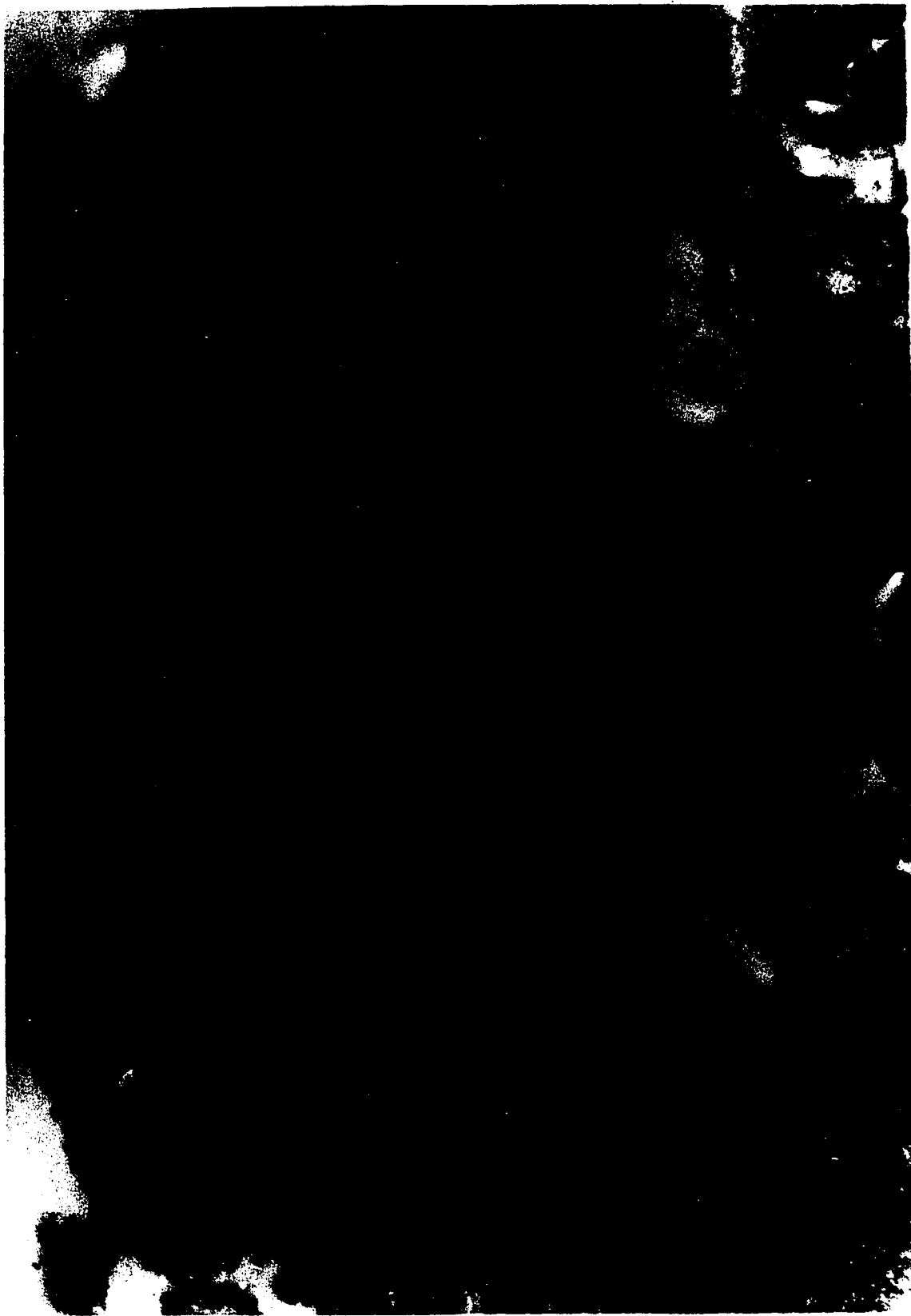


Figure 32

Figure 33

Case X, acquired interventricular septal defect. The endothelial cell lining (E) is appreciably thickened and contains many small vesicles. The perivascular space (p) contains collagen fibers and mesenchymal components, one of which has an enclosed fat inclusion (F). The epithelial lining of the alveolar space (A) is not increased in width. (Reynold's lead citrate and uranyl acetate, 24,400X)



Figure 33

Figure 34

Case XI, congestive heart failure. The endothelial (E) cell lining of the capillary is within the normal ranges of thickness, but attention is called to a fat inclusion (F) within this cell layer. Increased elastic fibers (e) and collagen fibers (c) are seen in the perivascular space. A mesenchymal cell (m) is also depicted in this area. No underlying vacuolization is seen beneath the alveolar type II cell (a₂) which forms part of the pulmonary surface lining of the alveolar space (A).

(Reynold's lead citrate and uranyl acetate, 16,700X)

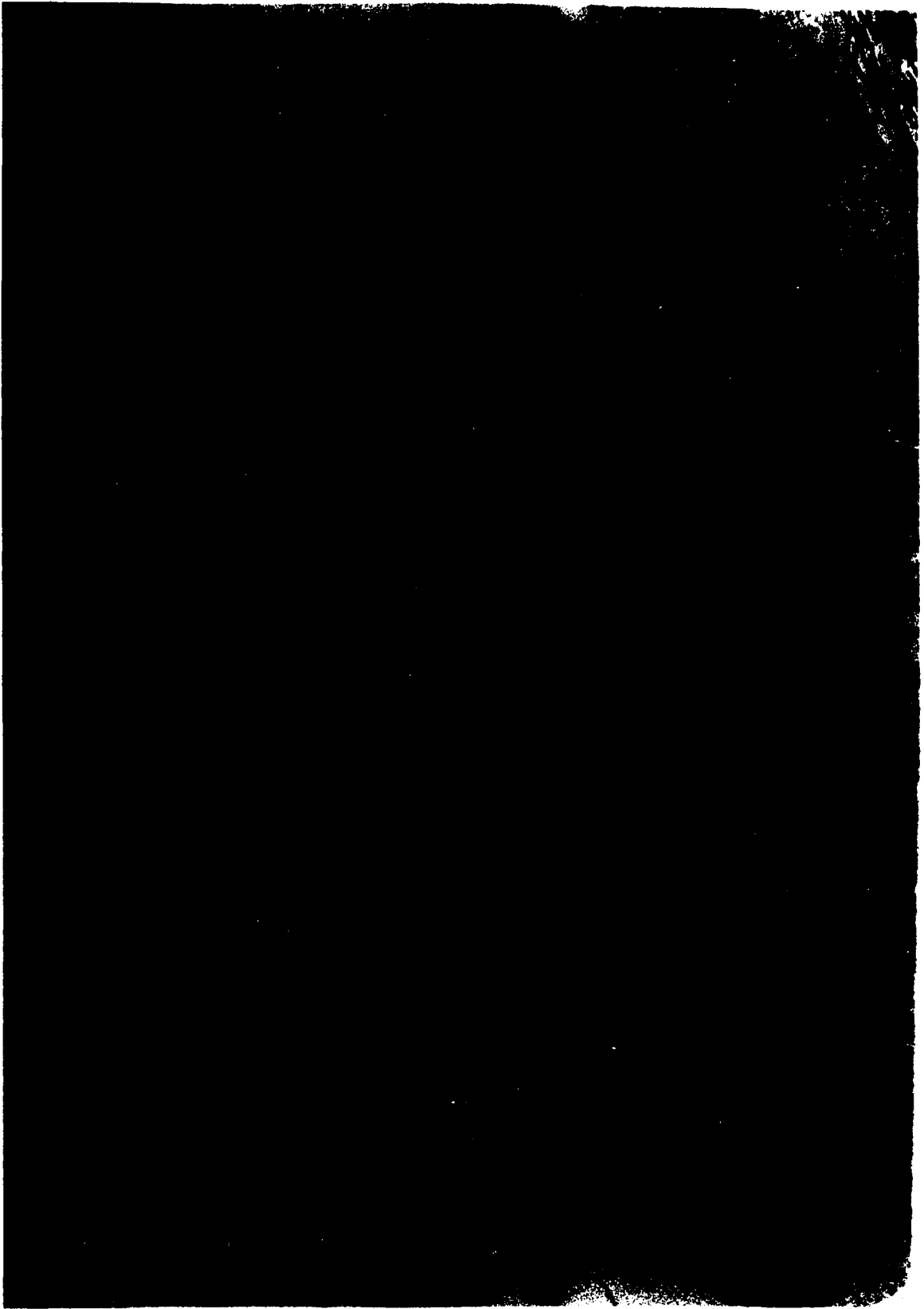
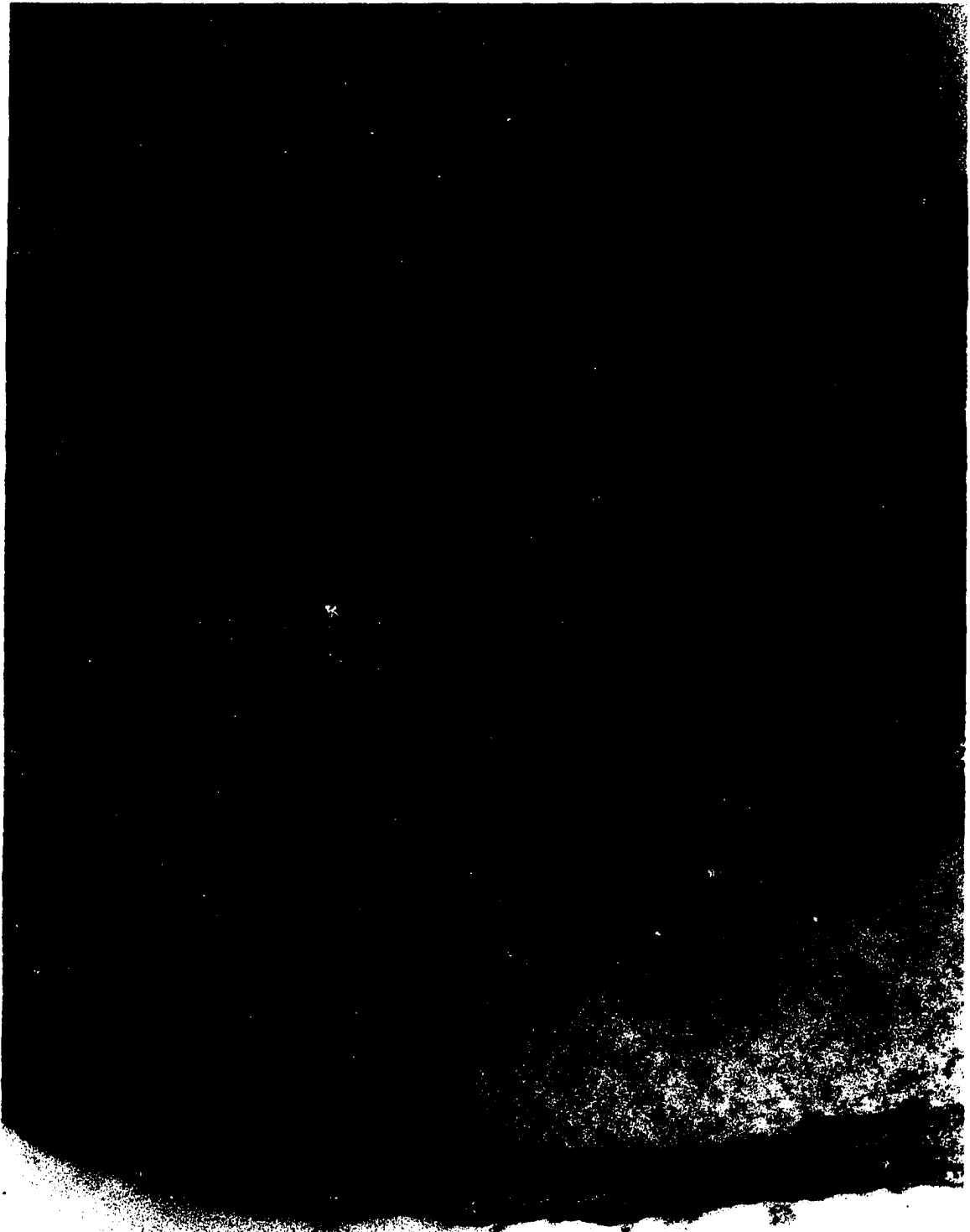


Figure 34

Figure 35

Case XI, congestive heart failure. This is a section through a septal wall with alveolar spaces (A) seen on both sides. There is increased elastic fiber (e) deposition and the elastic fibers themselves are very darkly stained and are without sharp borders. Collagen fibers (c) are also markedly increased in number and are heavily stained, but they can be separated from the elastic tissue by their characteristic periodicity. A mesenchymal cell component (m) with numerous ribosomes is seen within the markedly widened perivascular space. The capillary (C) is lined by a thin layer of endothelial cytoplasm. (Reynold's lead citrate and uranyl acetate, 12,900X)



A

Figure 35

Figure 36

Case XII, pulmonary fibrosis. This figure is a low power magnification and it demonstrates the remarkable fibrotic condition of the septal walls. All alveolar spaces (A) and capillaries (C) have been labelled to simplify orientation. Gross collagen deposition with increased cellular components are evident. The thin area labelled with a dash (-) is an alveolar lumen which has been cut tangentially. (Watson's lead hydroxide, 10,000X)

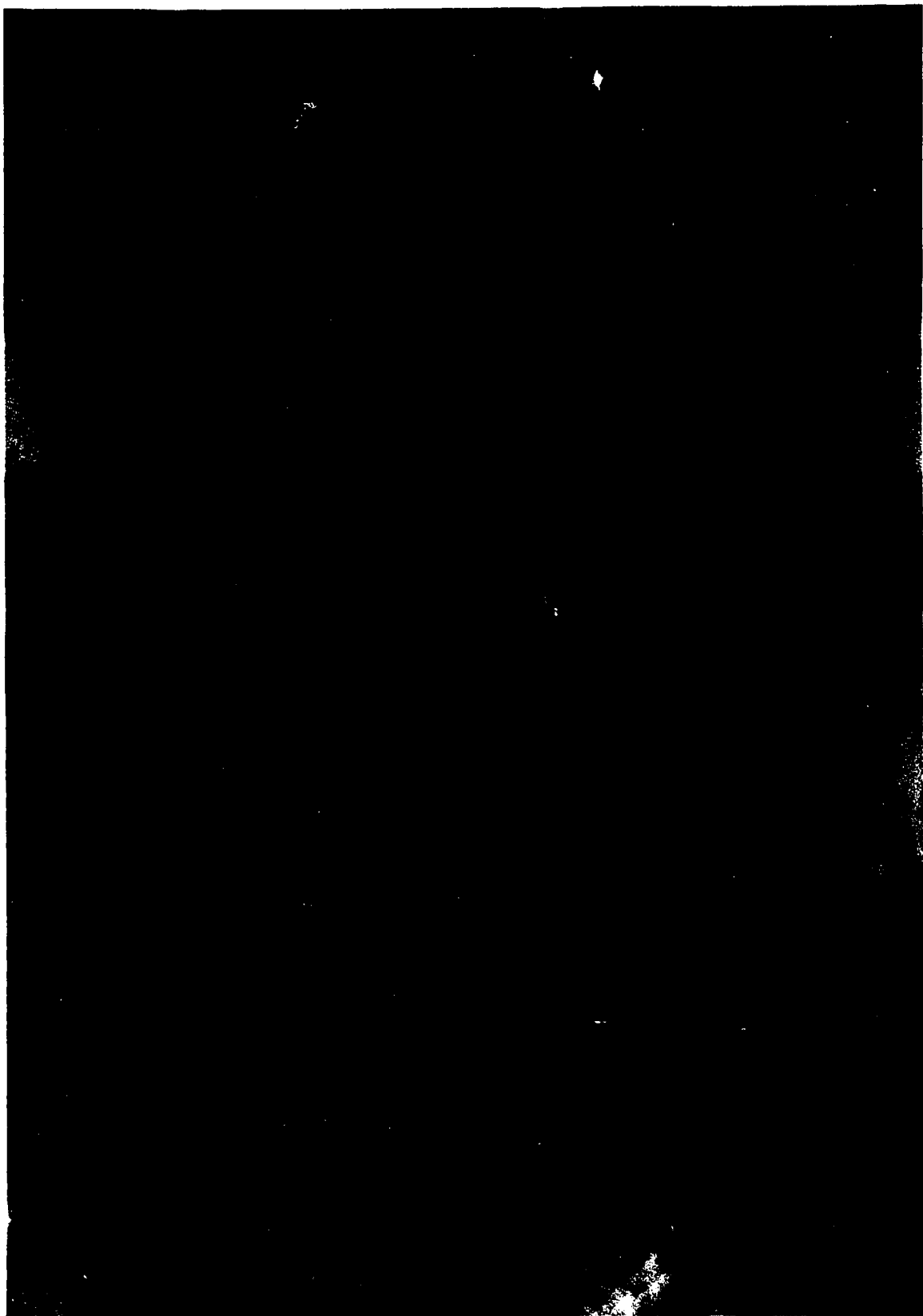


Figure 36

Figure 37

Case XII, pulmonary fibrosis. This area shows a normal configuration of the alveolar-capillary membrane. Increased reticular (r) and collagenous fibers are within the perivascular space (p). The alveolar and capillary basement membranes are quite narrow and well delineated. A large mesenchymal type cell (m) has, in some of its cytoplasmic borders, fine fibrillar elements which resemble reticular fibrils. An alveolar type II cell (a2) is situated above an area of vacuolization which contains the microvilli of the alveolar cell. The alveolar basement membrane is extremely thin and even appears to be lost in one area of this vacuolated space. This apparent loss of the alveolar basement membrane could possibly be due to artifact or to low magnification.

(Watson's lead hydroxide, 13, 300X)

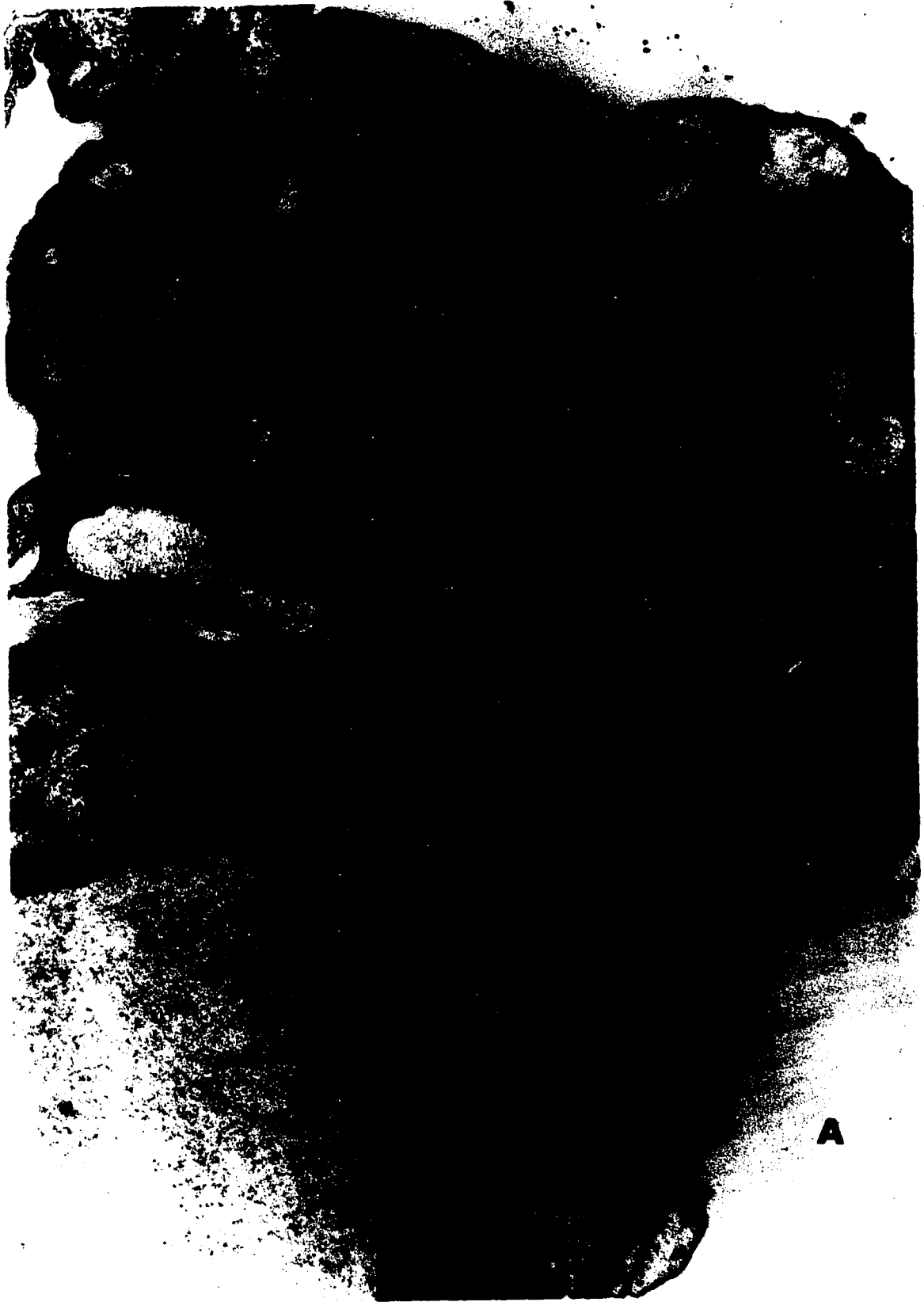


Figure 37

Figure 38

Case XII, pulmonary fibrosis. A cell which closely resembles a monocyte occupies the center of the figure. The cytoplasm contains numerous ribosomes and a well delineated Golgi apparatus (g). A mesenchymal cell component (m), containing ribosomes, mitochondria and a fat inclusion, is seen near the right margin. The areas labelled by (X) are seen to contain cross and longitudinal sections of collagen. This collagen is very lightly stained but the characteristic periodicity is evident.

(Watson's lead hydroxide, 19,200X)

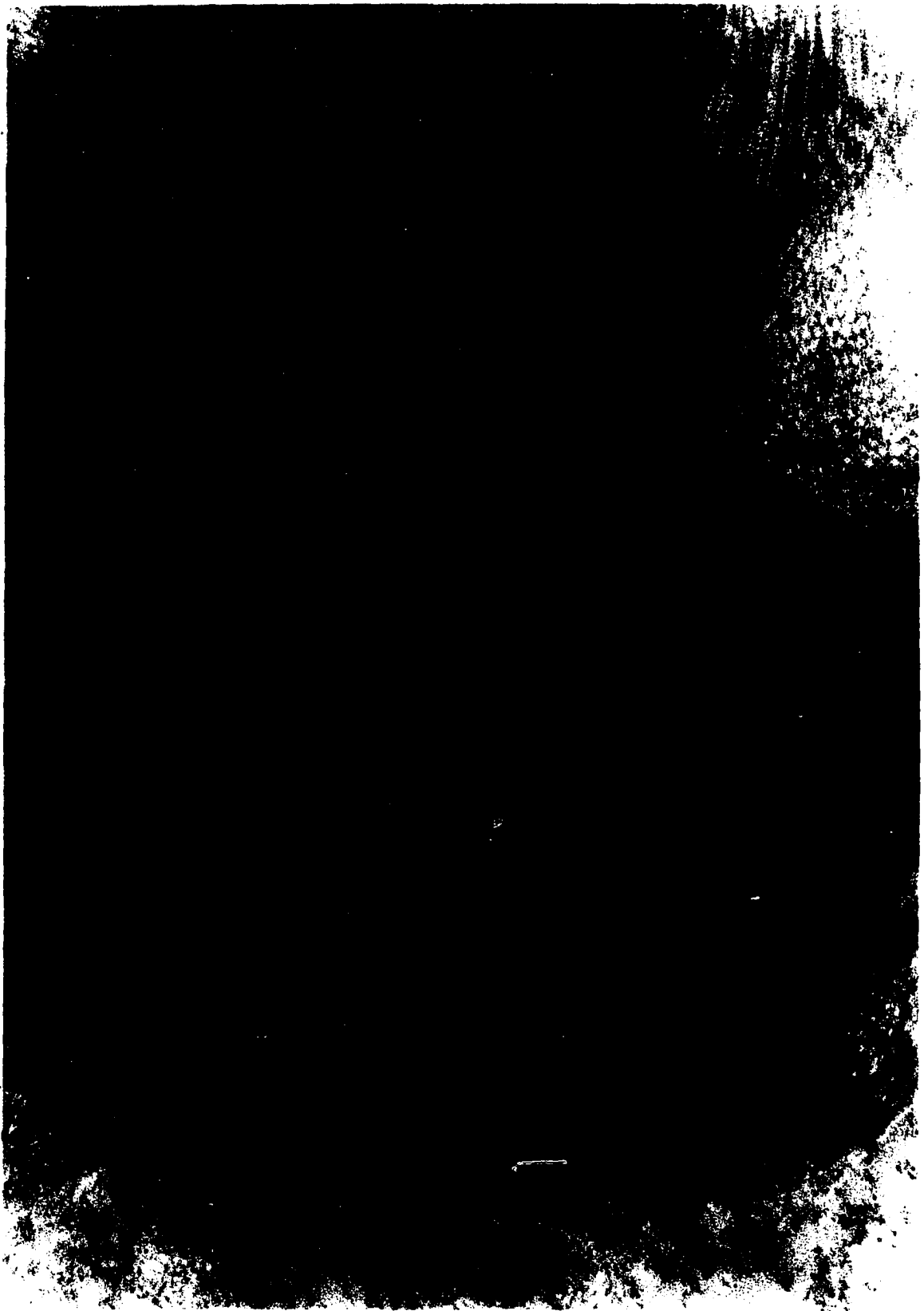


Figure 38

Figure 39

Case XII, pulmonary fibrosis. In the left upper portion of the figure, a large pale staining area can be seen. The white "holes" in this region are cross sections of collagen fibrils (c). This can be verified by comparing this area to a similar area in Figure 38. Two cells occupy most of the central portion of this figure (x) and (y). One of the cells (y) has a densely layered, rough endoplasmic reticulum and abundant mitochondria. It is probably a plasma cell. The other cell (x) has a rough endoplasmic reticulum and mitochondria, but the membranes are not closely packed and the intervening areas have a finely reticulated appearance.

(Watson's lead hydroxide, 13,300X)



Figure 39

Figure 40

Case XIII, congenital mitral stenosis. A portion of a red blood cell is seen in the capillary lumen (C). An endothelial cell nucleus (E) and its cytoplasmic extensions invest the capillary. A marked increase in width is seen in the capillary basement membrane (cb). Fine reticular fibers and mesenchymal cell components (m) are observed in the perivascular space. The perivascular space is greatly widened. Vacuolization is noted in the mesenchymal cell component. (uranyl acetate, 25,200X)

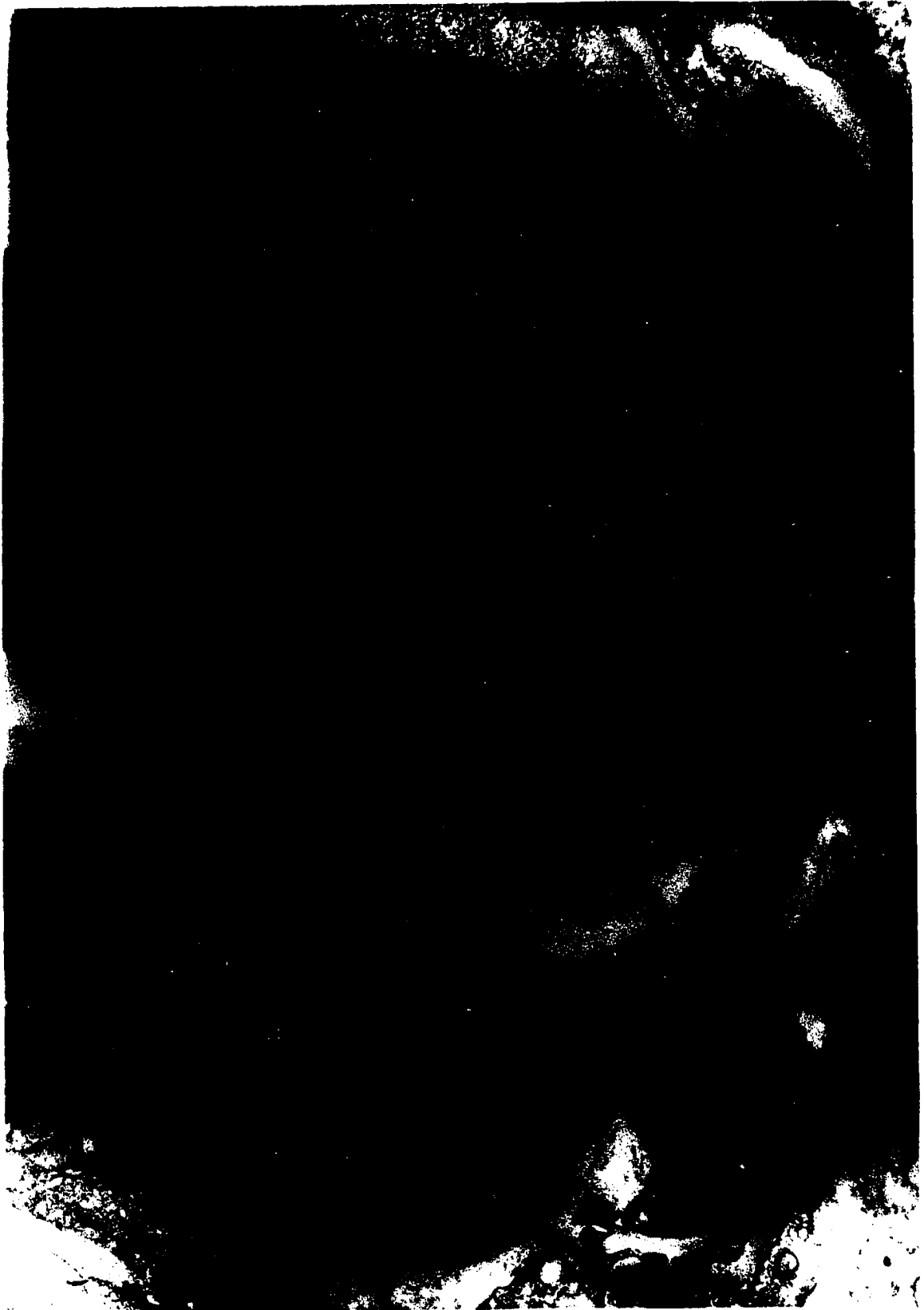


Figure 40

7A

Figure 41

Case XIII, congenital mitral stenosis. The alveolar type I epithelium lining the alveolar space (A) shows prominent vacuolization (v). Both basement membranes appear fused, but in some areas collagen and reticular fibrils are noted in the perivascular space (p). The capillary endothelium is not markedly increased in width.
(uranyl acetate and vanadatomolybdate, 29,400X)



Figure 41

Figure 42

Case XIII, congenital mitral stenosis. A tremendous widening of the perivascular space (p) is shown in this figure. There is increased collagen (c) and reticular (r) fiber deposition which fused into the alveolar basement membrane. The capillary basement membrane (cb) is markedly thickened. The alveolar type II cell (a2) shows vacuolization and the characteristic osmiophilic inclusions, but the microvilli are not prominent.

(uranyl acetate and vanadatomolybdate, 21,700X)

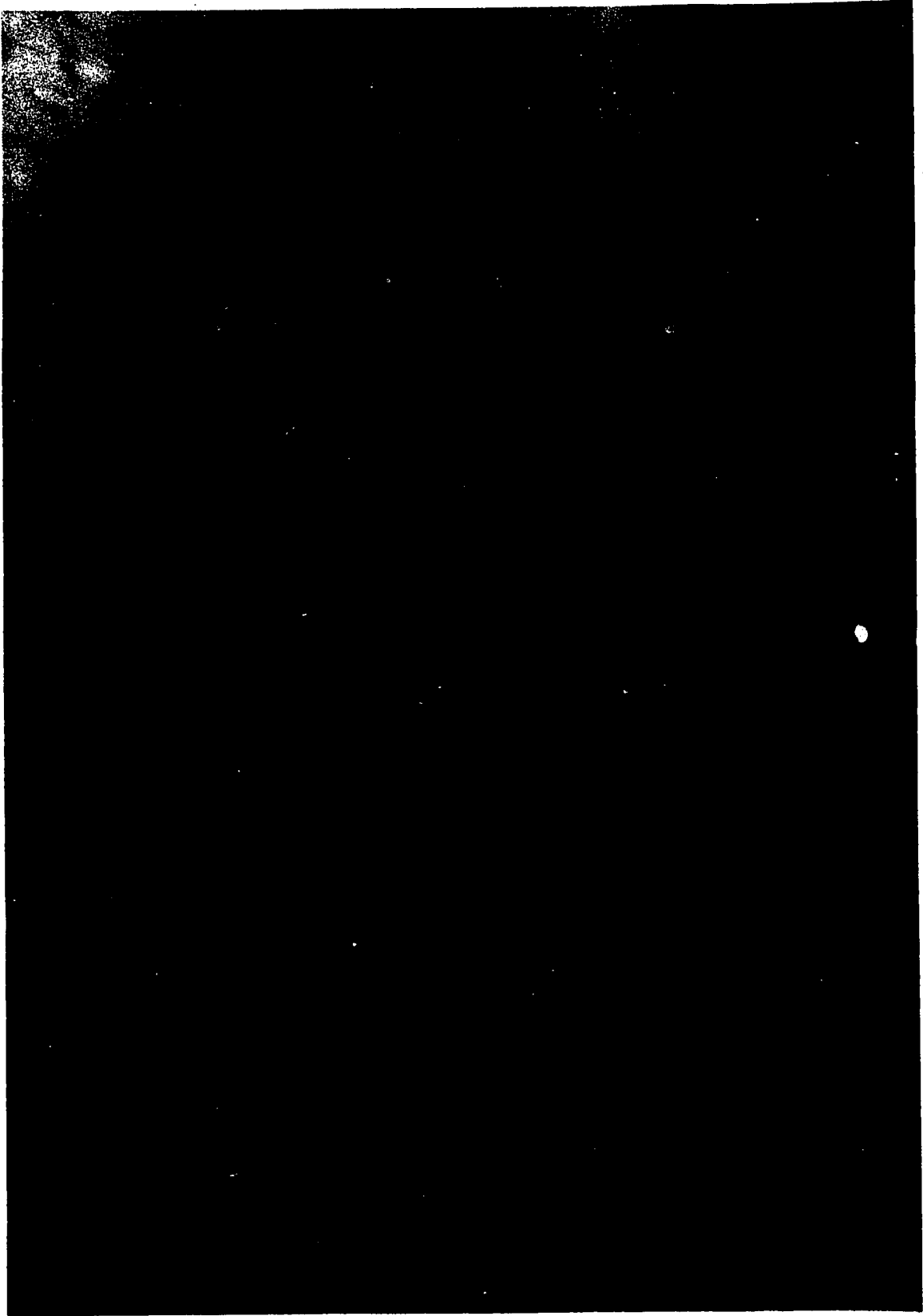


Figure 42

Figure 43

Case XIII, congenital mitral stenosis. This is an area through a septal wall. In the upper portion of the figure, an alveolar type II cell (a2) can be seen which contains vacuoles, an inclusion body, and numerous microvilli. The alveolar basement membrane fuses into "pockets" which contain collagen (c) and reticular (r) fibers. A mesenchymal cell component (m) rests in the perivascular space. Numerous small vesicles are seen in the alveolar type I lining of the alveolus (A).

(uranyl acetate, 29,400X)

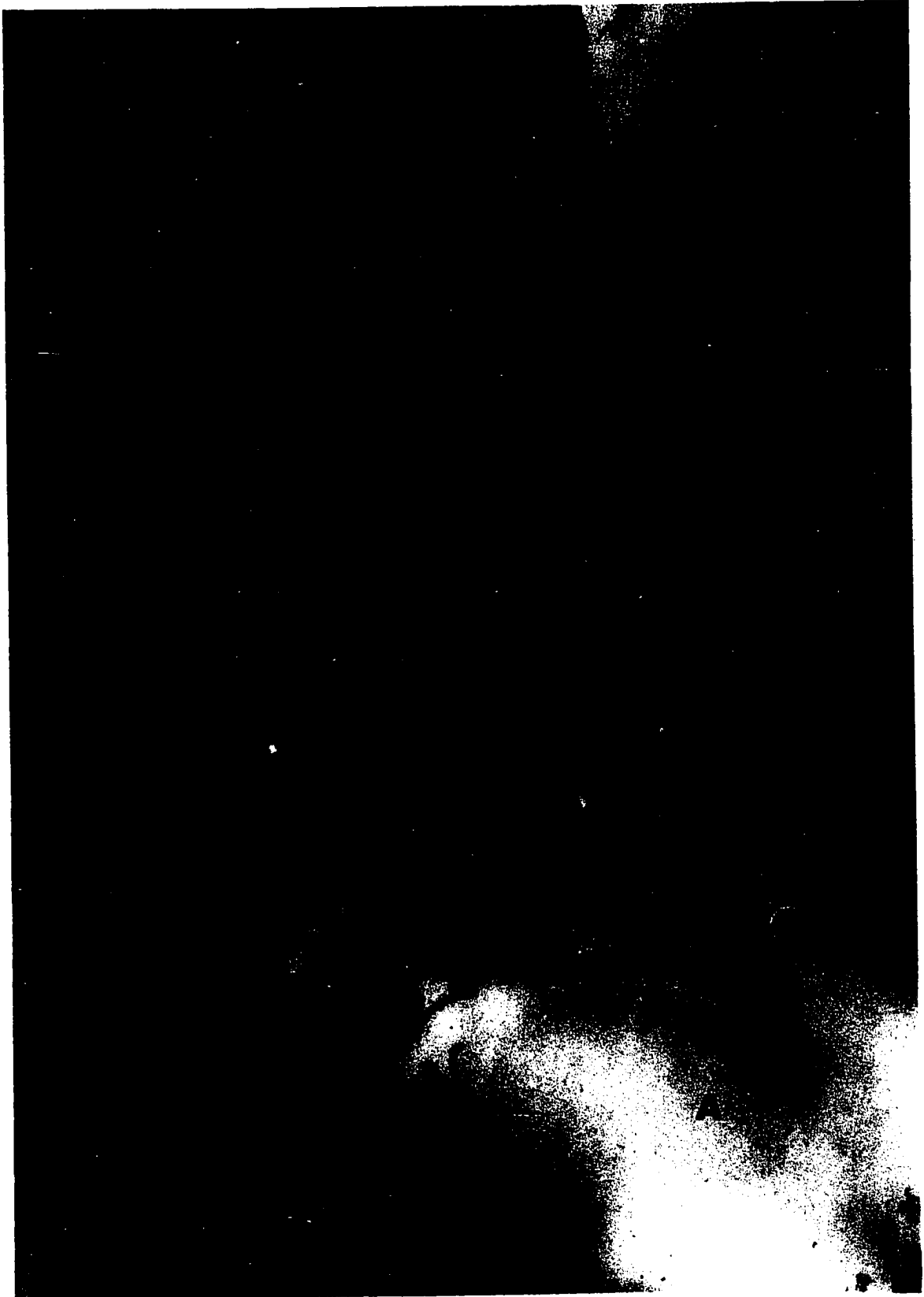


Figure 43

Figure 44

Case I, pulmonary stenosis. The reticular fibers are very fine and are not easily distinguished in the alveolar walls. (Gomori's reticulum - safranin O, 64X)

Figure 45

Case I, pulmonary stenosis. The alveolar septa show delicate strands of collagen. The collagen is more intensely stained in the interlobular area. Many free alveolar macrophages are present. (Koneff stain, 82X)

Figure 46

Case II, interventricular septal defect, left superior vena cava, and pulmonary hypertension. The alveolar septal walls show a definite increase in reticular fiber deposition and appear much thicker than those in Figure 44. (Gomori's reticulum - safranin O, 64X)

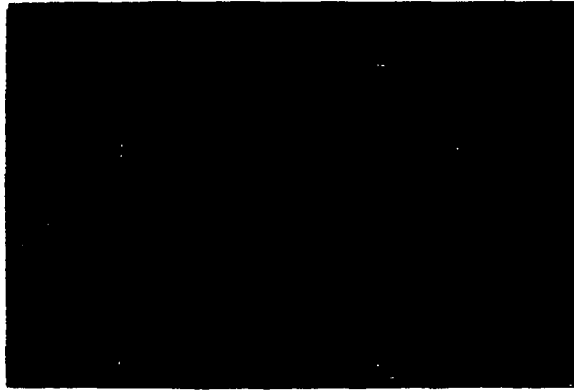


Figure 44



Figure 45



Figure 46

Figure 47

Case IV, atresia of a left common pulmonary vein, patent ductus arteriosus, interventricular septal defect and pulmonary hypertension. Increased collagen fibers and cells are depicted in the alveolar walls. There is also an abundance of free alveolar macrophages in the alveolar spaces. (Masson trichrome, 64X)

Figure 48

Case IV, atresia of a left common pulmonary vein, patent ductus arteriosus, interventricular septal defect and pulmonary hypertension. A marked increase of reticular fibers is evident in this figure. The capillaries are particularly well invested with a reticular network. (Gomori's reticulum - safranin O, 64X)

Figure 49

Case IV, atresia of a left common pulmonary vein, patent ductus arteriosus, interventricular septal defect and pulmonary hypertension. This preparation shows intensely staining collagen about the capillaries, whereas, the increased collagen within the septal walls have a delicate, pale-staining appearance. The septal walls are extensively widened. (Koneff stain, 64X)

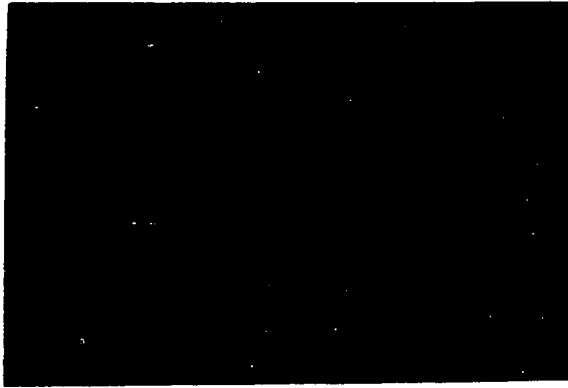


Figure 47

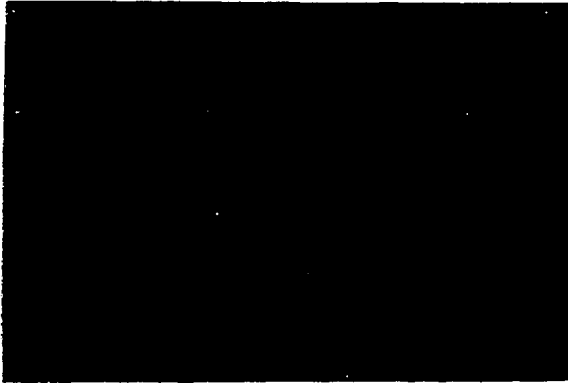


Figure 48

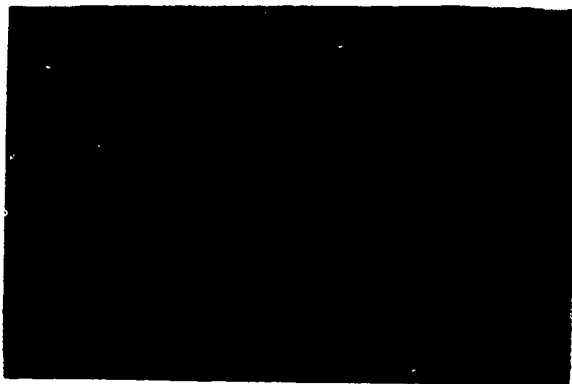


Figure 49

Figure 50

Case V, severe aortic stenosis. Attention is called to the cellularity evident in the alveolar walls. A "layering" effect is noted in some areas in which the cells appear pushed to the alveolar surfaces. The intervening area is clear and this is suggestive of an edematous condition in these areas. (Gallocyanin-chrome alum, 64X)

Figure 51

Case VI, acquired mitral stenosis. The alveolar septa show some areas of extensive collagen deposition. The capillaries appear quite hyperemic. (Masson trichrome, 64X)

Figure 52

Case VI, acquired mitral stenosis. The reticular fibers are particularly abundant about the vessel and are also easily observed within the alveolar walls. (Gomori's reticulum - safranin O, 64X)

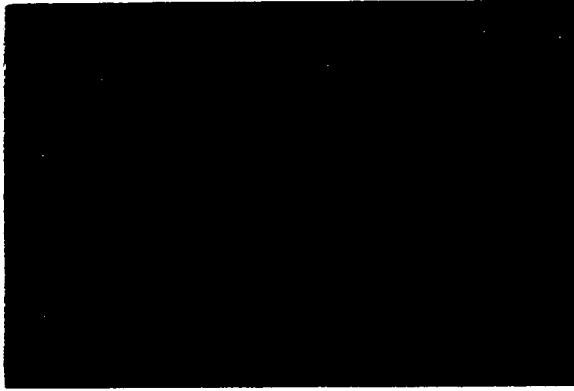


Figure 50

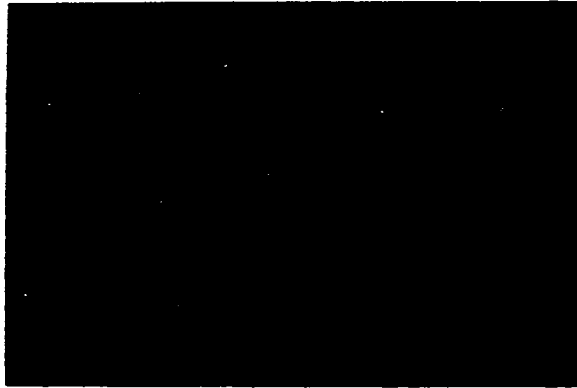


Figure 51

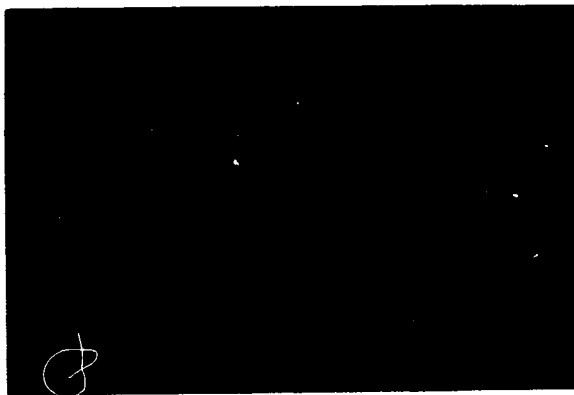


Figure 52

Figure 53

Case VII, acquired mitral stenosis. The alveolar spaces are filled with copious transudate. Numerous vacuoles are present. A marked increase of collagenous fibers is noted in the alveolar septa. Attention is called to the vessel in which extensive fibrosis had markedly compromised the lumen. (Koneff stain, 82X)

Figure 54

Case VII, acquired mitral stenosis. The alveolar walls are extensively laden with elastic tissue and appears to be thickened. (Orcein-fast green, 64X)

Figure 55

Case VII, acquired mitral stenosis. This case also has a marked reticular fiber increase in the septal walls. The reticular fibers form a very dense network in some areas. (Gomori's reticulum - safranin O, 82X)

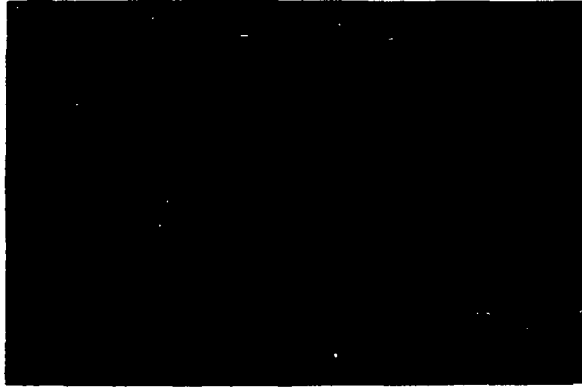


Figure 53

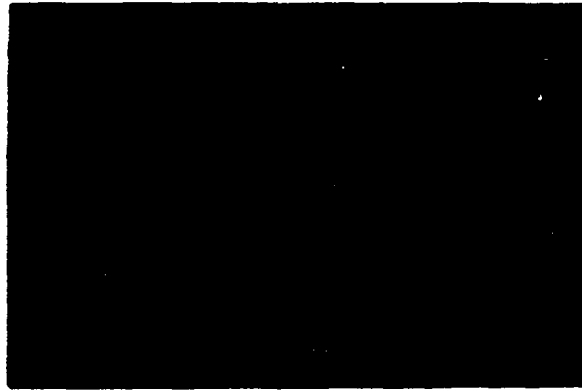


Figure 54

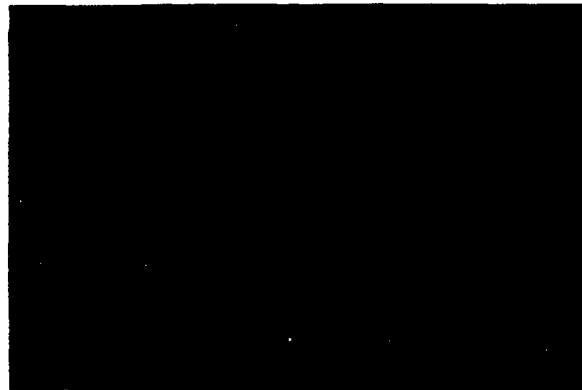


Figure 55

Figure 56

Case IX, acquired mitral stenosis. Extensive reticular fiber deposition is noted throughout the alveolar walls. Attention is called to the capillaries which are well invested with reticular fibers. (Gomori's reticulum - safranin O, 64X)

Figure 57

Case IX, acquired mitral stenosis. The blood vessel at the right border shows marked fibrosis of the tunica externa and some sub-endothelial thickening. The septal walls are very thick and a definite increase of collagen fibers and cells is noted. (Masson trichrome, 64X)

Figure 58

Case IX, acquired mitral stenosis. The elastic tissue deposition was increased in this case. The alveolar walls appear to be thickened markedly. (Orcein - fast green, 64X)

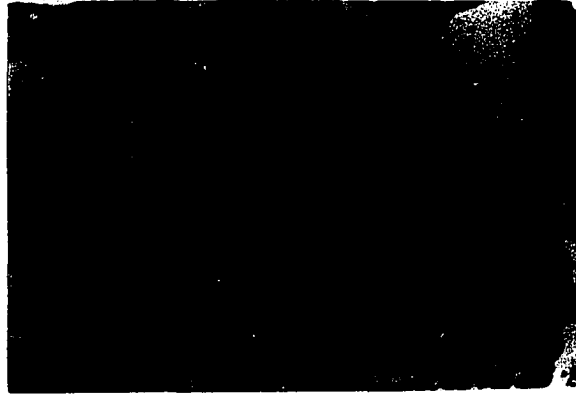


Figure 56



Figure 57



Figure 58

Figure 59

Case X, acquired interventricular septal defect. The alveolar walls are increased in width throughout most of the field. There is a moderate increase of reticular fibers in the alveolar walls. (Gomori's reticulum - safranin O, 64X)

Figure 60

Case X, acquired interventricular septal defect. This is a section through an interlobular septum with surrounding alveoli. Attention is called to the cuboidal lining epithelium along the septum and, in some areas, on the alveolar walls. The collagen only appears stained in the interlobular septum. (Koneff stain, 64X)

Figure 61

Case XI, congestive heart failure. In this preparation, the elastic tissue was only minimally increased. However, at the ultra-structural level, there was a definite elastic tissue increase. Attention is called to the very "smudgy" appearance of the elastic fibers. They are not clearly defined in this preparation. (Orcein - fast green, 64X)



Figure 59



Figure 60



Figure 61

Figure 62

Case XI, congestive heart failure. Even though the alveolar walls do not appear markedly increased in width, it is apparent that most of the component present within the wall is collagen. (Masson trichrome, 64X)

Figure 63

Case XIII, congenital mitral stenosis. The reticular fibers are markedly increased and appear closely interwoven. (Gomori's reticulum - safranin O, 64X)

Figure 64

Case XIII, congenital mitral stenosis. The darker staining cells formed the lining epithelial layer, whereas the cells with light, stippled chromatin material were the cells noted in the septal walls and free in the alveolar spaces. The increased cellularity noted at the ultrastructural level for this case is clearly evident here. (Turchini, 82X)

Figure 65

Case XIII, congenital mitral stenosis. In this reproduction, the areas of positive staining for elastic fibers are not well seen. Even though the fiber content was not increased, it was seen within the alveolar walls. (Orcein- fast green, 64X)



Figure 62

Figure 63

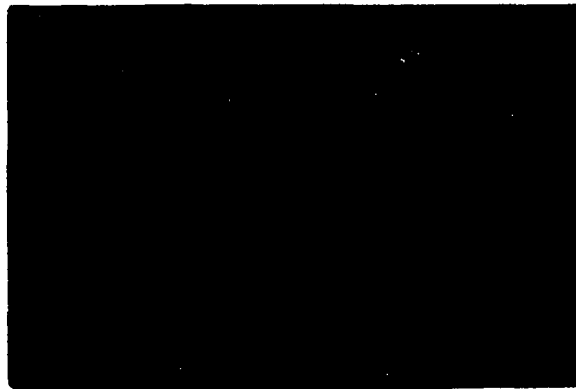


Figure 64



Figure 65

0

5

6

9

0